

ÉCOLE DE TECHNOLOGIE SUPÉRIEURE
UNIVERSITÉ DU QUÉBEC

THESIS PRESENTED TO
ÉCOLE DE TECHNOLOGIE SUPÉRIEURE

IN PARTIAL FULFILLMENT OF THE REQUIREMENTS FOR
THE DEGREE OF DOCTOR OF PHILOSOPHY
Ph.D.

BY
CARON François

A MAXIMUM LIKELIHOOD APPROACH TO VIDEO ERROR CORRECTION APPLIED
TO H.264 DECODING

MONTREAL, OCTOBER 7, 2013



Caron François 2013



This Creative Commons license allows readers to download this work and share it with others as long as the author is credited. The content of this work cannot be modified in any way or used commercially.

BOARD OF EXAMINERS

THIS THESIS HAS BEEN EVALUATED

BY THE FOLLOWING BOARD OF EXAMINERS:

Mr. Stéphane Coulombe, Thesis Director
Département de génie logiciel et des TI at l'École de technologie supérieure

Mr. François Gagnon, Committee President
Département de génie électrique at l'École de technologie supérieure

Mr. William Lynch, External Examiner
Department of Electrical & Computer Engineering at Concordia University

Mr. Pierre Dumouchel, Examiner
Département de génie logiciel et des TI at l'École de technologie supérieure

THIS THESIS WAS PRESENTED AND DEFENDED

IN THE PRESENCE OF A BOARD OF EXAMINERS AND PUBLIC

ON SEPTEMBER 5TH 2013

AT ÉCOLE DE TECHNOLOGIE SUPÉRIEURE

ACKNOWLEDGEMENTS

When I decided to pursue a Ph.D., nobody told me I had strapped in *the* rollercoaster ride of a lifetime. Well, that's not entirely true. Nobody told me I had *also* strapped in my loving spouse. So this is for you Jennifer.

Thank you for being *you*, and letting me be *me*. Thank you for having kept on a smile through all the *Oh my god, I am soooooooooo on to something!*, and the *I can't believe I lost so much time on a dead end. I'm never going to finish!* Thank you for having listened to me. Thank you for having pretended to listen to me. (Yes, I did bother her. A lot. When she was tired. Just after supper. On Friday nights. So sue me...) If it wasn't for you, I'm not sure I would still be sane. Through thick and thin, you supported me. You believed in me. Even when I started to doubt myself. And for that, I will forever be thankful.

I would also like to thank my thesis director, Stéphane Coulombe. You had faith in me ever since we started working together when I was still an undergrad. Your guidance has helped me become a better person at work and in my personal life. I strongly believe everybody should have a mentor like you have been for me.

My thanks go also to the members of the jury, Professors François Gagnon, William Lynch, and Pierre Dumouchel, who have accepted to devote their precious time to evaluating my thesis.

Finally, I would like to thank my family for their support. The impromptu meals and outings made me realize that there is life beyond work, and that I don't spend enough time enjoying it. Now that I am done, I fully intend to make a habit of having fun more often. Please help me keep this promise!

A MAXIMUM LIKELIHOOD APPROACH TO VIDEO ERROR CORRECTION APPLIED TO H.264 DECODING

CARON François

ABSTRACT

Video error concealment has long been identified as the last line of defense against transmission errors. This is especially true for real time video communication systems where retransmissions are rarely used because of timing constraints. Since error handling is outside the scope of video coding standards, decoders may choose to simply ignore the corrupted packets, or attempt to decode their content. Video error correction is a viable alternative to deal with transmission errors when corrupted packets reach their destination. Until now, these approaches have received little considerations. This is mainly because the proposed methods either rely on specific coding tools or constraints, or require far too many computations compared to video error concealment techniques.

In this thesis, we propose a novel video error correction method based on maximum likelihood decoding. The method estimates the likeliest syntactically valid video slice content based on the erroneous video packets rather than discarding the content, and concealing the missing information. Such content is obtained by combining the likelihood of the candidate codewords with the bit modification likelihood associated to each candidate. We propose two solutions centered around our maximum likelihood decoding approach. First, we introduce a slice-level video error correction method. Furthermore, we show how to integrate the soft-output information shared by the channel decoder to evaluate the bit modification likelihood. We also show that it is possible to use our maximum likelihood decoding approach when soft-output information is not available. Then, we refine the solution at the syntax-element-level. The final solution we obtain can be used in real-time communication systems as it is computationally inexpensive compared to the slice-level solution, or the solutions proposed in the literature.

Our final solution is then applied to the correction of videos conforming to the H.264 Baseline profile. We selected three 720x480 sequences, five 704x576 sequences, and one 720x576 sequence to run simulations. Each sequence was coded at a target bitrate of 1 Mbps, 1.2 Mbps, and 1.5 Mbps. All 27 sequences were then submitted to a noisy channel with a bit error rate ranging from 10^{-5} to 10^{-3} . Our 5400 observations show a PSNR improvement of 1.69 dB over the video error concealment method implemented in the H.264 reference software. Furthermore, our results also indicate a 0.42 dB PSNR improvement over state-of-the-art error concealment STBMA+PDE.

Keywords: video error correction, joint source-channel decoding, maximum likelihood decoding, H.264, real time video applications

LA CORRECTION D'ERREURS VIDÉO À L'AIDE DU MAXIMUM DE VRAISEMBLANCE APPLIQUÉE AU STANDARD VIDÉO H.264

CARON François

RÉSUMÉ

La dissimulation d'erreurs est l'approche *de facto* pour gérer les erreurs de transmission. C'est d'autant plus vrai pour les applications temps réel, car les retransmissions posent problème au maintien des courts délais de livraison requis. Conséquemment, il apparaît que toutes les approches de dissimulation d'erreurs partagent l'hypothèse qu'une erreur de transmission se manifeste par l'absence de données. Or, cette hypothèse ne s'avère pas toujours vraie. La correction d'erreurs vidéo se veut donc une alternative viable à la dissimulation d'erreurs lorsque les paquets endommagés atteignent leur destination. Malheureusement, ces approches reçoivent peu d'attention.

Dans cette thèse, nous proposons une toute nouvelle approche pour corriger les erreurs de transmission à l'aide du maximum de vraisemblance. Notre méthode nécessite aucun outil de codage particulier, ni l'imposition de contraintes spécifiques. En combinant la vraisemblance des symboles valides potentiels à la vraisemblance des modifications proposées aux bits reçus, notre méthode sélectionne le contenu le plus probable transmis par l'encodeur. En premier lieu, une approche ciblant la totalité d'un paquet endommagé est proposée. De plus, nous montrons comment intégrer les probabilités des bits calculés par la couche physique afin d'obtenir une vraisemblance plus précise sur les modifications des bits. Par la suite, nous raffinons l'approche au niveau des éléments de la syntaxe. Cette deuxième approche réduit suffisamment la complexité pour permettre l'intégration de notre méthode à des applications en temps réel.

Par la suite, notre solution est appliquée au cas particulier du standard vidéo H.264. Nous nous concentrons sur le profil *Baseline*. Notre expérience porte sur trois séquences 720x480, cinq séquences 704x576 et une séquence 720x576. Chacune des séquences a d'abord été codée à trois reprises avec un débit cible de 1 Mbps, 1,2 Mbps et 1,5 Mbps. Par la suite, les 27 séquences obtenues ont été soumises à des erreurs de transmission. Le taux d'erreur des bits oscillait entre 10^{-5} et 10^{-3} . Au total, nous avons observé 5400 cas différents. Nos résultats indiquent une amélioration moyenne de 1,69 dB en PSNR par rapport aux résultats obtenus avec la méthode utilisée dans le décodeur de référence. Plus encore, nous avons observé une amélioration moyenne de 0,42 dB en PSNR par rapport aux résultats obtenus avec la meilleure méthode de dissimulation d'erreur issue de l'état de l'art.

Mot-clés : correction d'erreur vidéo, décodage conjoint source-canal, décodage du maximum de vraisemblance, H.264, applications temps réel

CONTENTS

	Page
INTRODUCTION.....	1
CHAPTER 1 VIDEO COMPRESSION AND TRANSMISSION	7
1.1 Typical Video Communication System	7
1.2 Proposed Video Communication System	7
1.3 Network Abstraction Layer Units	9
1.4 Video Coding Layer Units.....	10
1.5 Exponential-Golomb Codes	11
CHAPTER 2 LITERATURE REVIEW	13
2.1 Video Error Concealment	13
2.1.1 Spatial Error Concealment	13
2.1.2 Temporal Error Concealment	15
2.1.3 Hybrid Error Concealment	17
2.1.4 Concealment Order	21
2.2 Video Error Correction	23
2.2.1 List Decoding	23
2.2.2 Joint Source-Channel Decoding	25
2.2.3 Discussion.....	26
CHAPTER 3 MAXIMUM LIKELIHOOD VIDEO ERROR CORRECTION	29
3.1 Slice-Level Error Correction	29
3.1.1 Channel Decoding	31
3.1.2 Source Decoding.....	33
3.2 Syntax-Element-Level Error Correction	36
CHAPTER 4 H.264 BASELINE PROFILE VIDEO ERROR CORRECTION	39
4.1 Slice Header.....	39
4.1.1 <i>first_mb_in_slice</i>	40
4.1.2 <i>slice_type</i>	41
4.1.3 <i>pic_parameter_set_id</i>	42
4.1.4 <i>frame_num</i> and <i>pic_order_cnt_lsb</i>	42
4.2 Slice Data	43
4.2.1 <i>mb_type</i>	43
4.2.2 <i>mb_skip_run</i>	44
4.2.3 Intra4x4PredMode	45
4.2.4 <i>intra_chroma_pred_mode</i>	46
4.2.5 <i>sub_mb_type</i>	47
4.2.6 <i>mvd_l0</i>	48
4.2.7 <i>coded_block_pattern</i>	49

4.3	Early Termination	50
CHAPTER 5 EXPERIMENTAL RESULTS		51
5.1	Experimental Setup	51
5.2	Concealment and correction comparison	53
5.3	Hard-output and soft-output comparison	58
5.4	Decoding time.....	63
5.5	Current limitations	65
CHAPTER 6 CONTRIBUTIONS		67
CONCLUSION.....		69
ANNEX I	ERROR RESILIENCY COST	73
ANNEX II	RANDOM TAIL ASSUMPTION	79
ANNEX III	EXPERIMENTAL TEST SET	83
ANNEX IV	MATLAB NETWORK SIMULATOR	97
ANNEX V	EXPERIMENTAL OBSERVATIONS.....	99
BIBLIOGRAPHY		232

LIST OF TABLES

	Page
Table 1.1 Mapping of Exponential-Golomb codes to decimal values	12
Table 2.1 Average system time using different methods	21
Table 5.1 Average PSNR comparison for an average bitrate of 1000 kbps	54
Table 5.2 Average PSNR comparison for an average bitrate of 1200 kbps	55
Table 5.3 Average PSNR comparison for an average bitrate of 1500 kbps	56
Table 5.4 Comparison of the average PSNR with a QP of 37	61
Table 5.5 Comparison of the average PSNR with a QP of 32	62
Table 5.6 Comparison of the average PSNR with a QP of 27	63
Table 5.7 Comparison of the average PSNR with a QP of 22	64
Table 5.8 Average decoding time using four decoding approaches	64

LIST OF FIGURES

	Page
Figure 0.1 Visual quality cost of using error resilience	3
Figure 1.1 A widespread video communication system	8
Figure 1.2 A video communication system with correction of corrupted VCL NALUs .	9
Figure 1.3 Composition of a Network Abstraction Layer Unit	9
Figure 1.4 Composition of a coded slice.....	10
Figure 2.1 Spatial error concealment strategies	14
Figure 2.2 Boundary Matching Algorithm	16
Figure 2.3 Concealment order	22
Figure 2.4 Candidate slice generator for list decoding strategies	23
Figure 2.5 Representation of a sequence of codewords as navigation waypoints.....	25
Figure 5.1 Residual BER for rate-2/3 LDPC protected packets	52
Figure 5.2 Average PSNR gains over JM 16.0 with a channel SNR of 4 dB	57
Figure 5.3 Average PSNR gains over JM 16.0 with a channel SNR of 5 dB	57
Figure 5.4 Visual comparison of the 99-th frame of the <i>ice</i> sequence.....	58
Figure 5.5 Visual comparison of the 65-th frame of the <i>walk</i> sequence.....	59
Figure 5.6 Frame-by-frame PSNR of the <i>ice</i> sequence after transmission errors.....	60
Figure 5.7 Frame-by-frame PSNR of the <i>walk</i> sequence after transmission errors.....	60
Figure 5.8 Example of uncorrected transmission errors	65
Figure 5.9 Side-by-side distributions of PSNR gains over JM 16.0	66

LIST OF ABBREVIATIONS

4CIF	4 × Common Intermediate Format
ASO	Arbitrary Slice Ordering
AVC	Advanced Video Codec
BER	Bit Error Rate
BMA	Boundary Matching Algorithm
CABAC	Context-Adaptive Binary Arithmetic Coding
CAVLC	Context-Adaptive Variable-Length Coding
CIF	Common Intermediate Format
FMO	Flexible Macroblock Ordering
HEC	Hybrid Error Concealment
HVS	Human Visual System
IEC	International Electrotechnical Commission
IJSCD	Iterative Joint Source-Channel Decoding
ISO	International Organization for Standardization
JSCD	Joint Source-Channel Decoding
JVT	Joint Video Team
kbps	Kilo Bits Per Second
LLR	Log-Likelihood Ratio
MPEG	Moving Picture Experts Group
MTU	Maximum Transmission Unit

NAL	Network Abstraction Layer
NTSC	National Television System Committee
OBMA	Overlapped Boundary Matching Algorithm
PAL	Phase Alternating Line
PDE	Partial Differential Equation
PLR	Packet Loss Rate
PPS	Picture Parameter Set
PSNR	Peak Signal-to-Noise Ratio
QCIF	Quarter Common Intermediate Format
QP	Quantization Parameter
RTP	Real-time Transport Protocol
RVLC	Reversible Variable-Length Codeword
SEC	Spatial Error Concealment
SNR	Signal-to-Noise Ratio
SPS	Sequence Parameter Set
STBMA	Spatio-Temporal Boundary Matching Algorithm
TCP	Transmission Control Protocol
TEC	Temporal Error Concealment
UDP	User Datagram Protocol
VLC	Variable-Length Codeword

LIST OF SYMBOLS

I_t	The t -th picture in a video sequence.
S^*	The likeliest transmitted slice.
\hat{S}	A hypothetically transmitted slice.
\hat{S}_n	The n -th bit in the slice \hat{S} .
\tilde{S}	An actually received corrupted slice.
\tilde{S}_n	The n -th bit in the slice \tilde{S} .
H	A discrete random vector's support containing all slices possibilities.
\mathcal{R}	A discrete random vector of received bits.
\mathcal{R}_n	The n -th bit of the discrete random vector \mathcal{R} .
$\mathcal{R}_{c,i}$	The i -th codeword extracted from \mathcal{R} .
\mathcal{T}	A discrete random vector of transmitted bits.
\mathcal{T}_n	The n -th bit of the discrete random vector \mathcal{T} .
$\mathcal{T}_{c,i}$	The i -th codeword extracted from \mathcal{T} .
$\mathcal{T}_{c,i,n}$	The n -th bit of the i -th codeword in \mathcal{T} .
LLR_n	The log-likelihood ratio of the n -th bit in \mathcal{T} .
\hat{c}_i	The i -th codeword extracted from \hat{S} .
c_i^*	The i -th likeliest transmitted codeword in \mathcal{T} .
C_i	The set of valid codewords for the i -th decoded syntax element.
$\Delta(i)$	The number of bits preceeding the first bit of the codeword \hat{c}_i .
$L_C(\hat{S})$	The number of codewords in a hypothetical slice \hat{S} .

$L_B(\hat{c}_i)$	The number of bits in codeword \hat{c}_i .
β_i	The length of the longest codeword in C_i .
Ω_i	The set of context variables required to decode the i -th codeword in \hat{S} .
Ψ_i	The internal state of the decoder after decoding the i -th codeword in \hat{S} .
ρ	The estimated bit error rate.
μ	The average number of macroblocks in a slice.
σ	The standard deviation of the number of macroblocks in a slice.
$\delta(\cdot)$	The discrete Dirac function.
α	The probability that the <i>slice_type</i> syntax element uses a value above 4.
β	The probability that the <i>slice_type</i> syntax element uses a value of either 2 or 7.
y	A random signal that represents channel noise.
$FMIS$	A discrete random variable representing the value of the <i>first_mb_in_slice</i> syntax element.
$fmis$	The latest observed value of $FMIS$.
ST	A discrete random variable representing the value of the <i>slice_type</i> syntax element.
st	The observed value of ST in the current slice.
st_{Prev}	The observed value of ST in the previous slice.
FN	A discrete random variable representing the value of the <i>frame_num</i> syntax element.
fn_{Prev}	The observed value of FN in the previous slice.

$POCL$	A discrete random variable representing the value of the <i>pic_order_cnt_lsb</i> syntax element.
$pocl_{prev}$	The observed value of $POCL$ in the previous slice.
CS	A discrete random variable representing the value of the current macroblock's coding scheme.
cs_{Co}	The observed value of CS of the colocated macroblock in the previous frame.
$Addr$	A discrete random variable representing the raster index of a macroblock.
$addr$	The raster index of the current macroblock.
IPM	A discrete random variable representing the Intra4x4PredMode value of a 4x4 block in the current macroblock.
ipm_{loc}	The observed value of Intra4x4PredMode of a 4x4 block at location <i>loc</i> relative to the current 4x4 block.
$ICPM$	A discrete random variable representing the value of the <i>intra_chroma_pred_mode</i> syntax element.
$icpm_{loc}$	The observed value of $ICPM$ at location <i>loc</i> relative to the position of the current macroblock.
MVC	A discrete random variable representing the number of observed motion vectors in a macroblock.
mvc_{Co}	The observed value of MVC of the colocated macroblock in the previous frame.
MV	A discrete random vector representing the motion vector of a macroblock.
mv_{loc}	An observed motion vector at location <i>loc</i> relative to the current macroblock.
CBP	A discrete random variable representing the value of the <i>coded_block_pattern</i> syntax element.

cbp_{loc} The observed value of CBP at location loc relative to the current macroblock.

INTRODUCTION

Video coding uses both lossless and lossy compression. Significant compression is achieved by removing spatio-temporal redundancies (lossless coding), mostly through motion compensation. The remaining information is then quantized (lossy coding) to control the stream's size. As a result, the coded stream exchanged between the encoder and the decoder carries mostly prediction information, such as motion vectors, and quantized residual errors. The technology is very effective, but it requires that both ends stay synchronized. That is, the reconstructed pictures at the decoding side must be identical to those used at the encoding side so that the prediction values are the same.

The drawback, however, is that delivering the coded stream is a challenge. Transmission errors threaten the system's synchronization. Reconstructed pictures are expected to differ from the ones transmitted when parts of the stream are missing. What's more, the encoder is typically oblivious to these differences. It can (and probably will) use prediction values unknown to the decoder to compress later pictures. The residual errors transmitted will not make up for the fact that the temporal prediction information differs at the decoding side. Even without further transmission errors, the pictures at both ends would continue to differ until the stream is resynchronized. This is what is commonly referred to as drifting effects.

Communication protocols, such as TCP (Postel, 1981) that guarantee delivery cannot be relied upon as a universal solution to handle transmission errors. In fact, real-time video communication systems frequently use unreliable means to exchange information as their timing requirements exclude the deployment of some well-known error-recovery techniques (Wang and Zhu, 1998). For instance, video conferencing applications use UDP (Postel, 1980), as retransmission delays threaten their interactive nature. Broadcasting applications prevent the use of retransmission algorithms completely due to network flooding considerations (Y. Wang and Katsaggelos, 2000).

Both examples above shed light on the fact that error handling should be viewed as a correctness criterion. At the transmitting side, the encoder can address this by building coded streams

in such a way as to limit the impact of transmission errors. At the receiving side, the decoder should be ready to deal with the missing regions caused by transmission errors.

The introduction of new error resiliency tools in the ITU-T H.264 and the ISO/IEC MPEG-4 AVC video coding standard clearly show the importance of the transmission challenges (International Telecommunications Union, 2007). Slices ensure that packets are independently decodable to isolate the effects of packet loss. In previous coding standards, the prediction process could cross packet boundaries. The loss of a packet would interfere with the decoding process of subsequent packets, until a resynchronization marker could be parsed. Flexible macroblock ordering (FMO) breaks the traditional raster scan ordering so that missing regions are not necessarily consecutive macroblocks (Lambert *et al.*, 2006). These tools, along with other tools such as random intra refresh and arbitrary slice ordering (ASO), increase resiliency to transmission errors, but reduce coding efficiency. More precisely, they reduce the efficiency of the lossless coding, as the prediction process makes less accurate predictions in order to respect the slice boundaries.

This reduced efficiency needs to be understood from a bandwidth-limitation perspective. The direct consequence of adding resilience is that bigger prediction errors will make their way to the lossy coding part of the video encoder. To make sure the allocated transmission budget is respected, more aggressive compression will have to be applied. It comes as no surprise that the use of error resiliency is at the expense of visual quality when a bit rate budget cannot be exceeded.

Figure 0.1 shows the frame-by-frame peak signal-to-noise ratio (PSNR) of the first 100 frames of a sequence to illustrate just how much of an impact error resilience has on the picture quality. The same sequence was coded with various error resilience strategies using the Joint Model (JM) 18.2 reference software made available by the Joint Video Team (JVT) (Joint Video Team, 2011a). The higher the PSNR, the better the visual quality is. The sequence showing the highest PSNR uses no error resilience. This makes the compression very efficient, but very vulnerable to transmission errors. The loss of a single packet results in the loss of an entire picture. Something very difficult to recover from. The second strategy involves splitting each

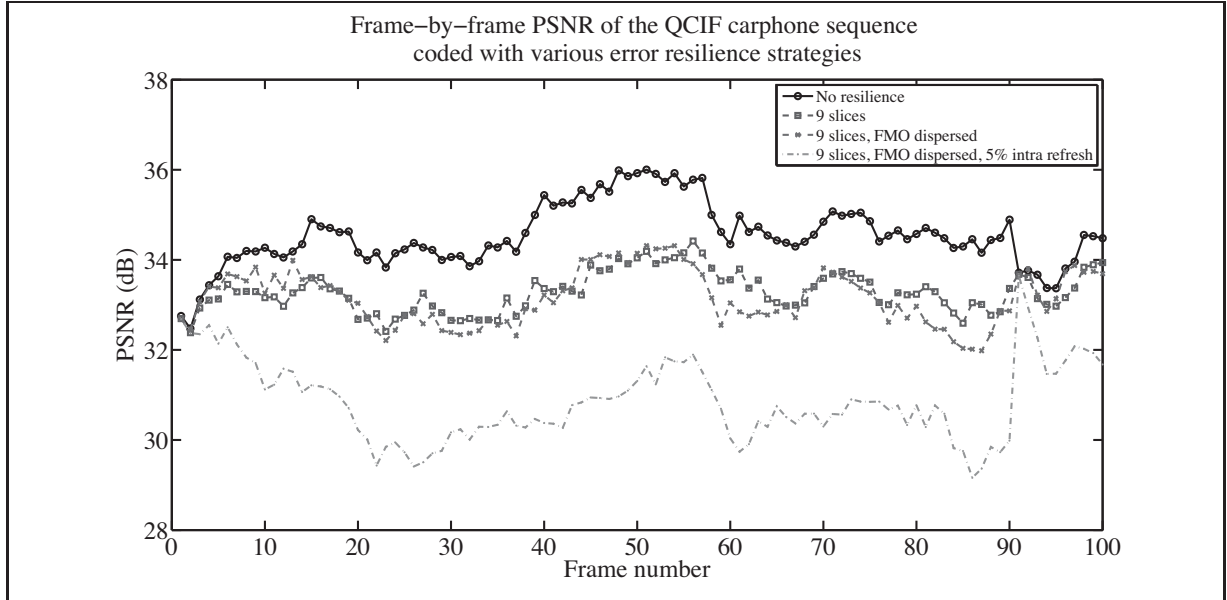


Figure 0.1 Visual quality cost of using error resilience

pictures into nine equal parts. This does reduce the visual quality, but makes the stream more robust. In this case, the loss of a packet results in the loss of one line of macroblocks in the picture. The third case also splits each picture into nine parts, but also makes sure consecutive macroblocks are in different slices. This further reduces the visual quality, but makes sure that each lost macroblock would be surrounded by its four direct neighbors. Finally, the last strategy is the costliest in terms of visual quality. It adds the use of five intra coded macroblocks in each picture (roughly 5% of each picture) to the previous strategy. These macroblocks are used to limit the drifting effect.

The lesson here is not to avoid using error resiliency. Rather, it is that error resiliency is a compromise made by the encoder so that the decoder has less trouble dealing with lost information. What's interesting is that the compromise becomes a sacrifice if no transmission errors occur.

On the other hand, transmission errors can be addressed at the decoding side with video error concealment. It is a mechanism (the last line of defense) outside the scope of video coding standards used to hide the fact transmission errors occurred. The fact it does not require additional bandwidth, and that it can be used with different standards explain its popularity. Yet, its

performance is tightly coupled to the coding parameters, as well as the sequence. The use of error resiliency can effectively increase concealment performance by providing it with additional neighboring information.

Having said that, error resilience and error concealment work under the assumption that all transmission errors are alike. That is, all transmission errors result in packet loss. Be that as it may, network congestion and physical phenomena, such as attenuation and fading, are different. The use of an error detection field in widely used communication protocols hold this to be true. Ideally, a different strategy should be used when a received packet contains transmission errors. The packet was received after all.

In fact, video communication systems belong to a class of applications that would benefit from using corrupted packets (Larzon *et al.*, 1999; Trudeau *et al.*, 2011). Accessing those packets gives the decoder the opportunity to recover at least some of the macroblocks that would have to be concealed otherwise. Moreover, small errors may even yield smaller differences than those introduced by the error concealment mechanism. In a perfect scenario, the transmission errors could even be corrected by the decoder, keeping both ends of the system synchronized.

The goal of our research was to correct transmission errors present in corrupted packets having reached their destination. We have successfully achieved this goal using a novel video error correction strategy where the video decoder estimates the most likely codewords counterbalanced with their Hamming distance from the received bits in the corrupted packet. More precisely, we have redefined the problem into a more manageable one for real-time communication systems. Then, we added support for joint source-channel decoding. Finally, we applied our findings to the Baseline profile of the H.264/AVC video coding standard.

In order to achieve our research goal, the following research objectives were defined:

- a. Propose a general mathematical framework to achieve video error correction at the bit-stream level, integrating the likelihood of alternative values (either entire slices, or single codewords), and the cost of modifying the received corrupted bits so that they match those of the alternatives' binary representation.

- b. Apply the general framework to H.264/AVC Baseline profile decoding.
- c. Compare our approach with solutions proposed in the literature using realistic corrupted sequences.

It is worth mentioning that, without minimizing the efforts required to achieve the first objective, the second objective is colossal! Firstly, the general mathematical framework had to be adapted and computationally simplified to be suitable for implementation in a real-life H.264 decoder. Secondly, an entire H.264/AVC Baseline profile decoder was designed and coded from the ground up to accomplish this project because the design of the reference software made available was ill-suited for the proposed research. This task is usually assigned to a team of software developers. This feat shows our conviction that the proposed solution is an elegant solution to a complicated problem.

This thesis is centered around our three ideas. First, we propose a maximum likelihood approach to video error correction that can be applied to any current video compression standard. Then, we add support for soft-output information so that the solution can be used in joint source-channel decoding (JSCD) fashion. Finally, we propose specific probability models for syntax elements present in H.264 Baseline profile streams.

In an effort to make this manuscript as readable as possible, it is organized into six chapters.

The first chapter presents an overview of video compression and video communications systems. It begins with the basic notions surrounding video compression and transmission. Then, a typical video communication system is compared to the one we propose to use. A reader comfortable with these notions may simply skim through this chapter.

The second chapter is dedicated to the proposed solutions found in the literature. A first section covers video error concealment strategies. The following section describes published video error correction strategies. We pay special attention to the inner workings of the published solutions, making it easier to appreciate the differences with our approach.

In the third chapter, we formulate our novel video error correction scheme. Starting with the initial definition of the problem, we derive a solution which is easier to evaluate. We take special care in describing the meaning of the equations, and their variables. The chapter concludes with the integration of soft-output information to our mathematical framework.

An application to the H.264 video standard is proposed in the fourth chapter. A short description of the H.264/AVC syntax elements are presented. Our assumptions are then stated. Finally, probability models for each syntax elements are proposed.

The fifth chapter presents the experimental results. In this section, we describe the experimental setup used to compare the results obtained with our proposed method against two different video error concealment strategies. Our observations and conclusions wrap up the chapter.

The sixth and final chapter summarizes our contributions. A recapitulation of the work achieved and its importance is clearly stated.

CHAPTER 1

VIDEO COMPRESSION AND TRANSMISSION

This chapter presents an overview of the H.264 video coding standard, and presents both a typical video communication system and a modified system that supports video error correction. The reader already familiar with the standard, may quickly skim through the last three sections.

1.1 Typical Video Communication System

A typical video communication system is shown in Figure 1.1. Each input picture passes through the video encoder, where at least one Network Abstraction Layer Unit (NALU) is created. Splitting each picture into multiple NALUs prevents the loss of entire pictures when packets are discarded due to network congestion. It is assumed that the communication protocol headers are added by the video encoder. The NALUs are then sent to the channel encoder, where they will be readied for transmission over an unreliable network.

Upon reception, the protected NALUs are handled by the channel decoder, where either hard and/or soft information is sent to the communication protocol stack. The resulting RTP packet is then processed at the video application control layer and checked from transmission errors. The units that fail the error detection test are discarded, and those that pass the test move on to the video decoder. The video decoder then reconstructs the picture with the intact information, and conceals any missing information.

1.2 Proposed Video Communication System

The typical communication system shown in the previous section needs to be modified if we are to exploit the corrupted packets. Figure 1.2 presents the modified system, where corrupted units that belong to the VCL are sent to a video error correction module.

In this system, the error detection test is still required, as intact packets can simply be decoded. However, corrupted packets are not discarded. They are sent to a maximum likelihood error

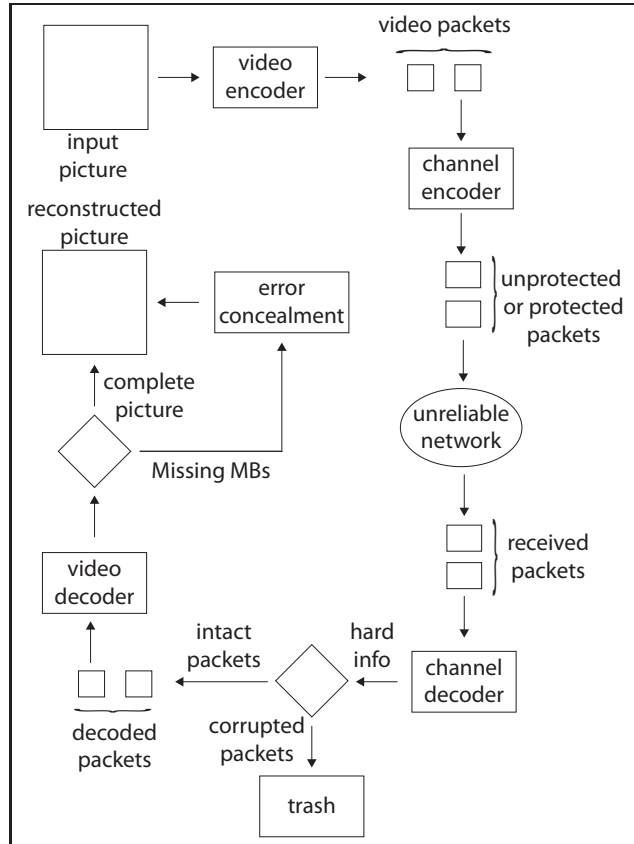


Figure 1.1 A widespread video communication system where corrupted packets are discarded

correction module where the corrupted information is transformed to create the most likely sequence of information. The output of the process is then passed to the video decoder, where normal reconstruction can take place. Because non-VCL units need to be correctly received, error correction is only applied to VCL units.

With the proposed approach, the reconstructed picture is expected to resemble more closely the coded picture than with a typical system. Furthermore, this will also keep both ends of the system better synchronized, reducing the drifting effects introduced by the loss of packets.

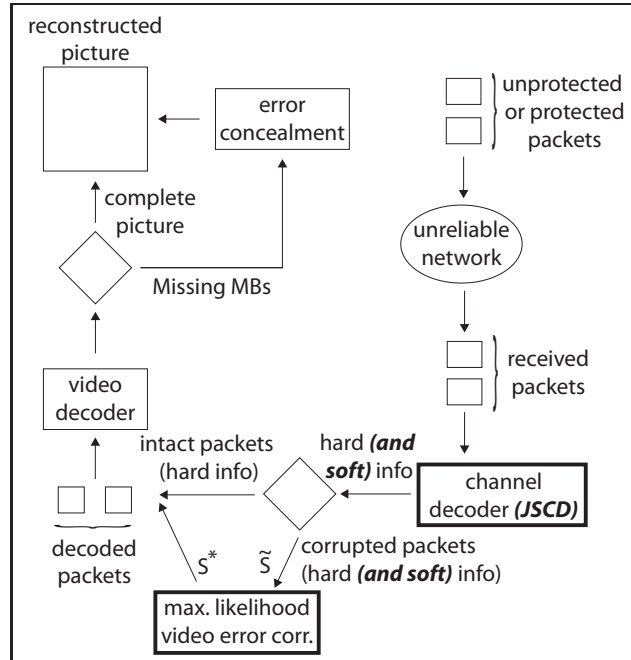


Figure 1.2 A video communication system with correction of corrupted VCL NALUs

1.3 Network Abstraction Layer Units

Once the communication protocol headers have been removed on the decoder side, NALUs are first processed at the Network Abstraction Layer (NAL). There, a one-byte header consisting of three fields (*forbidden_zero_bit*, *nal_ref_idc*, and *nal_unit_type*) is read (Figure 1.3).

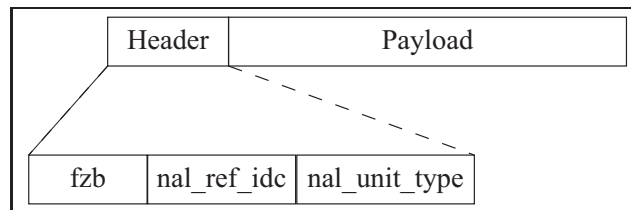


Figure 1.3 Composition of a Network Abstraction Layer Unit

The *forbidden_zero_bit* (fzb) syntax element, a 1-bit field, indicates the presence or absence of errors. The idea for this field is to allow network nodes to forward corrupted packets to their destination instead of discarding them (Wenger, 2003).

The *nal_ref_idc* syntax element, a 2-bit field, indicates the importance of the packet. It's value is used during the decoding of slices used for temporal references. Values above 0 indicate the presence of reference picture marking elements. In our work, we assume that such information is never used.

The *nal_unit_type* syntax element, a 5-bit field, indicates how to process the packet's remaining content. The supported profile influences the valid values here. Furthermore, each type is associated to either the Video Coding Layer (VCL) or the non-VCL. In our work, we assume that non-VCL units are sent using reliable means.

1.4 Video Coding Layer Units

VCL units, or slices of a coded picture, carry an unknown quantity of macroblocks. The decoding process checks for the *rbsp_stop_one_bit*, and up to seven *rbsp_alignment_zero_bit* as an indicator for the slice's end (Figure 1.4).

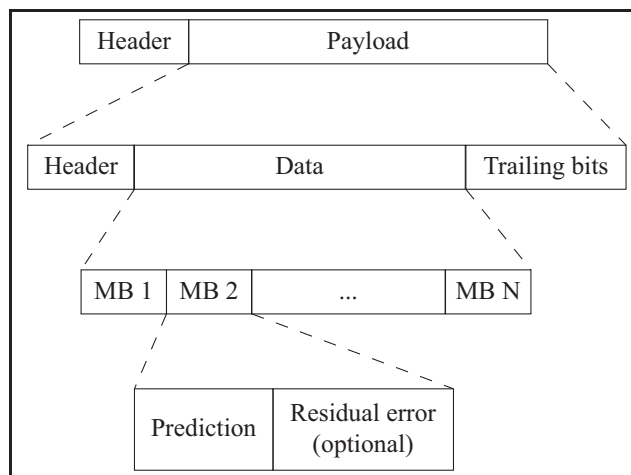


Figure 1.4 Composition of a coded slice

Each H.264 slice is independently decodable. That is, the prediction mechanisms are limited by the slice boundaries. The slice starts with a header, and is followed by the coded macroblocks. Each macroblock is described by its prediction information, and its residual information. The latter is optional, as the prediction process coupled with the quantization process may remove it entirely. When inter coding is used, any number of skipped macroblocks (macroblocks that are predicted well-enough) may be present between two coded macroblocks, or the end of the slice. This information is transmitted with the *mb_skip_run* syntax element.

It is important to mention that the H.264 standard does not use synchronization markers inside slices. Therefore, transmission errors may not be isolated to a particular location in the bitstream. The absence of synchronization markers, along with the unknown number of macroblocks carried in the slice, make it possible to create a very large number of syntactically valid slices using the number of bits received.

When the Extended profile is used, coded slices can be split into three partitions (Data Partitioning tool). The first partition carries the slice header and the prediction information such as the *mb_type*, *mvd_l0*, and *coded_block_pattern* syntax elements. The second and third partitions carry residual information (CAVLC or CABAC syntax elements). In our work, we consider that Data Partitioning is not used.

1.5 Exponential-Golomb Codes

The H.264 standard uses a combination of binary representation to efficiently compress the codewords. Shorter representations are associated to frequently used values, and longer ones, to rarely used values. Of the lot, Exponential-Golomb codes are the ones most used. These variable-length codewords (VLC) do not require predefined tables, making it easier to decode them. An example of the binary to decimal mapping is given in Table 1.1.

However, the regular structure of these codewords make them fragile to transmission errors. An erroneous bit at the start of a longer codeword inevitably creates a shorter, valid, codeword.

Table 1.1 Mapping of Exponential-Golomb codes to decimal values

Binary representation	Decimal value
1	0
010	1
011	2
00100	3
00101	4
00110	5
00111	6
0001000	7
...	...
000010000	15
...	...

CHAPTER 2

LITERATURE REVIEW

In this section, we first review video error concealment techniques. Although we have worked on error correction, both fields are complementary, as a concealment mechanism is required to deal with missing packets. Then, we take an in-depth look at published video error correction strategies. The inner workings are explained, and their weaknesses are brought to light through constructive criticism.

2.1 Video Error Concealment

Error concealment is used to hide the fact that parts of an image are missing. It exploits the spatio-temporal redundancies present in natural images. The idea is to make an educated guess of the value of each missing pixel. The function used to conceal the missing pixels is expected to perform increasingly better as more information (correctly decoded pixels, motion vectors, coding types, etc.) is made available to the decoder. This is the whole idea behind flexible macroblock ordering (FMO).

There are three families of estimation functions. Spatial error concealment (SEC) exploits the pixel values of the current frame. Temporal error concealment (TEC) takes advantage of the fact that consecutive pictures are usually similar. Hybrid error concealment (HEC) mixes the assumptions of both SEC and TEC to provide a better adapted estimation. All three families are further explained below. Implementation considerations are raised at the end of this section before video error correction is addressed.

2.1.1 Spatial Error Concealment

Sun and Kwok pioneered SEC for still images (Kwok and Sun, 1993; Sun and Kwok, 1995). They argued that boundaries had to be correctly restored to preserve an image's integrity. Wang (Wang *et al.*, 1993), on the other hand, defended the idea that the human visual system (HVS) favors smooth transitions between pixels. Both ideas are presented in Figure 2.1.

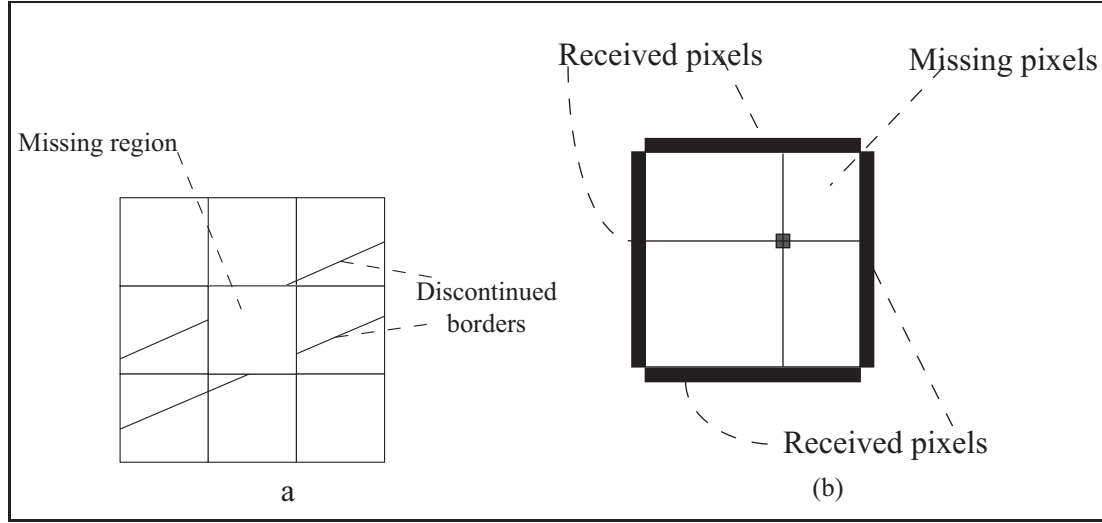


Figure 2.1 Spatial error concealment strategies: (a) Border reconstruction; (b) Multidirectional smoothing

Wang's solution is very simple to compute. A missing pixel \hat{p} is obtained using a bilinear interpolation with the closest boundary pixels p_N (above), p_S (below), p_E (to the right), and p_W (to the left). It is computed as:

$$\hat{p} = \frac{\frac{p_N}{d_N} + \frac{p_S}{d_S} + \frac{p_E}{d_E} + \frac{p_W}{d_W}}{\frac{1}{d_N} + \frac{1}{d_S} + \frac{1}{d_E} + \frac{1}{d_W}} \quad (2.1)$$

where d_i ($i = N, S, E, W$) are the distances between the pixel \hat{p} , and the boundary pixels p_i .

Sun and Kwok's solution, on the other hand, is computationally expensive. Edges are first detected in the pixel domain by applying a Sobel filter at the boundaries of the missing region. This requires that the eight connected neighbours are considered for this step. For each bordering pixel we have:

$$g_x = f(x+1, y-1) - f(x-1, y-1) + 2 \cdot f(x+1, y) - 2 \cdot f(x-1, y) + f(x+1, y+1) - f(x-1, y+1) \quad (2.2)$$

$$g_y = f(x-1, y+1) - f(x-1, y-1) + 2 \cdot f(x, y+1) - 2 \cdot f(x, y-1) + f(x+1, y+1) - f(x+1, y-1) \quad (2.3)$$

where g_x , and g_y are local gradients (each missing pixel has a pair of gradients). They are then used to determine the magnitude and angular direction of the edges with the following:

$$G = \sqrt{g_x^2 + g_y^2} \quad (2.4)$$

$$\Theta = \tan^{-1} \left(\frac{g_y}{g_x} \right) \quad (2.5)$$

The angular direction Θ is then rounded to the nearest 22.5 degree angle. Next, a projection operator (a function similar to the inverse discrete cosine transform (DCT)) is applied to the entire eight-connected region. Then, the magnitude and angular directions are used to estimate the coefficients that should have been received. The inverse projection operator is then applied to return to the pixel domain. Five to ten iterations are typically required when a good initial estimate is provided.

Since then, numerous refinements and approaches have been proposed to improve the performances of SEC. Still, when dealing with moving pictures, these differing views ignore the presence of additional information in the form of previously received images. When such information is present, it has been shown that TEC is a better alternative.

2.1.2 Temporal Error Concealment

TEC can be seen as a logical complement to motion compensation. Its goal is to find motion vectors, a goal shared by a video encoder. Unfortunately, the encoder's motion estimation strategy cannot be reproduced due to the missing pixels in the region we wish to conceal.

Two schools of thought have emerged to deal with this problem. The first looks to reproduce the encoder's behavior and uses a simplified motion estimation algorithm to find the missing motion vectors. These algorithms rely on the fact that consecutive images are typically highly correlated. Popular algorithms include the boundary matching algorithm (BMA) (Lam *et al.*, 1993), and overlapping boundary matching algorithm (OBMA) (Chen *et al.*, 1997). An example is given in Figure 2.2.

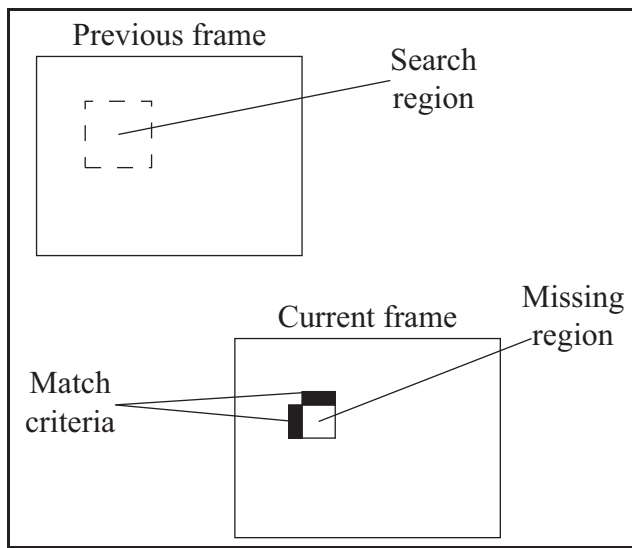


Figure 2.2 Boundary Matching Algorithm

The BMA cost function, for an $N \times N$ block, used to select the best motion vector is given by:

$$\begin{aligned}
 \text{BMA}(d_x, d_y) = & \sum_{x=x_0}^{x_0+N-1} (I(x, y_0 - 1, t) - I(x + d_x, y_0 + d_y, t - 1))^2 \\
 & + \sum_{x=x_0}^{x_0+N-1} (I(x, y_0 + N, t) - I(x + d_x, y_0 + d_y + N - 1, t - 1))^2 \\
 & + \sum_{y=y_0}^{y_0+N-1} (I(x_0 - 1, y, t) - I(x_0 + d_x, y + d_y, t - 1))^2 \\
 & + \sum_{y=y_0}^{y_0+N-1} (I(x_0 + N, y, t) - I(x_0 + d_x + N - 1, y + d_y, t - 1))^2
 \end{aligned} \tag{2.6}$$

where $I(\dots, t)$ stands for the current picture, $I(\dots, t - 1)$ is the reference frame (previous frame in this case), and the candidate motion vector is broken into its horizontal (d_x) and vertical (d_y) components. Its computation is a lighter version of the typical mean squared error used on an entire macroblock to search for the best motion vector candidate during the encoding process.

The motion vector associated to the lowest cost is declared the winner. The pixels in the reference frame the winning motion vector points to are then copied to the missing region in the current frame. The solution is expected to run in real-time, provided that the number of candidate motion vectors is kept low.

The second approach interpolates the missing motion vectors using the correctly received ones. These algorithms range from using the (0,0) motion vector (i.e. Frame Copy), copying the motion vector of the co-located macroblock in the previous picture (i.e. Motion Copy), to the use of the average or median motion vector of adjacent blocks (Wang and Zhu, 1998). The retrieved motion vectors are then used to copy the pixels from the reference frame to the current frame. This would be the equivalent of receiving motion vectors and no residual errors.

Both schools suffer from the same assumption. Consecutive pictures will not always be highly correlated. Scene changes, even if they are unfrequent, are a prime example of this. A movie trailer would be an extreme case, but a realistic one. An encoder's response to uncorrelated pictures can be to use intra coding. Alas, there is no TEC equivalent to intra coding. No matter what motion vector is retrieved, the absence of residual errors will be highlighted. For these cases, a more flexible approach would probably perform better.

2.1.3 Hybrid Error Concealment

HEC looks to address the limitations of both SEC and TEC, and combine their strengths. In certain cases, this will mean choosing between SEC and TEC. In other cases, this will mean combining both.

To our knowledge, STBMA+PDE (Chen *et al.*, 2008) is the state-of-the-art video error concealment algorithm. It starts by recovering the lost motion vectors with a modified BMA strategy named spatio-temporal boundary matching algorithm (STBMA), which combines spatial $D_{sm}^{spatial}$ and temporal $D_{sm}^{temporal}$ smoothness.

$$\text{STBMA}(d_x, d_y) = \alpha \times D_{sm}^{temporal} + (1 - \alpha) \times D_{sm}^{spatial} \quad (2.7)$$

where α is a weighting factor between 0 and 1. In their experiments, a weight of 0.5 is used so that both smoothness constraints have the same importance.

The temporal smoothness constraint is similar to the cost function of BMA. It is defined as:

$$\begin{aligned} D_{sm}^{temporal} = & \frac{1}{(w_N + w_S + w_W + w_E)M} \times \\ & [w_N \cdot \sum_{i=0}^{M-1} |I(x+i, y-1, t) - I(x+d_x+i, y+d_y-1, t-1)| + \\ & w_S \cdot \sum_{i=0}^{M-1} |I(x+i, y+M, t) - I(x+d_x+i, y+d_y+M, t-1)| + \\ & w_W \cdot \sum_{i=0}^{M-1} |I(x-1, y+i, t) - I(x+d_x-1, y+d_y+i, t-1)| + \\ & w_E \cdot \sum_{i=0}^{M-1} |I(x+M, y+i, t) - I(x+d_x+M, y+d_y+i, t-1)|] \end{aligned} \quad (2.8)$$

where w_i ($i = N, S, W, E$) are binary weights associated to the presence or absence of neighboring boundaries, M represents the length of a border (typically 16, the size of a macroblock), and $I(\dots, t)$, $I(\dots, t-1)$, d_x , and d_y hold the same meaning as in BMA.

The spatial smoothness constraint is more expensive to compute however. It is given by:

$$\begin{aligned}
D_{sm}^{spatial} &= \frac{w_N \times d_N + w_S \times d_S + w_W \times d_W + w_E \times d_E}{(w_N + w_S + w_W + w_E)M} \\
d_N &= \sum_{i=0}^{M-1} \left| \frac{\nabla(\Delta f(x+i, y, t))}{|\nabla(\Delta f(x+i, y, t))|} \cdot \frac{\nabla^\perp f(x+i, y, t)}{|\nabla^\perp f(x+i, y, t)|} \times |\nabla f(x+i, y, t)| \right| \\
d_S &= \sum_{i=0}^{M-1} \left| \frac{\nabla(\Delta f(x+i, y+M-1, t))}{|\nabla(\Delta f(x+i, y+M-1, t))|} \cdot \frac{\nabla^\perp f(x+i, y+M-1, t)}{|\nabla^\perp f(x+i, y+M-1, t)|} \times \right. \\
&\quad \left. |\nabla f(x+i, y+M-1, t)| \right| \\
d_W &= \sum_{i=0}^{M-1} \left| \frac{\nabla(\Delta f(x, y+i, t))}{|\nabla(\Delta f(x, y+i, t))|} \cdot \frac{\nabla^\perp f(x, y+i, t)}{|\nabla^\perp f(x, y+i, t)|} \times |\nabla f(x, y+i, t)| \right| \\
d_E &= \sum_{i=0}^{M-1} \left| \frac{\nabla(\Delta f(x+M-1, y+i, t))}{|\nabla(\Delta f(x+M-1, y+i, t))|} \cdot \frac{\nabla^\perp f(x+M-1, y+i, t)}{|\nabla^\perp f(x+M-1, y+i, t)|} \times \right. \\
&\quad \left. |\nabla f(x+M-1, y+i, t)| \right|
\end{aligned} \tag{2.9}$$

where $\nabla(\cdot) = [\delta(\cdot)/\delta x, \delta(\cdot)/\delta y]$ is the gradient operator, $\nabla^\perp(\cdot) = [-\delta(\cdot)/\delta y, \delta(\cdot)/\delta x]$ is the normal operator, and $|\Delta(\cdot)| = \delta^2(\cdot)/\delta^2 x + \delta^2(\cdot)/\delta^2 y$ is the Laplacian operator. The symbols w_i ($i = N, S, W, E$), M , $I(\dots, t)$, and $I(\dots, t-1)$ hold the same meanings as before.

In a typical implementation, these relevant operators can be calculated as:

$$|\nabla f(x, y)| = |\nabla^\perp f(x, y)| = \sqrt{\left[\frac{\delta f(x, y)}{\delta x} \right]^2 + \left[\frac{\delta f(x, y)}{\delta y} \right]^2} \tag{2.10}$$

$$\frac{\delta f(x, y)}{\delta x} = \frac{f(x+1, y) - f(x-1, y)}{2} \tag{2.11}$$

$$\frac{\delta f(x, y)}{\delta y} = \frac{f(x, y+1) - f(x, y-1)}{2} \tag{2.12}$$

$$\frac{\delta^2 f(x, y)}{\delta x} = f(x-1, y) - 2f(x, y) + f(x+1, y) \tag{2.13}$$

$$\frac{\delta^2 f(x, y)}{\delta y} = f(x, y-1) - 2f(x, y) + f(x, y+1) \tag{2.14}$$

Since the current block in $I(\dots, t)$ is lost, the candidate reference block in the previous picture is used to replace it. Next, the pixels pointed to by the winning motion vector are copied from the reference frame to the current frame. These values serve as the initial estimates to the partial differential equations (PDE) used to smooth the pixels through multiple iterations. This last step addresses the fact that the residual errors were also lost along with the motion vectors.

$$I^{k+1}(x, y, t) = I^k(x, y, t) + \lambda [c_N \cdot (\nabla_N I(x, y, t) - \nabla_N I(x, y, t-1)) + c_S \cdot (\nabla_S I(x, y, t) - \nabla_S I(x, y, t-1)) + c_W \cdot (\nabla_W I(x, y, t) - \nabla_W I(x, y, t-1)) + c_E \cdot (\nabla_E I(x, y, t) - \nabla_E I(x, y, t-1))] \quad (2.15)$$

where $0 < \lambda < 1$ is used to ensure numerical stability (in their work, $\lambda = 0.1$), k is the index of the iteration, and c_i ($i = N, S, W, E$) are weighting factors given by:

$$c_N = h(|\nabla_N I(x, y, t-1) - \nabla_N I(x, y, t)|) \quad (2.16)$$

$$c_S = h(|\nabla_S I(x, y, t-1) - \nabla_S I(x, y, t)|) \quad (2.17)$$

$$c_W = h(|\nabla_W I(x, y, t-1) - \nabla_W I(x, y, t)|) \quad (2.18)$$

$$c_E = h(|\nabla_E I(x, y, t-1) - \nabla_E I(x, y, t)|) \quad (2.19)$$

The above gradient operators are computed as the difference of neighboring samples, such as:

$$\nabla_N I(x, y, t) = I(x, y-1, t) - I(x, y, t) \quad (2.20)$$

$$\nabla_S I(x, y, t) = I(x, y+1, t) - I(x, y, t) \quad (2.21)$$

$$\nabla_W I(x, y, t) = I(x-1, y, t) - I(x, y, t) \quad (2.22)$$

$$\nabla_E I(x, y, t) = I(x+1, y, t) - I(x, y, t) \quad (2.23)$$

Furthermore, the function $h(\cdot)$, given below, serves to either attenuate small differences, or accentuate greater differences.

$$h(s) = \begin{cases} 1 - \exp(-s^2/\sigma_1^2), & s < T \\ \exp(-(s - T)^2/\sigma_2^2), & s \geq T \end{cases} \quad (2.24)$$

In their experiment, σ_1^2 , σ_2^2 , and T are parameters set to 0.5, 4, and 40, respectively.

Table 2.1 Average system time using different methods for a slice loss rate of 10%
(Adapted from (Chen *et al.*, 2008, p. 11))

Resolution	Time (sec)							
	BMA	STBMA	STBMA+PDE (max iterations per MB)					
			10	20	30	50	100	500
CIF	18.64	18.44	23.63	26.95	27.77	33.26	37.82	41.59
QCIF	4.23	4.30	5.59	6.52	6.66	8.25	9.63	10.78

From above, we can see that the approach is computationally expensive. Both the spatial smoothness D_{sm} and the PDE process rely on heavy use of gradients. The values in Table 2.1 are adapted from the published results in (Chen *et al.*, 2008) for common interchange format (CIF) and quarter CIF resolution sequences. The system used by the authors to obtain these results is not indicated in their experimental setup. The last six columns refer to the maximum number of iterations conducted by the refinement process. They clearly show that the refinement process introduces significant delays. Battery-operated devices or devices with less computational power may not be able to use this algorithm in real-time applications for this very reason.

2.1.4 Concealment Order

The concealment order is a fact frequently overlooked in the implementation of video error concealment algorithms. The common approach is to follow the raster scan order. For algorithms such as Frame Copy or Motion Copy, the order in which macroblocks are concealed

holds no importance, as the recovered values aren't used in the concealment process of the remaining missing regions.

For other algorithms, following the raster scan order may not be what provides the best visual results. In fact, better results are to be expected when the macroblocks with the most neighbors are concealed first (Qian *et al.*, 2009). This is especially true when some type of BMA is used to recover lost motion vectors.

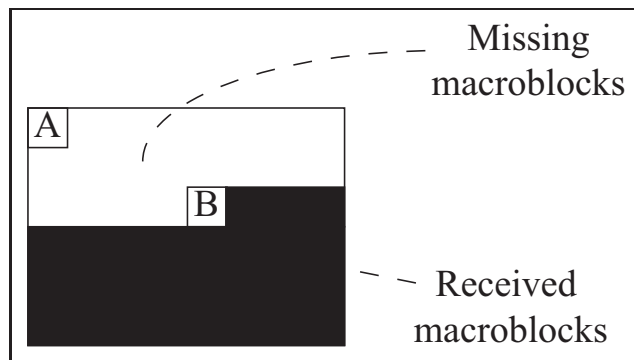


Figure 2.3 Concealment order

An example of a missing region is given in Figure 2.3. Macroblock A refers to the first macroblock that would be concealed following the raster scan order, and macroblock B, the last one concealed. In this example, macroblock A has no neighboring information, while B has two borders it can use. If any type of BMA is used, B is a better starting point than A, especially in high motion sequences.

In sorts, order determination and FMO share a common goal. They vie to provide the estimation function with as much information as possible. Hopefully, this translates to improved visual quality in the concealed regions.

2.2 Video Error Correction

Contrary to video error concealment, video error correction focuses on recovering the values that were actually sent. The objective can be seen as modifying the received bits into a likelier sequence of bits. This is done by taking advantage of the video standard's semantics.

Two distinct families of algorithms are proposed to modify the erroneous stream: list decoding and JSCD. Both families are discussed in detail below.

2.2.1 List Decoding

List decoding has been successfully applied to MPEG-2 (Aign, 1995), H.263 (Ding and Roy, 2004), MPEG-4 (Ma and Lynch, 2004) and H.264 (Levine *et al.*, 2007; Nguyen *et al.*, 2010; Farrugia and Debono, 2011).

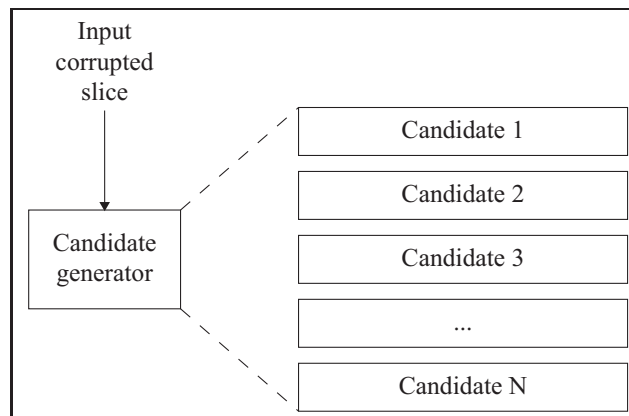


Figure 2.4 Candidate slice generator for list decoding strategies

The basic idea is to generate a list of candidate bitstreams ordered in decreasing order of likelihood (Figure 2.4). For instance, Levine (Levine *et al.*, 2007) and Nguyen (Nguyen *et al.*, 2010) sum the absolute soft-values of the flipped bits. The most likely slice candidates is the one with the lowest sum (0 if no bits were flipped). Each candidate is then sent to the video decoder, which acts as a validator. The correction process stops when the first valid bitstream is encoun-

tered. This termination criterion is challenged by (Farrugia and Debono, 2011). They argue that the most likely generated candidate, using this criterion, may not be the optimal solution. Rather, M valid candidates are kept. The winning candidate is decided using a pixel-domain alignment metric.

The main advantage of list decoding is that the slice candidate generator becomes a reusable entity. However, the approach comes with three problems. First, it is computationally complex. A bitstream containing N bits has 2^N possibilities. Even if the video packets were purposely kept small, there would still be too many options to consider. It goes without saying that an exhaustive search is out of the question if timing constraints are imposed. Second, decoupling the source semantics from the slice generator allows syntactically invalid candidates to be added to the list. Only once a candidate is processed will we know if it is valid. Third, the definition of a valid bitstream is not trivial. Multiple candidates may be syntactically valid. That is, they respect the video standard's syntax. Once reconstructed, each candidate may be significantly different due to the extensive use of VLCs.

To keep the computational complexity low, the number of candidates considered can be limited. For instance, only 300 candidates are considered in (Levine *et al.*, 2007) and (Nguyen *et al.*, 2010). Using the log-likelihood ratios (LLR) from the channel decoder, the least reliable bits are targeted to improve the chances of successfully correcting the transmission errors. Despite that, the compromise introduces the possibility that the actual solution may not be part of the candidate list. If that were the case, the winning slice would still desynchronize the system.

The second problem is solved by Nguyen *et al.* (2010). Their proposed virtual checker removes all candidate slices that follow a known erroneous path. This effectively reduces the computational complexity of the solution. On top of that, it makes iterative approaches more appealing, as less than the maximum number of candidates may be explored during each iteration.

To define what a valid slice is, the authors unanimously agree that additional constraints are required. The constraints imposed differ according to the authors and the video standards to which list decoding is applied. For example, the number of macroblocks expected to be de-

coded is used in (Nguyen *et al.*, 2010) to define a valid slice. This information is not part of the standard, as H.264 slices do not signal the number of macroblocks they carry, and the number of macroblocks carried can change from one slice to the next. Imposing such constraints guarantees that there won't be missing regions to conceal if a valid slice is found. Still, this limits the solution's portability, as it can only be used in scenarios where the decoder has detailed knowledge about the encoder's behavior.

2.2.2 Joint Source-Channel Decoding

JSCD has been applied to H.263 VLC decoding (Nguyen and Duhamel, 2004), H.264 CAVLC decoding (Weidmann *et al.*, 2004; Bergeron and Lamy-Bergot, 2004) and CABAC decoding (Sabeva *et al.*, 2006), and H.264 motion vectors (Wang and Yu, 2005). A fuzzy logic approach is also proposed for H.264 (Lee *et al.*, 2007). These implementations all use an iterative scheme (iterative JSCD, or IJSCD) to find a solution.

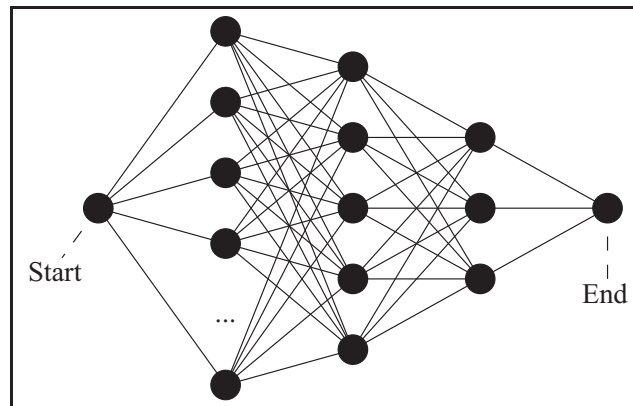


Figure 2.5 Representation of a sequence of codewords as navigation waypoints

JSCD can be viewed as a navigation algorithm, where each bit or codeword in the bitstream is a waypoint, as depicted in Figure 2.5. Combining the LLRs shared by the channel decoder with the source semantics, the objective is to find the most likely path that leads from one end of the stream to the other end. However, the sequential interpretation of the bitstream makes it

possible to reach a dead-end waypoint. An iterative approach (iterative JSCD or IJSCD) makes it possible to learn which paths to avoid.

JSCD removes the problem of proposing syntactically invalid candidates, with the exception of two cases. After visiting the last waypoint, the slice may still be invalid (too few bits). On the other hand, a valid slice may be formed before visiting the last waypoint (too many bits). IJSCD deals with both these cases.

Much like list decoding, JSCD is still left with the problem of defining the meaning of a valid slice. Again, this is caused by the extensive use of VLCs. To work around this problem, additional constraints are required to further define what constitutes a valid slice.

For example, (Bergeron and Lamy-Bergot, 2004) and (Sabeva *et al.*, 2006) work under the assumption that each slice carries an entire picture. This extra constraint enables them to only keep candidate slices that carry a predetermined number of macroblocks. In their respective experiments, they work with QCIF resolution sequences (99 macroblocks). Working with larger pictures would dramatically increase the computational complexity.

(Weidmann *et al.*, 2004) and (Wang and Yu, 2005), on the other hand, work with the H.264 Extended Profile. Enabling this profile lets the encoder split each slice into three partitions. From there, they assume that the partitions carrying the residual information are the only ones corrupted. Their assumption makes it possible for the decoder to know how many codewords are present in the corrupted partitions, since that information can be extracted from the partition carrying the headers. Regrettably, the use of the Extended profile is not widespread due to the additional complexity required to decode a partitioned stream.

Although their results show great gains when compared to video error concealment methods, the need for additional constraints make these methods difficult to deploy. A problem not encountered by video error concealment algorithms.

2.2.3 Discussion

The methods reviewed in the previous section all propose to correct transmission errors present in video streams. However, the complexity of these approaches limit their usefulness in low delay applications.

The list decoding approaches rely on a heavy process of generating a solution space. Limiting the size of the solution space to accelerate the process introduces the possibility that no candidate solution creates a valid stream, and in the end, video error concealment has to be used. Although these extreme cases have been addressed by keeping a maximum of information from the best candidate (Nguyen *et al.*, 2010), the amount of computations required to obtain a solution may be too heavy a burden for battery operated devices.

JSCD solutions on the other hand do not have to deal with the problem of generating a solution space. However, all the published methods impose additional constraints such as the number of macroblocks present in a corrupted packet, or the use of specific coding tools to demonstrate the correction capabilities. What is unclear is the importance of the constraints imposed. The fact that all the published methods use such constraint does give the impression that they are a requirement that will difficultly scale to real world applications.

In the next section, we present a lightweight video error correction solution better suited for low delay applications used in battery operated devices.

CHAPTER 3

MAXIMUM LIKELIHOOD VIDEO ERROR CORRECTION

In this chapter we propose a general mathematical solution for video error concealment. The first section of the chapter covers the problem at the slice level. The steps leading to our solution are discussed in detail. The second part of the chapter describes our novel maximum likelihood framework. Starting with the results obtained at the slice level, the problem is posed in a different manner that allows us to better exploit the source semantics.

For the remainder of the discussion, we assume that it is known *a priori* that the received slice is corrupted. The wide use of error detection mechanisms such as UDP's checksum (Larzon *et al.*, 1999) makes our assumption realistic.

3.1 Slice-Level Error Correction

Video error correction can be expressed as an optimization problem. Given that we know the received packet is corrupted, the objective is to modify the received information in such a way that we obtain the best balance between the cost of flipping bits (the more bits we flip, the less likely it becomes) and the credibility of the resulting content (based on the context, some syntax elements are more likely than others or impossible to receive). Applied to the H.264 video standard (International Telecommunications Union, 2007), the optimization problem can be described as selecting the most likely candidate slice. Note that what follows applies to any standard that uses a sequence of codewords taken from a defined syntax. JPEG, MPEG-2, H.263, MPEG-4, and HEVC all fall into this category.

In this discussion, we will assume that non-VCL NAL units (i.e. SPSs, PPSs, etc.) are sent using reliable means, and that fragmentation units (Wenger *et al.*, 2005) are not present. Let us first pose the problem as:

$$S^* = \arg \max_{\hat{S} \in H} \left\{ P(\mathcal{T} = \hat{S} | \mathcal{R} = \tilde{S}) \right\} \quad (3.1)$$

where \mathcal{R} is a discrete random vector of bits representing the received NALU, \tilde{S} is a realization of \mathcal{R} (the actually received NALU), \mathcal{T} is a discrete random vector of bits representing the transmitted NALUs, \hat{S} is one possible realization of \mathcal{T} , H is the discrete random vector's support containing the set of all possible realizations of \mathcal{T} (i.e., all possible transmitted NALUs), S^* is the likeliest realization of \mathcal{T} given the received NALU \tilde{S} , and $P(\mathcal{T} = \hat{S} | \mathcal{R} = \tilde{S})$ is the likelihood function (probability) that \hat{S} was sent, given that \tilde{S} was received.

In this context, it seems natural that both discrete random vectors \mathcal{R} and \mathcal{T} , and their realizations \tilde{S} and \hat{S} , contain the same number of bits since the number of bits is known, although they are corrupted. The use of discrete random vectors conveniently integrates this consideration, as any realization has the same finite set of dimensions, defined by the number of bits present in the received NALU \tilde{S} . As it happens, this consideration is consistent with the list decoding and JSCD approaches previously published. In fact, H , the discrete random vector's support, contains 2^N realizations, the exact size of the solution space (here N is the number of bits in the received NALU/the number of dimensions of the discrete random vectors and their realizations) explored by list decoding approaches.

The computational complexity required to solve (3.1) can be reduced if we consider that H only holds valid NALUs. However, generating such a solution space is a very difficult task to tackle (Weidmann *et al.*, 2004), one that requires knowledge held by the source decoder, as a valid NALU holds meaning at the application level.

Intuitively, we are aiming to find the NALU \hat{S} , composed of the likeliest codewords that holds the closest resemblance to the received NALU \tilde{S} . In other words, we are looking to make as few alterations as possible to the received bits, while improving the likeliness of the codewords. As such, the conditional distribution $P(\mathcal{T} = \hat{S} | \mathcal{R} = \tilde{S})$ in (3.1) can be interpreted as a compromise between the likeliness of the codewords present in \hat{S} , and its Hamming distance with \tilde{S} .

It is more convenient to rewrite (3.1) using Bayes' theorem. Its expanded form better illustrates our objective:

$$S^* = \arg \max_{\hat{S} \in H} \left\{ \frac{P(\mathcal{R} = \tilde{S} | \mathcal{T} = \hat{S}) \times P(\mathcal{T} = \hat{S})}{P(\mathcal{R} = \tilde{S})} \right\} \quad (3.2)$$

where $P(\mathcal{R} = \tilde{S} | \mathcal{T} = \hat{S})$ expresses the likelihood that the realization \tilde{S} was received given that the realization \hat{S} was sent, $P(\mathcal{T} = \hat{S})$ represents the probability that the realization \hat{S} was sent, and $P(\mathcal{R} = \tilde{S})$, the probability that the realization \tilde{S} was received. The latter probability is independent of \tilde{S} , and therefore, can be ignored. We can rewrite (3.2) as

$$S^* = \arg \max_{\hat{S} \in H} \left\{ P(\mathcal{R} = \tilde{S} | \mathcal{T} = \hat{S}) \times P(\mathcal{T} = \hat{S}) \right\} \quad (3.3)$$

As mentioned previously, our objective is to minimize the alterations to the received NALU \tilde{S} , while maximizing the effect they have in terms of likeliness of the codewords. In its current form, (3.3) can be solved using a JSCD approach. The likelihood $P(\mathcal{R} = \tilde{S} | \mathcal{T} = \hat{S})$ can be evaluated using the soft-output information provided by the channel decoder. The probability $P(\mathcal{T} = \hat{S})$ can be evaluated at the application layer by exploiting source semantics. In what follows, we first tackle the computation of the likelihood $P(\mathcal{R} = \tilde{S} | \mathcal{T} = \hat{S})$. Then, we show how to compute the probability $P(\mathcal{T} = \hat{S})$.

3.1.1 Channel Decoding

For the channel decoder, a NALU is nothing more than a sequence of bits. For convenience, let \mathcal{R}_n and \mathcal{T}_n be n -th bits of discrete random vectors \mathcal{R} and \mathcal{T} respectively, and let \tilde{S}_n and \hat{S}_n be n -th bits of the realizations \tilde{S} and \hat{S} respectively.

Thus, the Hamming distance can be used to evaluate $P(\mathcal{R} = \tilde{S} | \mathcal{T} = \hat{S})$, as we are only dealing with substitutions (erroneous bits). The distance represents the number of differing components between the realizations \hat{S} and \tilde{S} . More importantly, it can be interpreted as the number of successes in N independent Bernoulli trials with independent success rates.

$$P(\mathcal{R}=\tilde{S}|\mathcal{T}=\hat{S}) = \prod_{n=1}^N P(\mathcal{R}_n=\tilde{S}_n|\mathcal{T}_n=\hat{S}_n) \quad (3.4)$$

The conditional distribution $P(\mathcal{R}_n=\tilde{S}_n|\mathcal{T}_n=\hat{S}_n)$ in (3.4) represents the cost associated with either keeping (bits \tilde{S}_n and \hat{S}_n match) or flipping (bits \tilde{S}_n and \hat{S}_n differ) the n -th received bit. This cost combines both the possibility of a transmission error and the individual flipping cost of the n -th bit. The latter is more apparent if we rewrite (3.4) using Kolmogorov's definition of conditional events.

$$P(\mathcal{R}=\tilde{S}|\mathcal{T}=\hat{S}) = \prod_{n=1}^N \frac{P(\mathcal{R}_n=\tilde{S}_n \cap \mathcal{T}_n=\hat{S}_n)}{P(\mathcal{T}_n=\hat{S}_n)} \quad (3.5)$$

where the numerator represents the probability of transmitting \hat{S}_n , and receiving \tilde{S}_n , and the denominator represents the probability that \hat{S}_n was transmitted.

There are four outcomes for the numerator in (3.5). Two of them indicate a corrupted bit, and the two others, an intact bit. Assuming 0s and 1s are equally likely to be affected by transmission errors, let us assume that:

$$P(\mathcal{R}_n=\tilde{S}_n \cap \mathcal{T}_n=\hat{S}_n) = \begin{cases} \frac{\rho}{2} & , \hat{S}_n \neq \tilde{S}_n \\ \frac{1-\rho}{2} & , \hat{S}_n = \tilde{S}_n \end{cases} \quad (3.6)$$

where ρ is the estimated bit error rate (BER). Note that the assumption does not imply anything about the propability that a 0 or a 1 was transmitted. It simply states that transmission errors do not target 0s over 1s, or vice versa.

To evaluate the denominator in (3.5), the source decoder can use the LLRs provided by the channel decoder. LLRs represent the natural logarithm of the ratio of the probability that a 1 was sent over the probability a 0 was sent, given a random source of noise.

$$LLR_n = \ln \left(\frac{P(\mathcal{T}_n = 1|y)}{P(\mathcal{T}_n = 0|y)} \right) \quad (3.7)$$

where y is a random noise signal which represents channel noise (i.e., the source of bit errors), and LLR_n is the log-likelihood ratio associated with \hat{S}_n . Note that if the log-likelihood ratios are not available at the source layer, the decoder can assume that they are all 0. In fact, the decoder can assume any value, as long as all the received bits share the same LLR. This is the equivalent of telling the decoder that we do not have additional information on the received bits. For simplicity, y is assumed to be additive Gaussian noise in our simulations. From the computed LLR_n , the probability that \hat{S}_n was transmitted is:

$$P(\mathcal{T}_n = \hat{S}_n | y) = \begin{cases} \frac{1}{\exp(LLR_n) + 1} & , \hat{S}_n = 0 \\ \frac{\exp(LLR_n)}{\exp(LLR_n) + 1} & , \hat{S}_n = 1 \end{cases} \quad (3.8)$$

Now, we are interested in the probability $P(\mathcal{T}_n = \hat{S}_n)$, rather than in (3.8). Fortunately, the random noise present in (3.7) and (3.8) is a constraint in our solution. Our goal is to find the likeliest NALU, not to find the likeliest random noise that explains the received corrupted NALU. Therefore, let us assume that:

$$P(\mathcal{T}_n = \hat{S}_n) \approx P(\mathcal{T}_n = \hat{S}_n | y) \quad (3.9)$$

Integrating (3.6) and (3.8) into (3.5), we now have the means to evaluate the conversion cost associated with a candidate slice.

3.1.2 Source Decoding

At the application layer, a NALU is more meaningful if it is seen as a realization of a discrete random vector of codewords (i.e., $\hat{S} = [\hat{c}_1 \quad \hat{c}_2 \quad \dots \quad \hat{c}_M]$). We can partition \mathcal{T} and \mathcal{R} into

codewords. Let $\mathcal{T}_{c,i}$ and $\mathcal{R}_{c,i}$ be the i -th codewords of \mathcal{T} and \mathcal{R} , respectively, and \hat{c}_i be the i -th codeword of \hat{S} .

Inherently, with these definitions, $P(\mathcal{T} = \hat{S})$ represents the joint probability mass function of each codeword in the vector. This natural representation allows each realization \hat{S} to hold a differing number of dimensions, as variable-length codewords (VLC) are widely used at the application layer. However, this is not actually a problem since we are not considering other realizations. Thus, the realizations do not have to share a common number of dimensions at this stage.

$$P(\mathcal{T} = \hat{S}) = P(\cap_{i=1}^{L_C(\hat{S})} (\mathcal{T}_{c,i} = \hat{c}_i)) \quad (3.10)$$

where $L_C(\cdot)$ is a function returning the number of codewords in a NALU.

Using the Chain rule, (3.10) can be computed with greater ease. Additionally, the sequential dependencies between the codewords are better expressed in this way.

$$P(\mathcal{T} = \hat{S}) = \prod_{i=1}^{L_C(\hat{S})} P(\mathcal{T}_{c,i} = \hat{c}_i | \Psi_i \cap_{k=1}^{i-1} (\mathcal{T}_{c,k} = \hat{c}_k)) \quad (3.11)$$

where Ψ_i is the set of decoded codewords in past slices, as well as the decoding variables (decoder state variables), from past slices, and up to the i -th codeword in the current slice, such as the current MB's address. For the sake of compactness, let $\Omega_{c,i} = \Psi_i \cap_{k=1}^{i-1} (\mathcal{T}_{c,k} = \hat{c}_k)$. $\Omega_{c,i}$ can be interpreted as the set of variables which hold the context necessary to decode the i -th syntax element. Then, (3.11) becomes:

$$P(\mathcal{T} = \hat{S}) = \prod_{i=1}^{L_C(\hat{S})} P(\mathcal{T}_{c,i} = \hat{c}_i | \Omega_{c,i}) \quad (3.12)$$

Integrating (3.5) and (3.12) into (3.3), we now have:

$$S^* = \arg \max_{\hat{S} \in H} \left\{ \frac{\prod_{n=1}^N \frac{P(\mathcal{R}_n = \tilde{S}_n \cap \mathcal{T}_n = \hat{S}_n)}{P(\mathcal{T}_n = \hat{S}_n)}}{\prod_{i=1}^{L_C(\hat{S})} P(\mathcal{T}_{c,i} = \hat{c}_i | \Omega_{c,i})} \right\} \quad (3.13)$$

We can further refine the notations by acknowledging that each codeword is a vector of bits and write $\hat{c}_i = [\hat{c}_{i,1} \ \hat{c}_{i,2} \ \dots \ \hat{c}_{i,L_B(\hat{c}_i)}]$, where $L_B(\cdot)$ is a function returning dimension of a codeword, and $\hat{c}_{i,n}$ is the n -th vector component (i.e., n -th bit) of the realization \hat{c}_i . Let $\mathcal{T}_{c,i,n}$ be the n -th bit of the i -th codeword of \mathcal{T} .

Having split our original discrete random vector into smaller discrete random vectors, it would seem consistent to rewrite $P(\mathcal{R} = \tilde{S} | \mathcal{T} = \hat{S})$ in (3.3) as a product of distances at the codeword level to take advantage of this natural representation.

$$S^* = \arg \max_{\hat{S} \in H} \left\{ \prod_{i=1}^{L_C(\hat{S})} \frac{P(\mathcal{R} = \tilde{S} | \mathcal{T}_{c,i} = \hat{c}_i)}{P(\mathcal{T}_{c,i} = \hat{c}_i | \Omega_{c,i})} \right\} \quad (3.14)$$

where we have:

$$P(\mathcal{R} = \tilde{S} | \mathcal{T}_{c,i} = \hat{c}_i) = \prod_{n=1}^{L_B(\hat{c}_i)} \frac{P(\mathcal{R}_{\Delta(i)+n} = \tilde{S}_{\Delta(i)+n} \cap \mathcal{T}_{c,i,n} = \hat{c}_{i,n})}{P(\mathcal{T}_{c,i,n} = \hat{c}_{i,n})} \quad (3.15)$$

where $\Delta(i) = \sum_{k=1}^{i-1} L_B(\hat{c}_k)$. The sum expresses the position of the last bit belonging to the realization \hat{c}_{i-1} . When dealing with the first realization \hat{c}_1 , $\Delta(1) = 0$.

With the current form of (3.14), we still have to evaluate every candidate slice in the solution space H , a colossal task which is far too complex in practice.

The limitations of the published *list decoding* approaches are still present here, as flipping a bit at the channel layer, creating a different (yet valid) realization in H , does not guarantee that the realization \hat{S} will be valid at the application level.

3.2 Syntax-Element-Level Error Correction

We propose to solve the problem at the syntax-element-level. This is a more intuitive approach, which would also aid the decoding process. Codewords are sequentially decoded, and the valid realizations \hat{c}_i at each step of the decoding process are known (making error detection possible). Refining the problem at the syntax-element-level solves two important problems. Firstly, we no longer need to generate H , only the proper set of valid syntax elements at each stage of the decoding process. Secondly, we no longer need to deal with realizations \hat{S} that are valid at the channel level, but invalid at the application layer.

Fortunately, (3.14) can be modified to meet our goal. At each step of the decoding process, we want to select the optimal codeword as a function of previously decoded codewords:

$$c_i^* = \arg \max_{\hat{c}_i \in C_i} \left\{ P(\mathcal{R} = \tilde{S} | \mathcal{T}_{c,i} = \hat{c}_i) \times P(\mathcal{T}_{c,i} = \hat{c}_i | \Omega_{c,i}) \right\} \quad (3.16)$$

where c_i^* is the likeliest realization in the solution space C_i (the set of valid codewords for i -th decoded syntax-element). We start decoding with $i = 1$ and increment i as we decode the next codeword. Note that the likeliest sequence of codewords (3.14) (optimal solution), and the sequence of likeliest codewords (3.16) (greedy approach) are not necessarily the same. Therefore, it is expected that this syntax-element-level approach will find a different solution. Moreover, this approach accepts the fact that not all of the corrupted NALU's content may be recovered, as the decisions taken may lead to a step where the solution space C_i is empty. If such a case were to occur, the missing MBs would have to be concealed.

A slight modification to (3.16) is required to address VLCs. The initial optimization problem deals with discrete random vectors of equal lengths. Thus, $P(\mathcal{R} = \tilde{S} | \mathcal{T} = \hat{S})$ always considers the same number of independent Bernoulli trials. This is no longer the case, as C_i does not represent a discrete random vector's support. The realizations it contains do not have to share a common dimension.

As a result, a weighting factor needs to be added to even out the number of independent trials considered for each candidate. Without this factor, the maximization process would favor shorter realizations because they have smaller Hamming distances. This in fact penalizes longer codewords, codewords that are already expected to be less frequently used than shorter ones. (Weidmann *et al.*, 2004) uses the so-called random tail assumption to align sequences of different lengths. Additional information about this assumption is given in Annex II. We will do the same here (looking at (3.15)). We modify (3.16) to obtain the following optimization problem:

$$c_i^* = \arg \max_{\hat{c}_i \in C_i} \left\{ \begin{array}{l} P(\mathcal{R} = \tilde{S} | \mathcal{T}_{c,i} = \hat{c}_i) \times \\ \frac{1}{2}^{\beta_i - L_B(\hat{c}_i)} \times P(\mathcal{T}_{c,i} = \hat{c}_i | \Omega_{c,i}) \end{array} \right\} \quad (3.17)$$

where β_i is the length of longest codeword in C_i .

With this optimization problem, we can now select the likeliest codeword in C_i at each step in the decoding process, starting with c_1^* , and moving towards c_n^* . The likeliest codewords selected will affect the video decoder the same way a decoded codeword from an intact NALU would have, as our proposed solution does not affect the rest of the decoding process.

Exploiting the source semantics, a solution can now be tailored for each syntax element. It is also worth mentioning that the approach is independent of the video standard. We work with NALUs, introduced in the H.264 standard, but any term representing a sequence of codewords could have been used.

CHAPTER 4

H.264 BASELINE PROFILE VIDEO ERROR CORRECTION

The mathematical framework derived in the previous section explains how the likeliest code-word will be selected. The task at hand is to identify which information to use to evaluate $P(\mathcal{T}_{c,i} = \hat{c}_i | \Omega_{c,i})$ in (3.17) for each syntax element in the bitstream. In this section, we focus on H.264 Baseline Profile syntax elements, but the approach would also work for other profiles, previous standards (H.263, MPEG-2, etc.), as well as the new HEVC standard.

The models proposed in this section were all intuitively derived. We specifically favored simple models with low computational complexities. The observations required to evaluate the model parameters also had to be easy to gather. More exact models, obtained by studying the precise statistical behavior of the different syntax elements could be proposed to achieve even better results.

In this discussion, we assume that non-VCL NAL units (i.e., Sequence Parameter Sets, Picture Parameter Sets, etc.) are sent using reliable means, and that fragmentation units (Wenger *et al.*, 2005) are not present. We also assume that the corrupted slices were coded using the Baseline Profile, that the four constraint flags in the active Sequence Parameter Set are set to 0, and that the QP is constant for the entire frame. These constraints are imposed as a way to limit the scope of the thesis, not our method.

The first and second sections of the chapter cover the syntax elements found in the slice's header and body respectively. The third section of the chapter proposes an early termination strategy, since not all the syntax elements have been modeled.

4.1 Slice Header

We propose models for the first five fields of the slice header. We assume that the remaining fields use constant values throughout the sequence, simplifying the correction process. The fields are presented following their order in a coded slice.

4.1.1 *first_mb_in_slice*

The *first_mb_in_slice* syntax element represents the raster scan index of the first coded MB carried in the NALU. Under our current assumptions, the number of MBs carried in a NALU can be expressed as the difference between the values used in consecutive NALUs associated with the same picture. Since we know that transmission errors can affect the number of MBs extracted from a corrupted NALU, let us assume that the number of MBs carried in a NALU follows a Normal distribution.

$$P(FMIS = \hat{c}_i | \Omega_{c,i}) = \frac{1}{\sigma\sqrt{2\pi}} \exp\left(-\frac{(\hat{c}_i - (fmis_{prev} + \mu))^2}{2\sigma^2}\right) \quad (4.1)$$

where *FMIS* represents a discrete random variable representing the starting address of a NALU, *fmis_{prev}* is the previous observed value of *first_mb_in_slice*, μ is the observed average number of MBs carried in a NALU, and σ , the observed standard deviation. Both μ and σ should consider the coding type of the previously received NALU, as intra- and inter-coding are not expected to fit the same number of MBs in one NALU. Both μ and σ are obtained by studying the differences between the *first_mb_in_slice* values in consecutive slices.

It is worth mentioning that the last NALU associated with a picture should not be used to evaluate μ and σ . Limiting the maximum transmission unit (MTU) size of a packet introduces the possibility that the last NALU of a picture contains significantly fewer MBs than the other ones since MBs associated with different pictures cannot be transported together.

The codebook C_i should only contain the remaining undecoded addresses in the picture, starting with the last received value of *first_mb_in_slice* plus 1. This follows the logic that each MB is coded once. However, by limiting C_i , the probabilities will not sum to 1. Imposing the address 0 in C_i , the only valid address for the next picture, solves this problem elegantly. Its presence acknowledges the possibility that the next NALU starts a new picture. $P(FMIS = 0 | \Omega_{c,i})$ represents the complement of the summed probabilities. As NALUs are decoded, the probabil-

ity that the next NALU starts a new picture increases, which is exactly what happens with the above definition.

A special case exists if the previously received NALU was intact. Assuming that all NALUs are received in the correct order, the address following the last one used is expected. That value can be used as if a constant was expected instead of using (4.1).

4.1.2 *slice_type*

The *slice_type* syntax element indicates the coding type employed in the current NALU. The Baseline Profile restricts the outcomes to inter-coding (0 or 5), and intra-coding (2 and 7). The value used here has an influence on the allowed coding types the MBs can use. Additionally, values above 4, corresponding to the higher range, are used to indicate that all the slices associated with the current picture share the same coding type. Thus, the value of the *first_mb_in_slice* must be considered, since the effect of using a *slice_type* value above 4 is limited by the picture boundaries. We assume that the encoder does not mix values from the lower and higher ranges within a picture, because if it does, the only NALU using information in the higher range could be lost during transmission.

We can model the *slice_type* syntax as two pairwise independent Bernoulli trials. The first experiment checks for the range used, where a value in the range above 4 indicates success. The second experiment checks for the coding type, where the use of intra-coding indicates success. This can be expressed as:

$$P(ST = \hat{c}_i | \Omega_{c,i}) = \begin{cases} \alpha[\delta(\hat{c}_i - 5)(1 - \beta) + \delta(\hat{c}_i - 7)\beta] + \\ (1 - \alpha)[\delta(\hat{c}_i)(1 - \beta) + \delta(\hat{c}_i - 2)\beta] & , f_{mis} = 0 \\ \delta(\hat{c}_i)(1 - \beta) + \delta(\hat{c}_i - 2)\beta & , f_{mis} \neq 0, st_{prev} \leq 4 \\ \delta(\hat{c}_i - st_{prev}) & , f_{mis} \neq 0, st_{prev} > 4 \end{cases} \quad (4.2)$$

where ST is a discrete random variable representing the coding scheme used in a NALU, f_{mis} is the latest decoded value of $first_mb_in_slice$, st_{Prev} is the $slice_type$ value decoded in the previous NALU, $\delta(\cdot)$ is the discrete Dirac function, α represents the probability that a $slice_type$ value above 4 is used, and β represents the probability that the $slice_type$ uses intra-coding. Both probabilities are estimated from the previously reconstructed $slice_type$ values.

4.1.3 *pic_parameter_set_id*

The *pic_parameter_set_id* syntax element indicates which PPS is to be used during the decoding process of the current NALU. We assume that the coded streams always refer to the same PPS, and thus the value is a constant.

4.1.4 *frame_num* and *pic_order_cnt_lsb*

The *frame_num* and *pic_order_cnt_lsb* syntax elements are used to identify pictures. They both represent the least significant bits of monotonically increasing sequences, where the use of a new value is triggered when the value of $first_mb_in_slice$ equals 0 (the start of a new picture). Subclause 7.4.3 (International Telecommunications Union, 2007) specifically indicates that all NALUs belonging to the same picture shall use the same values of *frame_num* and *pic_order_cnt_lsb*. The only difference is that *pic_order_cnt_lsb* typically uses an increment of 2 instead of 1. Assuming that slices may be damaged, but never lost, this behavior indicates that we only need to consider two outcomes: either the same values present in the previous NALU are used, or the least significant bits of the next value in the monotonically increasing sequence are used. The syntax elements cannot be modeled as a single field because they are not necessarily contiguous.

$$P(FN = \hat{c}_i | \Omega_{c,i}) = \begin{cases} \delta(\hat{c}_i - fn_{Prev}) & , f_{mis} \neq 0 \\ \delta(\hat{c}_i - lsb(fn_{Prev} + 1)) & , f_{mis} = 0 \end{cases} \quad (4.3)$$

where FN is a discrete random variable representing the $frame_num$ value used by a NALU, fn_{prev} is the $frame_num$ value decoded in the previous NALU, and $lsb(\cdot)$ is the modulo operator using the SPS value $log2_max_frame_num_minus4$.

$$P(POCL=\hat{c}_i|\Omega_{c,i}) = \begin{cases} \delta(\hat{c}_i - pocl_{prev}) & , fmis \neq 0 \\ \delta(\hat{c}_i - lsb(pocl_{prev} + 2)) & , fmis = 0 \end{cases} \quad (4.4)$$

where $POCL$ is a discrete random variable representing the $pic_order_cnt_lsb$ value used by a NALU, $pocl_{prev}$ is the $pic_order_cnt_lsb$ value decoded in the previous NALU. In this case, the modulo operator uses the SPS value $log2_max_pic_order_cnt_lsb_minus4$.

4.2 Slice Data

The syntax elements used to communicate the prediction mechanisms used have all been modeled, with the exception of the mb_qp_delta syntax element. Our assumption that the QP is fixed for the entire sequence makes this value constant. However, we do not take advantage of this assumption to use the syntax element as a synchronization marker.

4.2.1 mb_type

There are 26 intra-, and six inter-coding schemes available. 31 of those 32 schemes are signaled with the mb_type syntax element. The P_Skip coding scheme is inferred by the use of the mb_skip_run syntax element, when it is present.

Inter-coding schemes can only be used in NALUs whose $slice_type$ syntax element uses inter-coding. Intra-coding schemes can be used in both intra and inter NALUs. Moreover, the MBs's location in the current NALU has an influence on the available intra 16x16 coding schemes. These coding schemes use predetermined luminance prediction modes (see Table 7 - 11 in Rec. H.264 (International Telecommunications Union, 2007)) that may be unavailable given the MB's location and the current slice's boundaries.

In addition to the addresses of the NALU *slice_type* and of the MB, we can also consider the coding schemes used by the neighboring spatio-temporal MBs. To keep the model simple, we consider the coding scheme used by the colocated MB in the previous frame.

$$P(CS = \hat{c}_i | \Omega_{c,i}) = P(CS = \hat{c}_i | st) \times P(CS = \hat{c}_i | addr) \times P(CS = \hat{c}_i | cs_{Co}) \quad (4.5)$$

where CS is a discrete random variable representing the coding scheme used, st is the latest decoded value of *slice_type*, st_{prev} has the same meaning as in (4.2), $addr$ indicates the address of the current MB, and cs_{Co} indicates the coding scheme used by the colocated MB in the previous frame.

Note that the coding scheme is used rather than the *mb_type* syntax element. This is because the value of *mb_type* for the colocated MB may not be available if *mb_skip_run* was used. This general definition will still lead to the selection of a valid *mb_type* value, as the codebook C_i will be populated as such.

4.2.2 *mb_skip_run*

The *mb_skip_run* syntax element is only present when the current slice uses inter prediction. It indicates the number of skipped MBs before the next coded one, or the end of the slice/frame. Since a MB is either coded or skipped, let us use these as the two outcomes of a Bernoulli trial. Then, the syntax element can be modeled as a Geometric distribution, where a success is defined as a coded MB, or the end of the slice/frame. As was the case with the *mb_type* syntax element, the probability of success is expected to vary with the MB's location in the frame. This is expressed through independent success rates.

$$\begin{aligned}
P(\text{mb_skip_run} = \hat{c}_i | \Omega_{c,i}) = \\
\prod_{n=0}^{\hat{c}_i-1} P(CS = \text{P_Skip} | \Omega_{c,i} \cap \text{Addr} = \text{addr} + n) \times \\
(1 - P(CS = \text{P_Skip} | \Omega_{c,i} \cap \text{Addr} = \text{addr} + \hat{c}_i))
\end{aligned} \tag{4.6}$$

where each term in the product, as well as the final term (the one outside the product) is evaluated using (4.5). However, the address at which the conditional probability will be evaluated is specified by the discrete random variable Addr . Here, \hat{c}_i is the number of skipped MBs before the next coded MB, or the end of the slice. The codebook C_i should be populated only with the values leading to the last valid address. This also requires that the probability of using any coding scheme at an address outside the frame equals 0. When the last entry in C_i is evaluated, the final term in (4.6) refers to the MB following the last valid one. That probability would thus be 1, keeping only the product of the probability that all the remaining MBs are skipped.

4.2.3 Intra4x4PredMode

Intra-coded MBs, with the exception of I_PCM MBs, use spatial prediction on both luminance and chrominance values to remove redundancies. While the luma prediction modes are built into the intra 16x16 coding schemes, intra 4x4 MBs use one of nine prediction modes for each of the 4x4 blocks it contains.

The mode selection is signaled using two syntax elements: *prev_intra4x4_pred_mode_flag* and *rem_intra4x4_pred_mode*. The former indicates whether the mode the decoder derived matches or differs from the one used. The latter, present when *prev_intra4x4_pred_mode_flag* equals 0, indicates which of the eight remaining modes to use.

The MB's current location plays the same role here as it did with the *mb_type* syntax element, limiting the available modes when the required neighboring information is unavailable.

Modeling both fixed-length syntax elements as a VLC makes the correction process more accurate. First, it integrates *rem_intra4x4_pred_mode*'s conditional presence into the correction process. Second, it takes advantage of the derivation process built into the decoder (International Telecommunications Union, 2007, Section 8.3.1.1). This results in a richer syntax element. Furthermore, the probability distribution is better tailored to our needs. We will use Intra4x4PredMode (*IPM*), the standard variable used to explain the derivation process, to represent the joint distribution of the syntax elements.

$$P(IPM = \hat{c}_i | \Omega_{c,i}) = P(IPM = \hat{c}_i | addr) \times P(IPM = \hat{c}_i | ipm_W) \times P(IPM = \hat{c}_i | ipm_N) \quad (4.7)$$

where *ipm_W* and *ipm_N* are the left and above Intra4x4PredMode values used in the derivation process for the current 4x4 block. The conditional distributions used in (4.7) are in fact pmfs built from the observed prediction modes in the previously decoded intact slices; one tracking the correlation with the MB's left neighbor, and the other tracking the correlation with the MB's top neighbor.

4.2.4 *intra_chroma_pred_mode*

The *intra_chroma_pred_mode* syntax element indicates which of the four prediction modes is to be used. The MB's location also affects the available types.

The syntax element can be corrected using the product of two conditional distributions; one tracking the correlation with the MB's left neighbor, and the other tracking the correlation with the MB's top neighbor.

$$P(ICPM = \hat{c}_i | \Omega_{c,i}) = P(ICPM = \hat{c}_i | addr) \times P(ICPM = \hat{c}_i | icpm_W) \times P(ICPM = \hat{c}_i | icpm_N) \quad (4.8)$$

where $ICPM$ is a discrete random variable representing the *intra_chroma_pred_mode* used, and $icpm_W$ and $icpm_N$ are the chrominance prediction modes used by the west and north MBs, respectively. The conditional distributions used in (4.8) are also custom built mass functions from the observed decoded values in previous intact NALUs.

4.2.5 *sub_mb_type*

Motion compensation, used to reduce temporal redundancies, is described using motion vectors. To improve coding efficiency, the H.264 standard introduced a more sophisticated motion compensation scheme compared to earlier standards. The latest value of *mb_type* indicates how many motion vectors are associated with the current MB. Additionally, when the coding scheme is either P_8x8 or P_8x8ref0, the syntax element *sub_mb_type* will be present to further segment the MB's displacement.

sub_mb_type elements always come in groups of four consecutive values. This can be exploited to build a more meaningful syntax element. Each value of *sub_mb_type* tells the decoder how many motion vectors to extract. The total number of motion vectors provides a convenient means to evaluate the probability of the joint distribution; convenient because we can observe the number of motion vectors used at any MB for any coding scheme.

In spite of the fact that counting motion vectors is computationally light, the joint distribution is less accurate with respect to the vector count of each 8x8 block. To address this consideration, we assume that all possible outcomes leading to the same number of motion vectors follow a Uniform distribution. The conversion cost evaluated by the channel decoder will help decide which codeword is the likeliest.

$$P(MVC = \hat{c}_i | \Omega_{c,i}) = \frac{1}{N_i} \times P(MVC = \hat{c}_i | mvc_{Co}) \quad (4.9)$$

where MVC is a discrete random variable used to represent the number of motion vectors associated with an MB, N_i is the number of combinations associated with a given number of motion vectors per MB (for instance, there are 8 combinations where $MVC = 5$, and only 1

combination where $MVC = 16$), and mv_{Co} represents the number of motion vectors used by the colocated MB in the previous frame. The conditional distribution is built using the observed values decoded in intact NALUs.

4.2.6 *mvd_l0*

The *mvd_l0* syntax element represents the difference, both horizontal and vertical, between the selected motion vector during motion estimation, and that predicted from the available neighboring ones. The correction process can take advantage of the fact they come in pairs, and model them as a single codeword.

The correction process can also exploit the derivation process to build a more precise model (International Telecommunications Union, 2007, Section 8.4.1). The *mvd_l0* values are added to the predicted values to obtain a final motion vector. To ensure that each slice is independently decodable, the prediction process is limited by the slice boundaries. At the start of each slice, the prediction motion vector will be (0,0), as no information will be available. In high motion sequences, we expect that this will lead to high prediction errors. As the decoding of the slice progresses, the derivation process should yield better predictors. Thus, the slice boundaries make it difficult to model the residual displacement.

Unlike the derivation process, the proposed correction process can use the available spatio-temporal motion vectors to build a motion vector field (MVF). The correction process can then use the MVF to build conditional distributions with the available spatio-temporal vectors. The optimal number of distributions used depends on the sequence and the coding parameters. We propose to use the product of five distributions. These five distributions, 4-connected neighbors and the co-located macroblock, were selected as a way to favor the motion vectors that are most similar to the ones used by their neighbors.

$$P(MV = (\hat{c}_i, \hat{c}_{i+1}) | \Omega_{c,i}) = \prod_{n \in \{W, N, C, E, S\}} P(MV = (\hat{c}_i, \hat{c}_{i+1}) | mv_n) \quad (4.10)$$

where mv_W and mv_N refer to the west and north motion vectors in the current frame, and mv_C , mv_E and mv_S , to the colocated, east and south motion vectors in the previous frame, all with respect to the current location.

The conditional distributions can all be evaluated using a joint Normal distribution centered at mv_n with $n \in \{W, N, C, E, S\}$. The standard deviation can be tracked using the previously decoded motion vectors in intact slices.

4.2.7 *coded_block_pattern*

The *coded_block_pattern* syntax element communicates the presence or absence of residual coefficients, and is used by both inter and intra 4x4 MBs. The value is also built into the intra 16x16 coding schemes, but they use less precise masks. The syntax element is a reordered exponential Golomb code. The ordering differs for inter and intra 4x4 MBs, but the mapped values hold the same meaning.

There are 48 values, meant to be interpreted as a 6-bit binary mask. This makes it difficult to track occurrences alone, as a value of 8 and a value of 4 both mean that a single 8x8 block contains residual information.

We can exploit the CAVLC decoding process here to help us build a model. The VLC table is selected using the *coeff_token* values of the left and top 4x4 blocks. This tells us that there is a strong correlation between neighboring blocks. We can mimic this behavior and use two conditional distributions, one tracking the above occurrences, and the other tracking the western occurrences.

$$\begin{aligned}
P(CBP = \hat{c}_i | \Omega_{c,i}) &= P(CBP = \hat{c}_i | cs) \times \\
&P(CBP = \hat{c}_i | cbp_W) \times P(CBP = \hat{c}_i | cbp_N)
\end{aligned} \tag{4.11}$$

where CBP is a discrete random variable representing the *coded_block_pattern* value of an MB, cs is the latest decoded value of *mb_type*, and cbp_W and cbp_N refer to the *coded_block_pattern* values west and north of the current MB, when they are available.

4.3 Early Termination

Errors in the residual information leading to a syntactically valid sequence of codewords are problematic, since the prediction information is interlaced with the residual information. Upon desynchronization, the correction process will force the use of a valid codeword in any modeled syntax element, no matter how unlikely. To address this problem, we use a threshold to stop the correction process when the selected codeword seems too unlikely. Exploiting the fact that most codewords are short, it becomes highly improbable that multiple bits inside the same codeword are erroneous, even at very high bit error rates. Thus, we propose to stop the correction process when the Hamming distance between the likeliest codeword and the received bits is greater than 1.

Furthermore, our implementation uses a greedy approach to find the series of likeliest codewords. A single codeword is retained at each step, and the remaining outcomes are discarded. Type I errors (i.e., changing intact bits) and type II errors (i.e., keeping corrupted bits) may desynchronize the bitstream, leading to an unlikely path requiring that multiple bits be flipped. To avoid following such a path, we stop the correction process when the ratio of flipped bits over interpreted bits exceeds 10^{-2} . Once the decoding process stops, either because the slice was entirely decoded, an error was detected, or a threshold was reached, the extracted MBs are reconstructed and the missing ones, if any, are concealed.

CHAPTER 5

EXPERIMENTAL RESULTS

In this chapter, we demonstrate the correction performances of our proposed approach. We choose to evaluate the PSNR of the reconstructed sequences as a comparison mean. We could have opted for other metrics, and other statistics, but the image quality speaks louder, and facilitates the comparison of future strategies with ours.

The chapter is separated into five sections. The first section describes the experimental setup used. Our assumptions are clearly highlighted, and the tools used are noted. The second section presents our observations in compact form and discusses them in detail. The actual observations are available in Annex V. The third section compares hard-output maximum likelihood decoding (HO-MLD) against soft-output maximum likelihood decoding (SO-MLD). The fourth section presents decoding times to show that both HO-MLD and SO-MLD could be implemented in real-time applications. The last section illustrates our proposed method's current limits to serve as motivation to further improve it.

5.1 Experimental Setup

The first 120 frames of the NTSC (720x480) sequences *driving*, *opening-ceremony*, *whale-show*, 4CIF (704x576) sequences *city*, *crew*, *harbour*, *ice*, *soccer*, and PAL (720x576) sequence *walk* were coded using the JM 18.2 (Joint Video Team, 2011a).

The Baseline profile was used, and an Intra frame was forced between every 30 frames. The MBs were coded following the raster scan order, and arbitrary slice ordering was not used. Following the recommendations in (Connie *et al.*, 2008), the maximum transmission unit (MTU) size was set to 200 bytes. As a result, each slice carries a variable number of MBs. Each sequence was coded with three different QP values. They were selected to produce streams with target bitrates of around 1 Mbps, 1.2 Mbps, and 1.5 Mbps.

As an experiment, a frame between the 61st and the 110th was randomly selected for corruption in each coded sequence. The first 60 frames were purposely kept intact so that our decoder can gather information such as the frequency of I and P slices, the average number of MBs carried in each slice, the average difference between the predicted motion vector and the actual motion vector, etc. The transmission of the slices belonging to the selected frame was simulated using a rate-2/3 low-density parity-check (LDPC) code (200 bytes unprotected packets, 300 bytes with protection), binary phase shift keying (BPSK) modulation, and an additive white Gaussian noise (AWGN) channel. The latter two were used, as was the case for (Levine *et al.*, 2007; Nguyen *et al.*, 2010; Farrugia and Debono, 2011; Wang and Yu, 2005; Lee *et al.*, 2007). The transmission simulation was repeated 10 times for each sequence, to ensure that the location of the erroneous bits did not bias our conclusions.

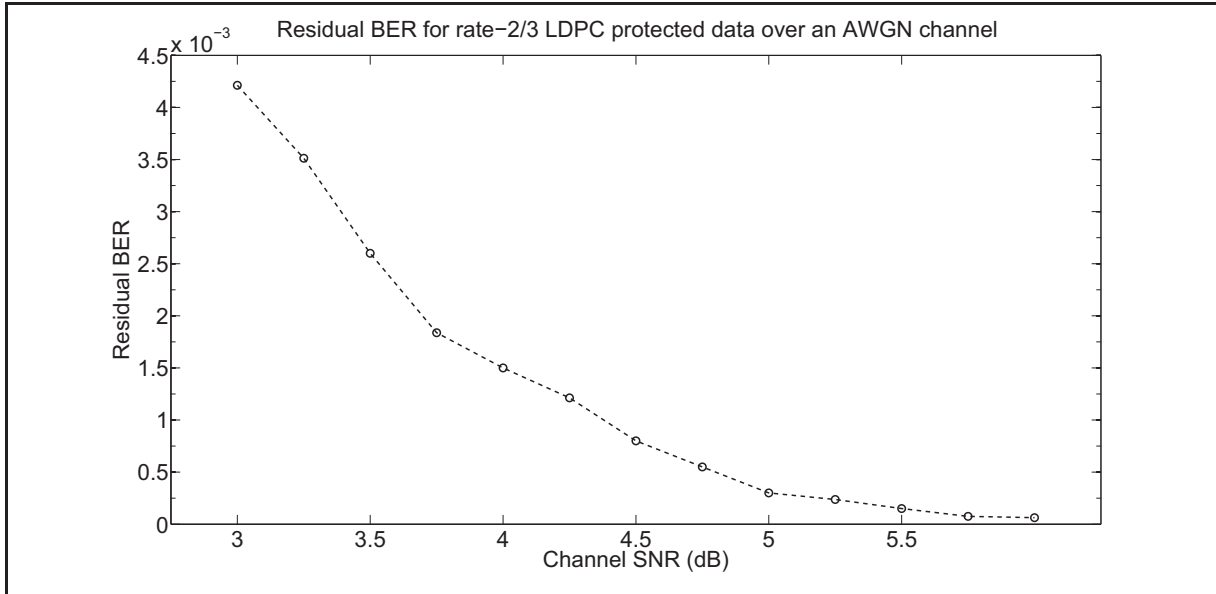


Figure 5.1 Residual BER for packets protected with a rate-2/3 LDPC code and submitted to an AWGN channel.

The actual choice of the coding rate is outside the scope of the experiment. Our interest lay in the bit error rate (BER) after the packet was decoded by the channel decoder (the LDPC codes are used to correct as many transmission errors as possible). Fig. 5.1 shows a plot mapping the channel conditions to the BERs under our experimental setup. The values in the graph indicate

the amount of remaining errors, as a ratio, after the LDPC codes have been used to correct transmission errors. We refer to this as residual errors. The experiment used channel SNRs of 4 dB (10^{-3} BER), and 5 dB (10^{-6} BER) to simulate both harsh and moderate transmission conditions. With the selected MTU, this translates to packet loss rates (PLR) of 80% for harsh conditions, and 1% under moderate conditions.

The experiment was conducted 10 times at each channel SNR. During the transmission simulations, the corrupted slices were identified to allow the mimicking of the error detection mechanism. Using this information, we created complementary streams in which the corrupted slices were discarded, as a typical communication system would have done. Essentially, this was done to avoid having to modify the H.264 reference software to enable it to accept corrupted slices.

The streams containing corrupted slices were first decoded using our H.264 decoder, and soft-output maximum likelihood decoding (SO-MLD) was applied to the corrupted slices. Then, the complementary streams carrying only intact slices were decoded twice, concealing the missing MBs: once using the JM 16.0 (the error concealment mechanism is broken in more recent versions (Joint Video Team, 2011b)) default error concealment mechanism (frame copy), and once using STBMA+PDE (Chen *et al.*, 2008), which, to our knowledge, is the best error concealment mechanism. The missing MBs, following the application of SO-MLD, were also concealed using STBMA+PDE.

5.2 Concealment and correction comparison

The average PSNR of the frames containing corrupted slices are presented in Tables 5.1, 5.2, and 5.3. Columns 2, 3, and 4 refer to the experiments using a channel SNR of 4 dB, while columns 5 to 7 refer to the experiments using a channel SNR of 5 dB. The differences between the results obtained with JM 16.0 and those obtained with STBMA+PDE and SO-MLD appear between parentheses.

The results indicate that SO-MLD outperforms JM 16.0 in all cases, with the exception of the *opening-ceremony*, and *whale-show* sequences. In both cases, the coding behavior is difficult to predict, resulting in an increase in false positive, as well as false negative, detections.

Moreover, the results also show that on average, SO-MLD performs better than STBMA+PDE for the vast majority of the sequences studied. Overall, STBMA+PDE's PSNR gain is 0.76 dB over JM 16.0 at a channel SNR of 4 dB, and 1.77 dB at a channel SNR of 5 dB, while SO-MLD's gain is 1.42 dB at a channel SNR of 4 dB, and 1.96 dB at a channel SNR of 5 dB. Both increases are an indication that exploiting corrupted slices yields better results.

Table 5.1 Comparison of the average PSNR (dB) observed with the three decoding approaches for a target bitrate of 1000 kbps

Sequences	Channel SNR (dB)						
	Intact	4			5		
		JM16.0	STBMA + PDE	SO-MLD	JM16.0	STBMA + PDE	SO-MLD
driving	29.33	20.67	21.64 (+0.98)	22.75 (+2.09)	23.49	26.20 (+2.71)	26.22 (+2.72)
opening- ceremony	27.76	26.37	26.10 (-0.27)	26.12 (-0.25)	27.12	27.16 (+0.04)	27.12 (+0.00)
whale-show	24.12	22.26	22.20 (-0.06)	22.42 (+0.16)	23.10	23.08 (-0.02)	23.27 (+0.17)
city	32.39	25.08	26.57 (+1.50)	26.90 (+1.83)	27.57	30.37 (+2.80)	29.99 (+2.41)
crew	33.63	25.88	26.15 (+0.27)	26.73 (+0.85)	28.80	29.81 (+1.00)	30.03 (+1.23)
harbour	28.58	23.18	24.10 (+0.92)	24.33 (+1.15)	25.23	26.58 (+1.35)	26.48 (+1.25)
ice	40.33	24.85	25.80 (+0.95)	27.32 (+2.47)	28.43	31.36 (+2.93)	32.28 (+3.86)
soccer	31.30	22.50	22.42 (-0.08)	23.67 (+1.17)	25.44	26.21 (+0.77)	27.15 (+1.71)
walk	28.30	16.56	18.12 (+1.56)	19.35 (+2.79)	19.88	22.67 (+2.79)	23.35 (+3.47)
average	30.64	23.94	23.68 (+0.64)	24.40 (+1.36)	25.45	27.05 (+1.60)	27.32 (+1.87)

Table 5.2 Comparison of the average PSNR (dB) observed with the three decoding approaches for a target bitrate of 1200 kbps

Sequences	Channel SNR (dB)						
	Intact	4			5		
		JM16.0	STBMA + PDE	SO-MLD	JM16.0	STBMA + PDE	SO-MLD
driving	30.15	20.48	21.54 (+1.06)	22.56 (+2.08)	23.18	25.75 (+2.57)	25.98 (+2.81)
opening- ceremony	28.37	26.77	26.41 (-0.36)	26.51 (-0.26)	27.55	27.57 (+0.02)	27.56 (+0.01)
whale-show	24.66	22.47	22.43 (-0.04)	22.71 (+0.24)	23.32	23.33 (+0.01)	23.68 (+0.37)
city	32.99	24.88	26.83 (+1.95)	27.06 (+2.18)	27.78	31.13 (+3.35)	30.37 (+2.59)
crew	34.18	24.97	25.27 (+0.30)	25.95 (+0.98)	29.56	30.81 (+1.25)	31.17 (+1.62)
harbour	29.19	24.47	25.09 (+0.61)	25.29 (+0.82)	25.63	27.11 (+1.49)	26.94 (+1.32)
ice	40.89	24.79	25.51 (+0.72)	27.11 (+2.32)	28.46	31.18 (+2.72)	31.83 (+3.37)
soccer	31.76	22.36	22.61 (+0.25)	24.04 (+1.69)	24.41	26.46 (+2.05)	26.94 (+2.53)
walk	28.93	16.62	18.38 (+1.76)	19.49 (+2.87)	20.31	23.25 (+2.94)	23.56 (+3.24)
average	31.24	23.09	23.79 (+0.70)	24.52 (+1.43)	25.58	27.40 (+1.82)	27.56 (+1.98)

Figs. 5.2 and 5.3 compare the average gains of STBMA+PDE and SO-MLD over JM 16.0 at each target bitrate. When the channel conditions are harsh (Fig. 5.2), we can see that SO-MLD performs relatively better compared to STBMA+PDE. Since most of the packets are corrupted, retrieving the corrupted packets rather than discarding them does in fact yield better results. When the channel conditions are moderate, the improvement is smaller, as fewer packets are discarded. However, in Fig. 5.3, we can clearly see that STBMA+PDE provides significant PSNR gains over JM 16.0.

A visual inspection of the results obtained further confirms that SO-MLD should be integrated into real-time video communication systems. Fig. 5.4 shows the original 99-th frame of the *ice* sequence coded at 1.2 Mbps, and transmitted with a channel SNR of 5 dB. The luminance differences between the frames produced with the three approaches are also presented to highlight the problem areas.

Table 5.3 Comparison of the average PSNR (dB) observed with the three decoding approaches for a target bitrate of 1500 kbps

Sequences	Channel SNR (dB)						
	Intact	4			5		
		JM16.0	STBMA + PDE	SO-MLD	JM16.0	STBMA + PDE	SO-MLD
driving	30.68	20.42	21.21 (+0.78)	22.51 (+2.08)	23.48	26.49 (+3.01)	26.20 (+2.72)
opening- ceremony	29.98	27.65	27.38 (-0.26)	26.90 (-0.74)	28.85	28.93 (+0.08)	29.14 (+0.28)
whale-show	25.28	22.54	22.53 (-0.01)	22.44 (-0.11)	23.83	23.84 (+0.01)	24.07 (+0.24)
city	33.87	24.76	27.35 (+2.59)	26.89 (+2.13)	27.88	31.20 (+3.32)	30.14 (+2.26)
crew	35.37	25.97	26.41 (+0.44)	27.38 (+1.41)	29.35	30.91 (+1.56)	31.15 (+1.80)
harbour	30.10	23.61	24.97 (+1.36)	24.86 (+1.25)	25.26	27.03 (+1.77)	26.71 (+1.45)
ice	41.73	24.83	25.82 (+0.99)	27.27 (+2.44)	28.50	31.57 (+3.07)	32.21 (+3.71)
soccer	33.06	21.36	22.12 (+0.77)	23.30 (+1.95)	25.24	26.45 (+1.21)	27.60 (+2.36)
walk	29.65	17.02	18.95 (+1.93)	19.74 (+2.72)	22.23	25.26 (+3.03)	25.78 (+3.55)
average	33.30	23.13	24.08 (+0.95)	24.59 (+1.46)	26.07	27.96 (+1.90)	28.11 (+2.04)

Fig. 5.5 shows another example in which SO-MLD performs better than JM 16.0 and STBMA+PDE. The 65-th frame of the *walk* sequence is presented, along with the luminance differences between the intact frame and the reconstructed frames.

In both cases, fewer differences are introduced when using SO-MLD. This is important not only for the current frame, but for the subsequent ones, as fewer visible drifting effects will be seen.

This is the case in the first example. The errors surrounding the skater in the center of the picture, better handled by STBMA+PDE, lead to inferior PSNR over time (Figure 5.6).

In the second case, the instantaneous improvements are noteworthy. In fact, the system is practically resynchronized around the 80-th frame, 11 frames before the forced intra frame that resynchronizes the stream (Figure 5.7).

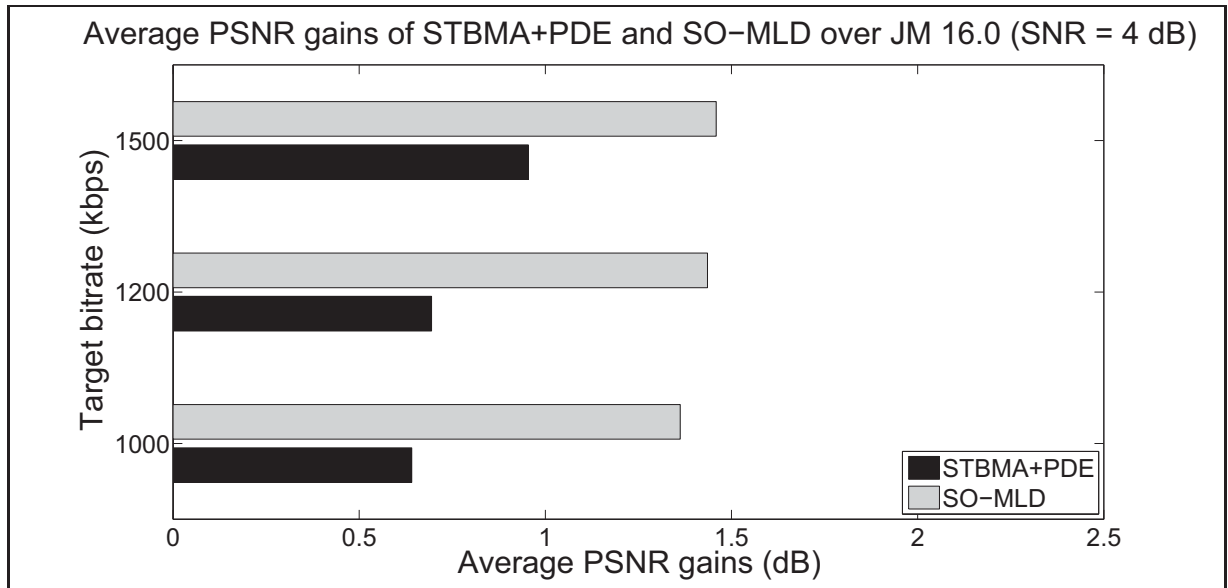


Figure 5.2 Average PSNR gains of STBMA+PDE and SO-MLD over JM 16.0 when the channel SNR is 4 dB

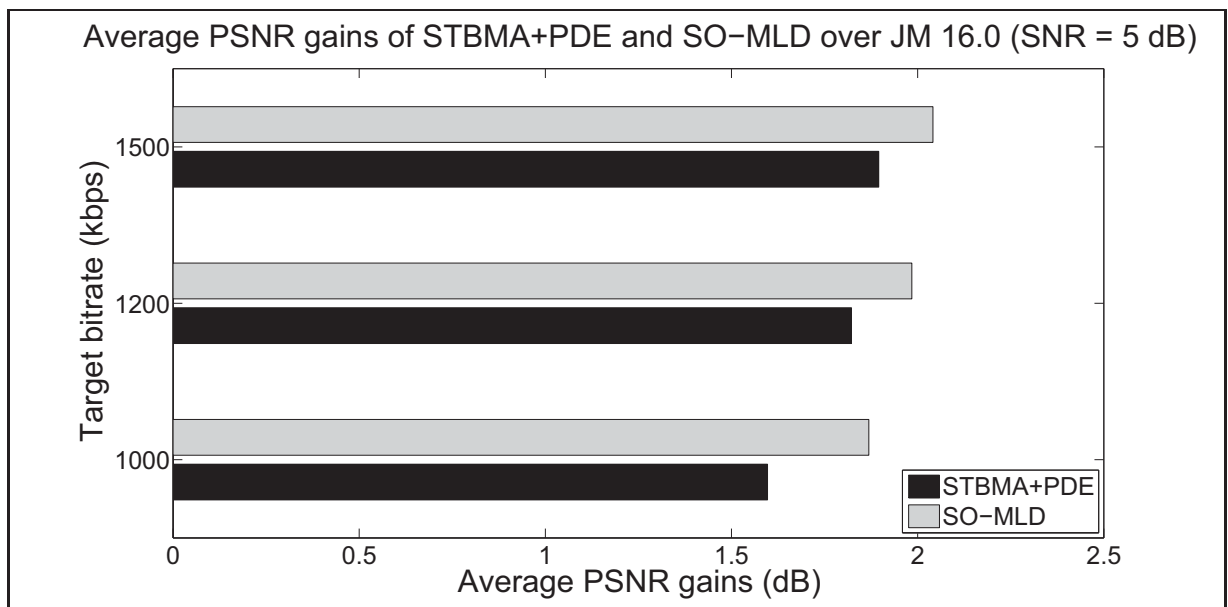


Figure 5.3 Average PSNR gains of STBMA+PDE and SO-MLD over JM 16.0 when the channel SNR is 5 dB

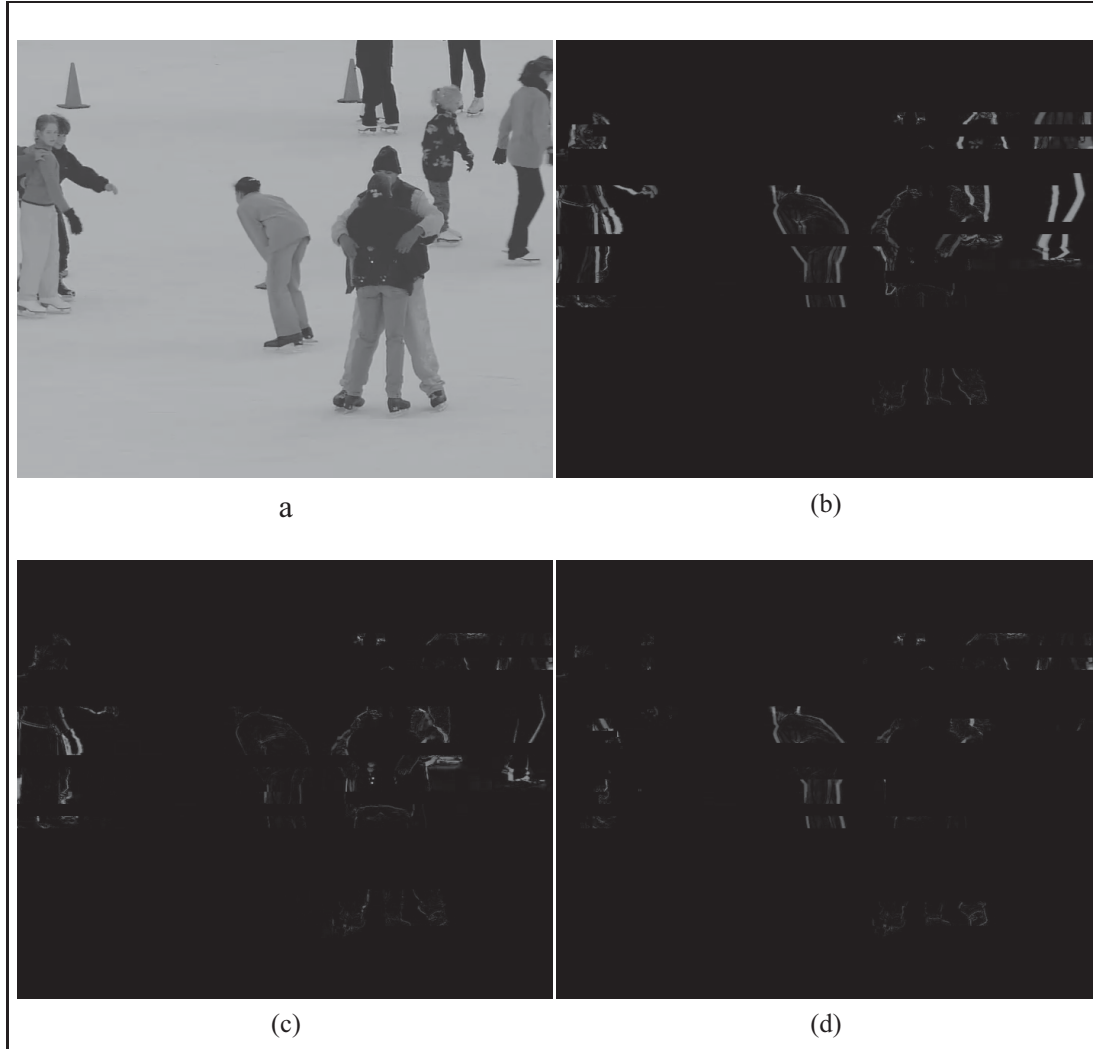


Figure 5.4 Visual comparison of the 99-th frame of the *ice* sequence coded at 1200 kbps, and submitted to a channel SNR of 5 dB: (a) The intact frame (41.02 dB); (b) Luminance difference from the intact frame using JM 16.0 to decode the corrupted frame (26.42 dB); (c) Luminance difference from the intact frame using STBMA+PDE to decode the corrupted frame (31.24 dB); and (d) Luminance difference from the intact frame using SO-MLD to decode the corrupted frame (34.66 dB).

5.3 Hard-output and soft-output comparison

As a second experiment, the same 120 frames of sequences used in the previous experiment were used to compare the performances of our proposed method when soft-output information is available, and when it is not. The same configurations were used (Baseline profile, intra

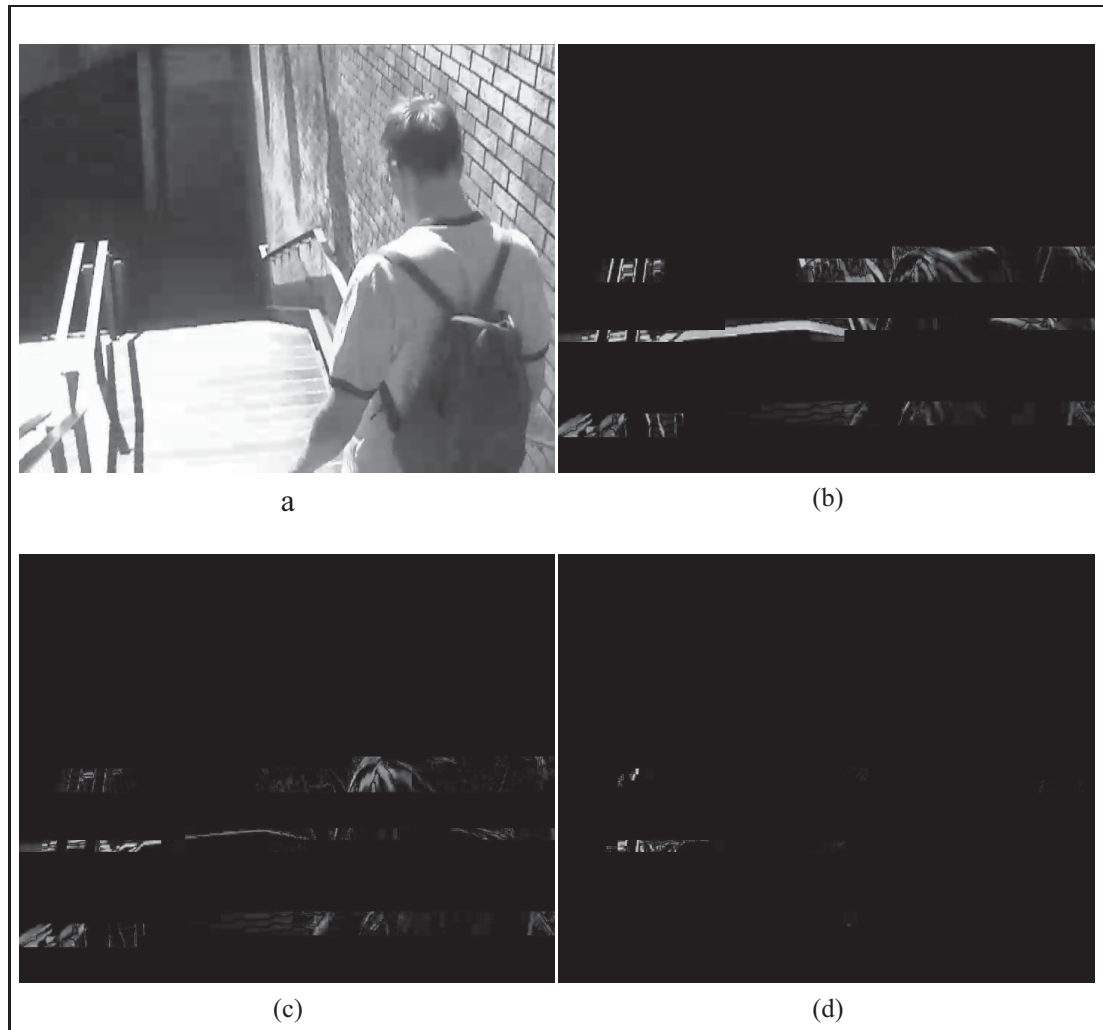


Figure 5.5 Visual comparison of the 65-th frame of the *walk* sequence coded at 1500 kbps, and submitted to a channel SNR of 5 dB: (a) The intact frame (29.88 dB); (b) Luminance difference from the intact frame using JM 16.0 to decode the corrupted frame (21.61 dB); (c) Luminance difference from the intact frame using STBMA+PDE to decode the corrupted frame (25.75 dB); and (d) Luminance difference from the intact frame using SO-MLD to decode the corrupted frame (28.97 dB)

refresh rate, resilience scheme, MTU size, etc.). However, the sequences were coded with fixed QP values of 22, 27, 32, and 37.

Transmission simulations were conducted in the same manner as they were for the first experiment. A single frame between the 61st and the 110th was selected, keeping all other frames

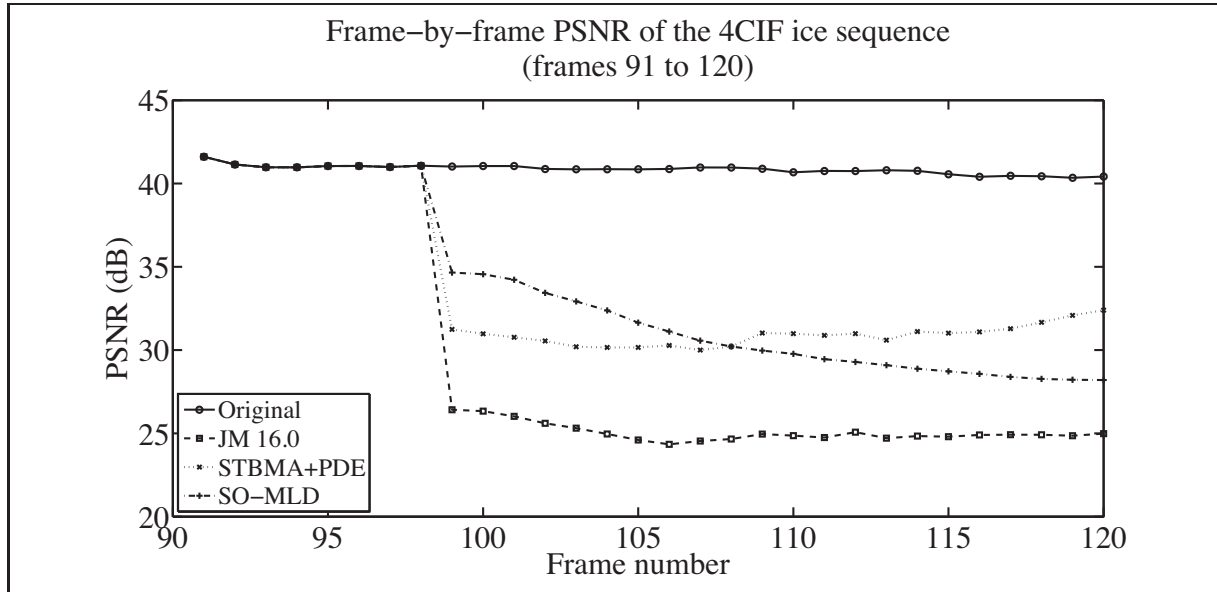


Figure 5.6 Frame-by-frame PSNR of the 4CIF *ice* sequence after transmission errors

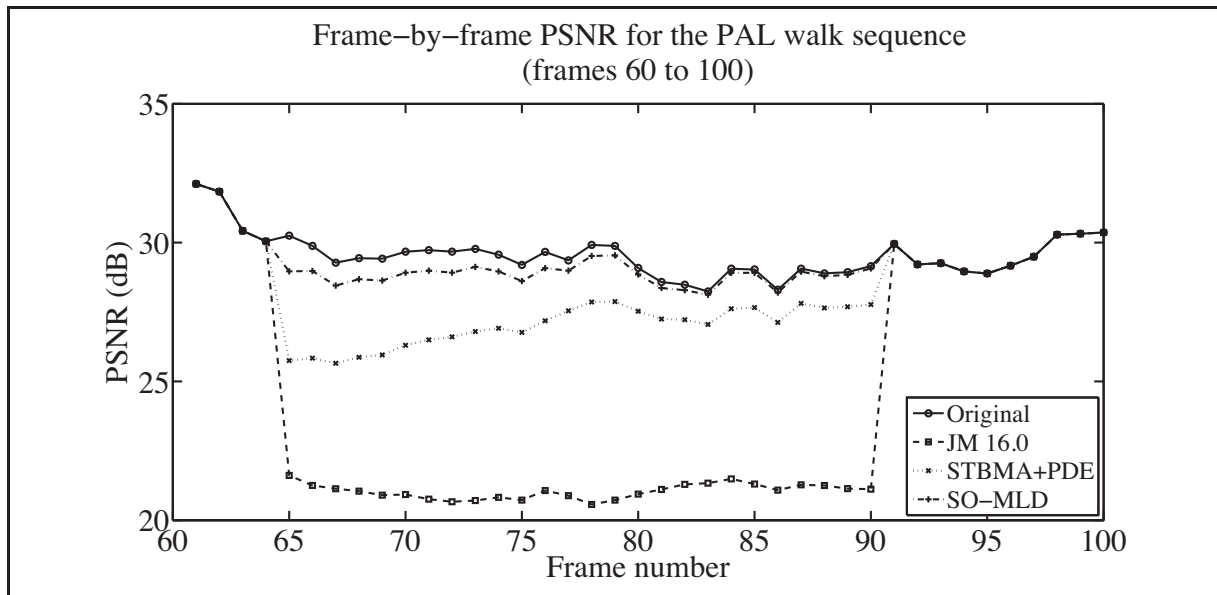


Figure 5.7 Frame-by-frame PSNR of the PAL *walk* sequence after transmission errors

intact. The simulations were repeated 30 times per frame, and 10 different frames were randomly selected as a way to ensure that our conclusions were not biased.

The corrupted streams were decoded using SO-MLD and HO-MLD. They were also decoded using the error concealment feature in the JM 16.0 and state-of-the-art error concealment STBMA+PDE to show that HO-MLD also performs better than error concealment.

Table 5.4 Comparison of the average PSNR (dB) observed with the four decoding approaches for streams coded with a fixed QP of 37

Sequences	Channel SNR								
	Intact	4 dB				5 dB			
		JM16.0	STBMA + PDE	SO-MLD	HO-MLD	JM16.0	STBMA + PDE	SO-MLD	HO-MLD
driving	30.15	20.44	21.69 (+1.25)	22.80 (+2.36)	22.06 (+1.63)	23.60	26.44 (+2.84)	26.52 (+2.93)	25.59 (+1.99)
opening- ceremony	27.76	26.34	26.18 (-0.16)	26.14 (-0.20)	26.14 (-0.20)	27.12	27.02 (-0.10)	26.96 (-0.17)	26.91 (-0.21)
whale-show	28.22	23.20	23.24 (+0.03)	23.97 (+0.76)	23.64 (+0.43)	25.39	25.50 (+0.11)	26.07 (+0.68)	25.77 (+0.38)
city	29.89	24.96	25.43 (+0.45)	26.44 (+1.46)	26.41 (+1.43)	27.38	28.68 (+1.29)	28.61 (+1.22)	28.60 (+1.22)
crew	33.16	25.42	25.52 (+0.10)	26.40 (+0.98)	26.01 (+0.59)	28.52	29.25 (+0.73)	29.76 (+1.23)	29.42 (+0.90)
harbour	30.09	24.60	25.27 (+0.67)	25.47 (+0.87)	25.47 (+0.86)	26.25	27.63 (+1.38)	27.33 (+1.08)	27.29 (+1.04)
ice	36.17	24.77	24.94 (+0.17)	25.81 (+1.04)	25.32 (+0.55)	28.47	29.39 (+0.92)	30.16 (+1.69)	29.80 (+1.33)
soccer	31.30	21.23	21.84 (+0.61)	22.84 (+1.61)	22.40 (+1.17)	24.73	25.64 (+0.91)	26.47 (+1.74)	25.94 (+1.20)
walk	31.79	18.51	20.64 (+2.13)	21.43 (+2.91)	20.06 (+1.55)	20.79	23.33 (+2.54)	24.77 (+3.98)	24.01 (+3.22)
average	30.94	23.28	23.82 (+0.53)	24.59 (+1.30)	24.17 (+0.88)	25.81	26.99 (+1.18)	27.41 (+1.6)	27.04 (+1.23)

The average PSNR (in dB) for all four methods are given in Tables 5.4, 5.5, 5.6, and 5.7. The average PSNR of the intact frames are also given as a comparison basis.

The results indicate that SO-MLD outperforms JM 16.0 in all cases, with the exception of the *opening-ceremony* sequence. Moreover, the results also show that on average, SO-MLD and HO-MLD perform better than STBMA+PDE for the majority of the sequences studied. Overall, STBMA+PDE's PSNR gain is 1.15 dB over JM 16.0 at a channel SNR of 4 dB, and 2.39 dB at a channel SNR of 5 dB, while SO-MLD's gain is 1.82 dB at a channel SNR of 4 dB, and 2.72 dB at a channel SNR of 5 dB, and HO-MLD's gain is 1.43 dB at a channel

Table 5.5 Comparison of the average PSNR (dB) observed with the four decoding approaches for streams coded with a fixed QP of 32

Sequences	Channel SNR								
	Intact	4 dB				5 dB			
		JM16.0	STBMA + PDE	SO-MLD	HO-MLD	JM16.0	STBMA + PDE	SO-MLD	HO-MLD
driving	33.43	20.47	21.95 (+1.47)	22.77 (+2.30)	22.21 (+1.73)	23.89	26.32 (+2.43)	27.21 (+3.31)	26.39 (+2.50)
opening- ceremony	31.46	28.50	28.28 (-0.23)	28.56 (+0.06)	28.18 (-0.32)	29.93	30.13 (+0.20)	30.27 (+0.33)	30.17 (+0.24)
whale-show	31.98	23.69	23.82 (+0.13)	24.65 (+0.95)	24.39 (+0.70)	26.75	27.01 (+0.26)	27.80 (+1.05)	27.52 (+0.77)
city	32.99	25.14	26.79 (+1.65)	27.37 (+2.23)	27.41 (+2.27)	27.73	30.56 (+2.83)	30.00 (+2.27)	30.18 (+2.45)
crew	35.80	26.17	26.59 (+0.42)	27.95 (+1.78)	27.28 (+1.11)	29.10	30.45 (+1.35)	30.96 (+1.85)	30.67 (+1.57)
harbour	33.58	24.02	25.96 (+1.95)	25.41 (+1.39)	25.05 (+1.13)	27.12	29.53 (+2.42)	29.17 (+2.05)	28.51 (+1.39)
ice	38.76	25.02	25.51 (+0.49)	26.77 (+1.75)	26.27 (+1.25)	28.57	30.49 (+1.92)	31.33 (+2.77)	31.01 (+2.44)
soccer	34.27	19.87	21.68 (+1.81)	21.71 (+1.84)	21.47 (+1.60)	25.50	27.63 (+2.13)	28.40 (+2.90)	27.92 (+2.42)
walk	35.21	18.27	20.12 (+1.85)	21.18 (+2.91)	19.76 (+1.49)	22.13	25.57 (+3.44)	26.09 (+3.96)	25.61 (+3.48)
average	34.16	23.46	24.52 (+1.06)	25.15 (+1.69)	24.67 (+1.21)	26.75	28.63 (+1.89)	29.02 (+2.28)	28.66 (+1.92)

SNR of 4 dB, and 2.37 dB at a channel SRN of 5 dB. The results indicate that the gap between STBMA+PDE and SO-MLD/HO-MLD closes with improved channel conditions. On average, SO-MLD yields 0.33 dB better PSNR than STMA+PDE at a channel SNR or 5 dB, while HO-MLD performs similarly. This is a slight decrease compared to the 0.67 dB gain at a channel SNR of 4 dB. However, with improved channel conditions, the number of intact macroblocks increases, making it harder for SO-MLD/HO-MLD to distinguish itself since there are less corrupted macroblocks to recuperate. Inversely, as the channel conditions worsen, error correction actually helps error concealment perform better as it reduces the size of the concealment region and provides error concealment with better/more information which results in better quality concealed MBs.

Table 5.6 Comparison of the average PSNR (dB) observed with the four decoding approaches for streams coded with a fixed QP of 27

Sequences	Channel SNR								
	Intact	4 dB				5 dB			
		JM16.0	STBMA + PDE	SO-MLD	HO-MLD	JM16.0	STBMA + PDE	SO-MLD	HO-MLD
driving	37.12	20.66	22.51 (+1.85)	22.95 (+2.30)	22.45 (+1.79)	23.92	28.84 (+4.92)	28.65 (+4.73)	27.78 (+3.86)
opening- ceremony	35.39	29.86	29.55 (-0.32)	30.03 (+0.17)	29.65 (-0.21)	32.26	32.93 (+0.67)	32.99 (+0.73)	33.04 (+0.78)
whale-show	36.30	23.94	24.16 (+0.22)	24.86 (+0.92)	24.67 (+0.73)	26.51	27.63 (+1.13)	28.57 (+2.06)	28.23 (+1.72)
city	36.64	24.71	28.34 (+3.64)	28.86 (+4.15)	28.39 (+3.68)	27.73	33.84 (+6.11)	33.87 (+6.14)	33.27 (+5.53)
crew	38.59	26.04	26.67 (+0.63)	28.00 (+1.95)	27.42 (+1.38)	28.75	30.57 (+1.83)	31.50 (+2.75)	30.86 (+2.12)
harbour	37.32	23.15	26.08 (+2.93)	24.53 (+1.38)	24.31 (+1.16)	28.55	30.68 (+2.13)	30.08 (+1.54)	29.87 (+1.32)
ice	41.30	25.14	26.05 (+0.92)	27.53 (+2.40)	26.94 (+1.80)	29.26	32.18 (+2.91)	32.98 (+3.71)	32.54 (+3.27)
soccer	37.88	22.05	23.06 (+1.01)	23.96 (+1.91)	23.49 (+1.43)	24.99	28.35 (+3.36)	28.34 (+3.45)	28.15 (+3.16)
walk	38.97	17.45	19.71 (+2.26)	20.68 (+3.23)	20.47 (+3.02)	21.67	26.36 (+4.70)	26.34 (+4.68)	26.21 (+4.54)
average	37.72	23.67	25.13 (+1.46)	25.71 (+2.04)	25.31 (+1.64)	27.07	30.15 (+3.08)	30.37 (+3.30)	29.99 (+2.92)

5.4 Decoding time

While conducting the second experiment, we also collected the decoding time of all four approaches for all the simulations we ran as a way to measure the complexity of the different approaches.

The simulations were conducted on an iMac equipped with a 3.4 GHz Intel i7 processor, 8 Gb of 1333 DDR3 RAM running OS X 10.7. Our decoder was implemented using the C++ programming language, and compiled favoring execution speed over program size. Our implementation of the STBMA+PDE algorithm uses a maximum of 30 iterations in the PDE step. Table 5.8 summarizes the average decoding time per frame for all 9 sequences since the tests sequences share similar resolutions. The decoding times are in milliseconds per frame, and they are separated by channel SNR and QP since the amount of errors and the stream quality both affect the decoding and concealment time.

Table 5.7 Comparison of the average PSNR (dB) observed with the four decoding approaches for streams coded with a fixed QP of 22

Sequences	Channel SNR								
	Intact	4 dB				5 dB			
		JM16.0	STBMA + PDE	SO-MLD	HO-MLD	JM16.0	STBMA + PDE	SO-MLD	HO-MLD
driving	41.03	20.51	22.29 (+1.79)	23.12 (+2.62)	22.59 (+2.09)	24.15	29.41 (+5.25)	29.27 (+5.12)	29.34 (+5.18)
opening- ceremony	39.37	32.02	32.33 (+0.31)	32.69 (+0.67)	33.15 (+1.13)	30.62	30.42 (-0.20)	29.86 (-0.75)	29.39 (-1.23)
whale-show	40.92	24.29	24.45 (+0.17)	25.08 (+0.79)	24.92 (+0.64)	27.30	28.27 (+0.97)	30.19 (+2.89)	29.75 (+2.45)
city	40.91	24.74	28.92 (+4.17)	28.92 (+4.17)	28.48 (+3.73)	28.27	34.67 (+6.41)	34.27 (+6.00)	33.97 (+5.70)
crew	41.87	25.94	26.48 (+0.54)	27.90 (+1.96)	27.15 (+1.21)	28.96	30.96 (+2.00)	32.07 (+3.11)	31.64 (+2.68)
harbour	41.18	24.25	26.41 (+2.16)	25.70 (+1.45)	25.46 (+1.22)	27.45	31.06 (+3.61)	30.23 (+2.78)	29.89 (+2.44)
ice	43.61	24.56	25.46 (+0.89)	27.30 (+2.73)	26.78 (+2.21)	28.32	31.98 (+3.66)	32.73 (+4.41)	32.10 (+3.79)
soccer	41.93	21.21	23.03 (+1.83)	23.51 (+2.30)	23.38 (+2.17)	24.90	29.05 (+4.15)	29.53 (+4.63)	29.32 (+4.41)
walk	42.98	17.83	19.89 (+2.06)	21.39 (+3.56)	21.48 (+3.65)	22.23	27.16 (+4.93)	27.48 (+5.26)	27.35 (+5.13)
average	41.53	23.93	25.47 (+1.55)	26.18 (+2.25)	25.93 (+2.00)	26.91	30.33 (+3.42)	30.63 (+3.71)	30.31 (+3.39)

Table 5.8 Average decoding time per standard definition frame measured in milliseconds using the four decoding approaches on all test sequences

Channel SNR	QP	JM 16.0	STBMA+PDE	SO-MLD	HO-MLD
4 dB	22	27	28	33	32
	27	21	22	24	23
	32	17	18	22	20
	37	13	14	16	15
5 dB	22	27	28	29	28
	27	21	21	22	22
	32	17	18	18	18
	37	14	15	15	15

The results indicate that both SO-MLD and HO-MLD have slightly longer decoding times than STBMA+PDE. This can be explained by the fact that the concealment only approaches decode (far) less packets. Accounting for the fact that our approach deals with all packets (corrupted in

addition to intact), the increase in complexity is acceptable, even for real-time communication systems. Note that neither the decoder nor the error correction method have been optimized yet.

5.5 Current limitations



Figure 5.8 Example of uncorrected transmission errors in the CAVLC syntax elements creating valid codewords

We conclude the chapter with an example when our proposed method performs poorly. This is the *worst* case from our set of observations, resulting in 7.65 dB loss compared to the JM 16.0. Figure 5.8 shows the 61-st frame of the *opening-ceremony* sequence coded with a target bitrate of 1500 kbps. The picture strictly uses intra coding, dramatically increasing the presence of CAVLC coefficients. The numerous artefacts present all have to do with errors creating syntactically valid, yet erroneous, codewords.

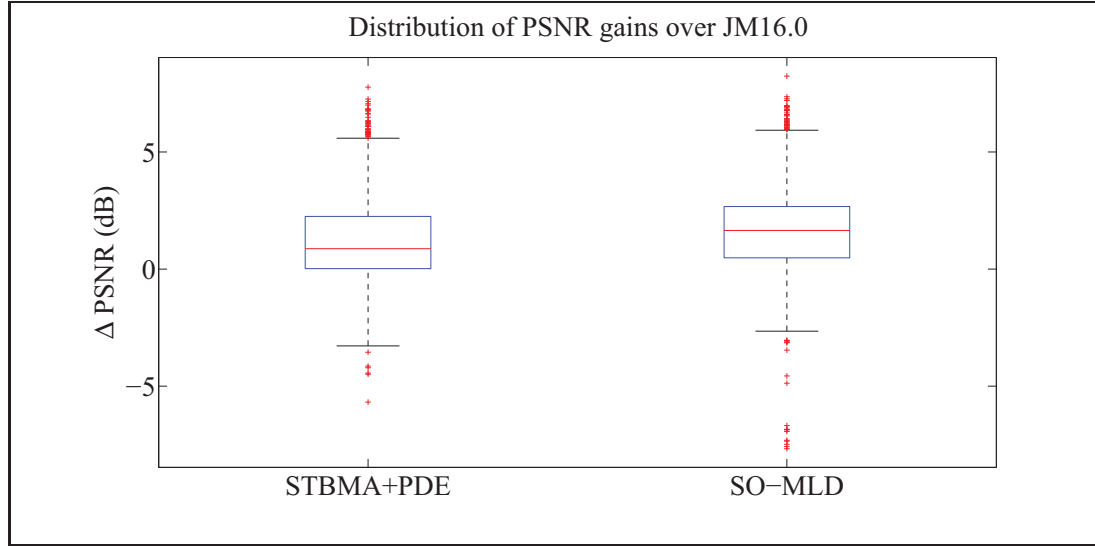


Figure 5.9 Side-by-side distributions of STBMA+PDE's and SO-MLD's PSNR gains over JM 16.0

This should serve as motivation to continue the research. The experimental results already show that our proposed method, on average, performs better than state-of-the-art error concealment STBMA+PDE. Yet, there are numerous negative outliers in our observations. Figure 5.9 presents, side-by-side, STBMA+PDE's and SO-MLD's PSNR gain distribution over JM 16.0. Modeling the CAVLC syntax elements should take care of these negative outliers. Furthermore, it should also shift the rest of the distribution upwards, as the outliers aren't the only cases where annoying artefacts caused by uncorrected errors in the residual syntax elements are present.

CHAPTER 6

CONTRIBUTIONS

In this chapter, we reexamine the three ideas around which this thesis is centered, and align them with the work accomplished. For clarity, the ideas and achievements are listed below.

- We have successfully proposed a novel video error correction mechanism, both at the slice level and the syntax-element level. Our framework evaluates the probability of candidate codewords at the application level, and assigns a cost to modify the received corrupted bitstream to reproduce the binary representation of each codeword. The framework then selects the most likely value by combining both the codeword probabilities and the modification costs.
 - A first provisional patent entitled *Method and System for Video Error Correction Based on Maximum Likelihood* (Caron and Coulombe, 2012a), covering our novel approach, was filed on May 14th 2012.
 - A paper entitled *A Maximum Likelihood Approach to Video Error Correction Applied to H.264 Decoding* (Caron and Coulombe, 2012b), describing the framework, was presented on September 13th 2012 at the Sixth International Conference on Next Generation Mobile Applications, Services, and Technologies, held in Paris, France. We have received the best paper award for this publication.
- We have extended our initial approach with the integration of soft-output information shared by the channel decoder with the video decoder. The Hamming distance first used now accounts for the fact that our confidence in each of the received bits is not uniformly distributed.
 - A second provisional patent entitled *Method and System for Video Error Correction Based on Maximum Likelihood Using Hard or Soft Information From the Channel Decoder* was filed on January 21st 2013 (Caron and Coulombe, 2013a).

- A conference paper entitled *A Maximum Likelihood Approach to Correct Transmission Errors for Joint Source-Channel Decoding of H.264 Coded Video*, describing the integration of soft-output information to our novel maximum likelihood decoding framework was accepted to the twentieth International Conference on Image Processing that will be held in Melbourne, Australia, from the 15th, to the 18th of September 2013 (Caron and Coulombe, 2013b).
- A PCT application, combining both provisional patent applications, entitled *Method and System for Video Error Correction* (Caron and Coulombe, 2013d) was filed on May 14th 2013.
- We have successfully applied our novel video error correction approach to a subset of H.264 Baseline profile syntax elements. Our experimental results show that our approach outperforms both standard and state-of-the-art video error concealment strategies at bit error rates in the range of 10^{-3} to 10^{-6} inclusively.
 - A journal paper entitled *Video Error Correction Using Soft-Output Maximum Likelihood Decoding Applied to H.264 Baseline Profile* (Caron and Coulombe, 2013c), describing in details the framework and the models we used for each of the syntax elements we cover has been submitted in May 2013 to the IEEE Transactions on Circuits and Systems for Video Technology.

As a final note, we would like to mention that our proposed solution has also gathered attention from the industry. We have found a company interested to commercialize our technology. This is perhaps the most unexpected, but clearest, indication that we have truly contributed towards solving a complicated problem.

CONCLUSION

Video communication systems are built using contrasting ideologies. On the one hand, the video encoder removes spatio-temporal redundancies to achieve better compression. In doing so, better visual quality is available given a limited amount of data. On the other hand, the channel encoder adds redundancies to combat transmission errors. The more redundancies are added, the better suited the stream is to reach its destination still intact.

Faced with these opposing goals, the design of a system that offers both quality and robustness requires expertise in many fields. Our research deals with the delicate aspect of video transmission. More specifically, with the handling of received corrupted packets. Our goal was to use these packets instead of discarding them, a goal we have achieved.

Our novel maximum likelihood video error correction method has already shown great promise. The experimental results indicate that SO-MLD performs better than state-of-the-art video error concealment STBMA+PDE. Taking into account that we haven't modeled all the H.264 Baseline profile syntax element, and that our simulations weren't built to minimize the presence of CAVLC syntax elements, these performances are very encouraging.

Furthermore, the proposed solution is independent from the H.264 video standard to which we applied it. It could be applied to existing video standards such as H.261, MPEG-2, H.263, MPEG-4, or the new H.265 standard. With each standard, new syntax element probability models can be derived to exploit the binary representation used and the encoder's behavior. The particularities of each standard can also be applied to improve the correction capabilities.

With our proposed approach, the video decoders can now play a bigger role in the robustness aspect of video transmission. This can effectively relax the compromises the video encoder must make to help packets reach their destination.

Yet, the proposed solution is still young, and we are left with many unexplored ideas. Ideas we share here as recommendations for research problems. They are presented in no particular order.

The computational complexity of the solution can be reduced by taking advantage of our early termination criterion. During the maximization process of a codeword, the codebook containing the valid candidates should be limited to those having a Hamming distance of 1 or less. The longest codewords are typically less than 50 bits. At most, there would be 51 candidates for each syntax element, greatly reducing the number of candidates to study. For example, NTSC sequences have 1350 macroblocks (1350 *first_mb_in_slice* candidates). 21 bits are required to code 1349 (the last valid address) using an unsigned exponential Golomb code. Instead of exploring all 1350 candidates, only 22 would be checked. The approach is expected to produce slightly different results, as cases where there are multiple errors in the same codeword will take different decisions.

The CAVLC and CABAC syntax elements should be modeled. This is perhaps the project leading to the best immediate results. The coding process already removes spatio-temporal redundancies. By modeling the distribution of the quantized residual errors, a probable set of candidates could be generated. Using this, probabilities for each syntax element could be derived. Another idea would be to integrate pixel-domain information. If a range of luminance or chrominance values can be determined, the decoding process can take this into account to assign probabilities to the codewords of a syntax element.

Support for the Main and Extended profile can be added. These profiles offer more coding tools such as bidirectional coding (Main profile) and data partitioning (Extended profile). The later would make it possible to have more reliable information during the correction process. For instance, the number of motion vectors could be known. The correction process would then have to correct the residual motion vectors.

The maximization process can be improved by keeping more candidates at each step or by using an iterative approach. Our proposed solution only keeps the most likely codeword at each decoding step. However, in some cases, the second, third, and fourth candidates are almost as likely as the winning candidates. By keeping more candidates, or by using an iterative approach, more transmission errors could be corrected.

Pixel-domain information, such as border alignment, could be introduced to the framework. This would be especially useful for the motion vectors, as transmission errors in the least significant bits of the signed exponential Golomb codewords used are difficult to deal with.

ANNEX I

ERROR RESILIENCY COST

In this annex, the configuration files used and the output of the JM 18.2 are presented. The default comments present in the configuration files were removed for presentation purposes. They can be found in the *encoder_baseline.cfg* file shipped with the reference software. Specific comments were left in Listing I.1 to draw attention to the differing lines in each example. To save space, only the lines that differ from the first configuration file are shown afterwards. The first 100 values of the SnrY values outputted by the reference software were used to construct the plot shown in Figure 0.1.

1 No Resiliency

Listing I.1: Configuration file with no error resiliency

```
# New Input File Format is as follows
# <ParameterName> = <ParameterValue> # Comment
#
# See configfile.h for a list of supported ParameterNames
#
# For bug reporting and known issues see:
# https://ipbt.hhi.fraunhofer.de

#####
# Files
#####
InputFile           = "carphone_qcif.yuv"
InputHeaderLength   = 0
StartFrame          = 0
FramesToBeEncoded   = 382
FrameRate           = 30.0
SourceWidth         = 176
SourceHeight        = 144
SourceResize        = 0
OutputWidth         = 176
OutputHeight        = 144

TraceFile           = "trace_enc.txt"
ReconFile           = "test_rec.yuv"
OutputFile          = "test.264"
StatsFile           = "stats.dat"

#####
# Encoder Control
#####
ProfileIDC          = 66
IntraProfile        = 0
LevelIDC            = 40
IntraPeriod         = 90
```

```

IDRPeriod                = 0
AdaptiveIntraPeriod      = 0
AdaptiveIDRPeriod        = 0
IntraDelay               = 0
EnableIDRGOP             = 0
EnableOpenGOP            = 0
QPISlice                 = 28
QPPSlice                 = 28
FrameSkip                = 0
ChromaQPOffset           = 0
DisableSubpelME          = 0
SearchRange              = 32

MEDistortionFPel         = 0
MEDistortionHPel         = 2
MEDistortionQPel         = 2
MDDistortion             = 2
SkipDeBlockNonRef        = 0
ChromaMCBuffer           = 1
ChromaMEEnable           = 0
ChromaMEWeight           = 1

NumberReferenceFrames    = 1

PList0References         = 0
Log2MaxFNumMinus4        = 0
Log2MaxPOCLsbMinus4      = -1

GenerateMultiplePPS      = 0
SendAUD                  = 0
ResendSPS                 = 0
ResendPPS                 = 0

MbLineIntraUpdate        = 0
RandomIntraMBRefresh     = 0    # Do not force intra MBs per picture

#####
# PSlice Mode types
#####
PSliceSkip                = 1
PSliceSearch16x16         = 1
PSliceSearch16x8          = 1
PSliceSearch8x16          = 1
PSliceSearch8x8           = 1
PSliceSearch8x4           = 1
PSliceSearch4x8           = 1
PSliceSearch4x4           = 1

DisableIntra4x4           = 0
DisableIntra16x16         = 0
DisableIntraInInter       = 0
IntraDisableInterOnly     = 0
Intra4x4ParDisable        = 0
Intra4x4DiagDisable       = 0
Intra4x4DirDisable        = 0
Intra16x16ParDisable      = 0
Intra16x16PlaneDisable    = 0
ChromaIntraDisable        = 0
EnableIPCM                = 0

DisposableP               = 0
DispPQPOffset             = 0

PreferDispOrder           = 1
PreferPowerOfTwo          = 0
FrmStructBufferLength     = 16

```



```

ChangeQPFrame      = 0
ChangeQPI          = 0
ChangeQPP          = 0
ChangeQPB          = 0
ChangeQPSI         = 0
ChangeQPSP         = 0

#####
# Output Control, NALs
#####
OutFileMode        = 0

#####
# Picture based Multi-pass encoding
#####
RDPictureDecision  = 0
RDPsliceBTest      = 0
RDPictureMaxPassISlice = 1
RDPictureMaxPassPSlice = 2
RDPictureMaxPassBSlice = 3
RDPictureFrameQPPSlice = 0
RDPictureFrameQPBSlice = 0
RDPictureDeblocking = 0
RDPictureDirectMode = 0

#####
# Deblocking filter parameters
#####
DFParametersFlag   = 0
DFDisableRefISlice = 0
DFAlphaRefISlice   = 0
DFBetaRefISlice    = 0
DFDisableNRefISlice = 0
DFAlphaNRefISlice  = 0
DFBetaNRefISlice   = 0
DFDisableRefPSlice = 0
DFAlphaRefPSlice   = 0
DFBetaRefPSlice    = 0
DFDisableNRefPSlice = 0
DFAlphaNRefPSlice  = 0
DFBetaNRefPSlice   = 0

#####
# Error Resilience / Slices
#####
SliceMode          = 1
SliceArgument       = 99  # 1 Picture = 1 Slice

num_slice_groups_minus1 = 0 # no FMO
slice_group_map_type    = 0

slice_group_change_direction_flag = 0
slice_group_change_rate_minus1    = 85
SliceGroupConfigFileName           = "sg0conf.cfg"

UseRedundantPicture = 0
NumRedundantHierarchy = 1
PrimaryGOPLength    = 10
NumRefPrimary       = 1

#####
# Search Range Restriction / RD Optimization
#####
RestrictSearchRange = 2
RDOptimization      = 1
I16RDOpt            = 0
SubMBCodingState    = 1

```

```

DistortionSSIM          = 0
DistortionMS_SSIM       = 0
SSIMOverlapSize        = 8
DistortionYUVtoRGB      = 0
CtxAdptLagrangeMult     = 0
FastCrIntraDecision     = 1
DisableThresholding     = 0
SkipIntraInInterSlices = 0
WeightY                 = 1
WeightCb                 = 1
WeightCr                 = 1

#####
# Explicit Lambda Usage
#####
UseExplicitLambdaParams = 0
UpdateLambdaChromaME   = 0
FixedLambdaISlice      = 0.1
FixedLambdaPSlice      = 0.1

LambdaWeightISlice     = 0.65
LambdaWeightPSlice     = 0.68

LossRateA               = 5
LossRateB               = 0
LossRateC               = 0
FirstFrameCorrect       = 0
NumberOfDecoders        = 30
RestrictRefFrames       = 0

#####
# Additional Stuff
#####
UseConstrainedIntraPred = 0

NumberOfLeakyBuckets    = 8
LeakyBucketRateFile     = "leakybucketrate.cfg"
LeakyBucketParamFile    = "leakybucketparam.cfg"

NumFramesInELayerSubSeq = 0

SparePictureOption      = 0
SparePictureDetectionThr = 6
SparePicturePercentageThr = 92

PicOrderCntType         = 0

#####
#Rate control
#####
RateControlEnable       = 1
Bitrate                 = 64000
InitialQP               = 0
BasicUnit               = 0
ChannelType             = 0
RCUpdateMode            = 0
RCISliceBitRatio        = 1.0
RCBSliceBitRatio0       = 0.5
RCBSliceBitRatio1       = 0.25
RCBSliceBitRatio2       = 0.25
RCBSliceBitRatio3       = 0.25
RCBSliceBitRatio4       = 0.25
RCBoverPRatio           = 0.45
RCIOverPRatio           = 3.80
RCMinQPPSlice           = 8
RCMaxQPPSlice           = 44
RCMinQPISlice           = 8

```

```

RCMaxQPISlice          = 36

#####
#Fast Mode Decision
#####
EarlySkipEnable        = 0
SelectiveIntraEnable    = 0

ReportFrameStats       = 0
DisplayEncParams       = 0
Verbose                = 1

#####
#Rounding Offset control
#####
OffsetMatrixPresentFlag = 0
QOffsetMatrixFile       = "q_offset.cfg"

AdaptiveRounding        = 1
AdaptRoundingFixed      = 1
AdaptRndPeriod          = 16

AdaptRndChroma          = 1

AdaptRndWFactorIRef     = 4
AdaptRndWFactorPRef     = 4
AdaptRndWFactorINRef    = 4
AdaptRndWFactorPNRef    = 4

AdaptRndCrWFactorIRef   = 4
AdaptRndCrWFactorPRef   = 4
AdaptRndCrWFactorINRef  = 4
AdaptRndCrWFactorPNRef  = 4

#####
#Fast Motion Estimation Control Parameters
#####
SearchMode              = 0

UMHexDSR                = 1
UMHexScale               = 3

EPZSPattern              = 2
EPZSDualRefinement       = 3
EPZSFixedPredictors      = 2
EPZSTemporal             = 1
EPZSSpatialMem           = 1
EPZSBlockType            = 1
EPZSMinThresScale        = 0
EPZSMedThresScale        = 1
EPZSMaxThresScale        = 2
EPZSSubPelME             = 1
EPZSSubPelMEBiPred       = 1
EPZSSubPelThresScale     = 2
EPZSSubPelGrid           = 1

#####
# SEI Parameters
#####
GenerateSEIMessage       = 0
SEIMessageText           = "H.264/AVC Encoder"

UseMVLimits              = 0
SetMVXLimit              = 512
SetMVYLimit              = 512

#####

```

```
# VUI Parameters
#####
# the variables below do not affect encoding and decoding
# (many are dummy variables but others can be useful when supported by the decoder)

EnableVUISupport = 0
```

2 Multiple Slices

Listing I.2: Configuration file with multiple slices

```
#####
# Error Resilience / Slices
#####
SliceMode = 1
SliceArgument = 11 # 1 Picture = 9 Slices
```

3 Multiple Slices and FMO

Listing I.3: Configuration file with multiple slices and FMO

```
#####
# Error Resilience / Slices
#####
SliceMode = 1
SliceArgument = 11 # 1 Picture = 9 Slices

num_slice_groups_minus1 = 1 # no FMO
slice_group_map_type = 1 # checkerboard pattern
```

4 Multiple Slices, FMO and Forced Intra Refresh

Listing I.4: Configuration file with multiple slices, FMO and forced intra refresh

```
#####
# Encoder Control
#####

RandomIntraMBRefresh = 5 # force 5 intra MBs per picture

#####
# Error Resilience / Slices
#####
SliceMode = 1
SliceArgument = 11 # 1 Picture = 9 Slices

num_slice_groups_minus1 = 1 # no FMO
slice_group_map_type = 1 # checkerboard pattern
```

ANNEX II

RANDOM TAIL ASSUMPTION

VLCs are engineered to award the shortest binary representations to the most probable values. From a compression standpoint, this design reduces the number of bits that have to be sent. However, from a correction standpoint, the design penalizes longer, less probable codewords. An example here works best to illustrate our point. To concentrate on the subject at hand, LLRs aren't considered.

Table-A II-1 Subset of a fictive codebook

Codeword	Binary representation	Length L
A	1	1
B	010	3
C	00111	5

Table-A II-1 presents a codebook containing three valid codewords, and their binary representation. Such a representation would be obtained with unsigned Exponential Golomb Codes. Now, consider that the bits 00111 were sent, and that the bits 00011 were received (the third bit is erroneous). Not only does the received sequence differs from all three entries in Table-A II-1, but modifying (flipping) any of the first three bits would lead us to find one of the entries. Note that there would be unused bits in two out of the three cases. However, the decoder has no way of knowing how many bits are associated to each codeword. Thus, the fact that there are unused bits is irrelevant in this case.

Table-A II-2 presents the likelihood of each symbol. The values listed in the second column represent the probability of each symbol given the previously decoded codewords. The third column indicates the number of matching bits M . The fourth column presents the number of differing bits E . Note that the sum of the values in columns three and four amount to the length of the codeword's binary representation L in Table-A II-1. The fifth column represents the bit modification likelihood. An estimated BER of 0.01 was used to obtain the results. The

Table-A II-2 A first example without the random tail assumption

Symbol	Conditional symbol probability $P(\hat{c}_{i,j} \cap_{k \in K_i} c_k^*)$	Matches M	Errors E	Bit modification likelihood $P(\tilde{S} \hat{c}_{i,j})$	Symbol likelihood $P(\tilde{S})$
A	0.50	0	1	$0.99^0 \times 0.01^1$	0.0050
B	0.33	2	1	$0.99^2 \times 0.01^1$	0.0032
C	0.17	4	1	$0.99^4 \times 0.01^1$	0.0016

likelihood that a bit is intact (1 - BER) is raised to the power M , while the likelihood that the bit is erroneous is raised to the power E . The last column is the product of second and fifth columns. The symbol associated to the highest value in the last column is considered the most likely symbol and is the value selected by the proposed decoder. Without the random tail assumption, the winning codeword is A (the wrong answer).

The flaw here has to do with the fact that longer codewords are more exposed to transmission errors. What's worse is that errors at the beginning of longer codewords convert them into shorter ones. Such a scenario is difficult to deal with unless the longer codeword's probability is far greater than the shorter one's given the previously decoded values. Note that without LLRs, this is even more difficult to distinguish, as our confidence in each bit follows a uniform distribution.

The uninterpreted bits following the shorter codewords need to be accounted for so that the same number of Bernoulli trials are considered. The random tail assumption does exactly this. Assuming that a video encoder is a good binary source, the 0s and 1s outputted can be considered equally likely.

The assumption conveniently deals with the cases where flipping the wrong bit creates a shorter codeword. Table-A II-3 presents the adjusted values initially evaluated in Table-A II-2. The first five columns hold the same meaning as before. The sixth column represent the random tail assumption where the probability of 0.5 (equally likely values) is raised to the power $L_{max} - (M + E)$, where L_{max} is the length of the largest codeword (which is 5 in our example). Given that we know that we received five bits, and that the length of each codeword is the sum of

Table-A II-3 An example with the random tail assumption

Symbol	Conditional symbol probability $P(\hat{c}_{i,j} \cap_{k \in K_i} c_k^*)$	Matches M	Errors E	Bit modification likelihood $P(\tilde{S} \hat{c}_{i,j})$	Tail	Symbol likelihood $P(\tilde{S})$
A	0.50	0	1	$0.99^0 \times 0.01^1$	0.5^4	0.0003
B	0.33	2	1	$0.99^2 \times 0.01^1$	0.5^2	0.0008
C	0.17	4	1	$0.99^4 \times 0.01^1$	0.5^0	0.0011

columns three and four, the exponent in column six is the difference between the received bits and the length of the binary representation of the codewords. The last column is now the product of the second, fifth and sixth columns. This time, we would select codeword C (the correct answer), as it is the value with the highest likelihood.

ANNEX III

EXPERIMENTAL TEST SET

In this annex, the configuration files used to generate the intact sequences are presented. To save space, a single complete configuration file is presented. The modifications to be brought to the file for the other test sequences are then listed. Also, the comments associated to the parameters were removed to lighten the presentation. The meaning of each parameter can be found with the default configuration parameter files shipped with the JM reference software.

1 Complete configuration file

Listing III.1: Complete configuration file for the *city* sequence coded at 1000 kbps

```
# New Input File Format is as follows
# <ParameterName> = <ParameterValue> # Comment
#
# See configfile.h for a list of supported ParameterNames
#
# For bug reporting and known issues see:
# https://ipbt.hhi.fraunhofer.de

#####
# Files
#####
InputFile           = "city_4cif.yuv"
InputHeaderLength   = 0
StartFrame          = 0
FramesToBeEncoded   = 120
FrameRate           = 30.0
SourceWidth         = 704
SourceHeight        = 576
SourceResize        = 0
OutputWidth         = 704
OutputHeight        = 576

TraceFile           = "trace_enc.txt"
ReconFile            = "city_1000kbps_200mtu.yuv"
OutputFile          = "city_1000kbps_200mtu.264"
StatsFile           = "stats.dat"

#####
# Encoder Control
#####
ProfileIDC          = 66
IntraProfile        = 0
LevelIDC            = 40

IntraPeriod         = 30
IDRPeriod           = 0
AdaptiveIntraPeriod = 0
AdaptiveIDRPeriod   = 0
IntraDelay          = 0
```

```

EnableIDRGOP          = 0
EnableOpenGOP         = 0
QPISlice              = 33
QPPSlice              = 33
FrameSkip             = 0
ChromaQPOffset        = 0

DisableSubpelME        = 0
SearchRange           = 32

MEDistortionFPel      = 0
MEDistortionHPel      = 2
MEDistortionQPel      = 2
MDDistortion          = 2
SkipDeBlockNonRef     = 0
ChromaMCBuffer        = 1
ChromaMEEEnable       = 0
ChromaMEWeight        = 1

NumberReferenceFrames = 1

PList0References      = 0
Log2MaxFNumMinus4     = 0
Log2MaxPOCLsbMinus4  = -1

GenerateMultiplePPS   = 0
SendAUD               = 0
ResendSPS             = 0
ResendPPS             = 0

MbLineIntraUpdate     = 0
RandomIntraMBRefresh  = 0

#####
# PSlice Mode types
#####
PSliceSkip            = 1
PSliceSearch16x16     = 1
PSliceSearch16x8      = 1
PSliceSearch8x16      = 1
PSliceSearch8x8       = 1
PSliceSearch8x4       = 1
PSliceSearch4x8       = 1
PSliceSearch4x4       = 1

DisableIntra4x4        = 0
DisableIntra16x16     = 0
DisableIntraInInter    = 0
IntraDisableInterOnly  = 0
Intra4x4ParDisable     = 0
Intra4x4DiagDisable    = 0
Intra4x4DirDisable     = 0
Intra16x16ParDisable   = 0
Intra16x16PlaneDisable = 0
ChromaIntraDisable     = 0
EnableIPCM             = 1

DisposableP           = 0
DispQPPOffset         = 0

PreferDispOrder        = 1
PreferPowerOfTwo       = 0
FrmStructBufferLength  = 16

ChangeQPFrame          = 0
ChangeQPI              = 0
ChangeQPP              = 0

```

```

ChangeQPB          = 0
ChangeQPSI         = 0
ChangeQPSP         = 0
#####
# Output Control, NALs
#####

OutFileMode        = 1

#####
# Picture based Multi-pass encoding
#####

RDPictureDecision  = 0
RDPSPliceBTest     = 0
RDPictureMaxPassISlice = 1
RDPictureMaxPassPSlice = 2
RDPictureMaxPassBSlice = 3
RDPictureFrameQPPSlice = 0
RDPictureFrameQPBSlice = 0
RDPictureDeblocking = 0
RDPictureDirectMode = 0

#####
# Deblocking filter parameters
#####

DFParametersFlag    = 0

DFDisableRefISlice  = 0
DFAlphaRefISlice    = 0
DFBetaRefISlice     = 0
DFDisableNRefISlice = 0
DFAlphaNRefISlice   = 0
DFBetaNRefISlice    = 0
DFDisableRefPSlice  = 0
DFAlphaRefPSlice    = 0
DFBetaRefPSlice     = 0
DFDisableNRefPSlice = 0
DFAlphaNRefPSlice   = 0
DFBetaNRefPSlice    = 0

#####
# Error Resilience / Slices
#####

SliceMode           = 2
SliceArgument        = 200

num_slice_groups_minus1 = 0
slice_group_map_type   = 0

slice_group_change_direction_flag = 0

slice_group_change_rate_minus1 = 85
SliceGroupConfigFileName      = "sg0conf.cfg"

UseRedundantPicture = 0
NumRedundantHierarchy = 1
PrimaryGOPLength    = 10

NumRefPrimary       = 1

#####
# Search Range Restriction / RD Optimization
#####

```

```

RestrictSearchRange      = 0
RDOptimization           = 1

I16RDOpt                = 0

SubMBCodingState         = 1

DistortionSSIM           = 0
DistortionMS_SSIM       = 0
SSIMOverlapSize         = 8
DistortionYUVtoRGB       = 0
CtxAdptLagrangeMult      = 0

FastCrIntraDecision      = 1
DisableThresholding      = 0
SkipIntraInInterSlices  = 0
WeightY                  = 1
WeightCb                 = 1
WeightCr                 = 1

#####
# Explicit Lambda Usage
#####
UseExplicitLambdaParams  = 0
UpdateLambdaChromaME    = 0
FixedLambdaISlice       = 0.1
FixedLambdaPSlice       = 0.1

LambdaWeightISlice      = 0.65
LambdaWeightPSlice      = 0.68

LossRateA               = 5
LossRateB               = 0
LossRateC               = 0
FirstFrameCorrect       = 0
NumberOfDecoders        = 30
RestrictRefFrames       = 0

#####
# Additional Stuff
#####

UseConstrainedIntraPred = 0

NumberOfLeakyBuckets    = 8
LeakyBucketRateFile     = "leakybucketrate.cfg"
LeakyBucketParamFile    = "leakybucketparam.cfg"

NumFramesInELayerSubSeq = 0

SparePictureOption      = 0
SparePictureDetectionThr = 6
SparePicturePercentageThr = 92

PicOrderCntType         = 0

#####
#Rate control
#####

RateControlEnable       = 0
Bitrate                 = 45020
InitialQP               = 0

BasicUnit               = 0
ChannelType             = 0
RCUpdateMode            = 0

```

```

RCISliceBitRatio      = 1.0
RCBSliceBitRatio0     = 0.5
RCBSliceBitRatio1     = 0.25
RCBSliceBitRatio2     = 0.25
RCBSliceBitRatio3     = 0.25
RCBSliceBitRatio4     = 0.25
RCBoverPRatio         = 0.45
RCIooverPRatio        = 3.80
RCMinQPPSlice         = 8
RCMaxQPPSlice         = 44
RCMinQPISlice         = 8
RCMaxQPISlice         = 36

#####
#Fast Mode Decision
#####
EarlySkipEnable       = 0
SelectiveIntraEnable   = 0

ReportFrameStats      = 0
DisplayEncParams      = 0
Verbose               = 1

#####
#Rounding Offset control
#####

OffsetMatrixPresentFlag = 0
QOffsetMatrixFile       = "q_offset.cfg"

AdaptiveRounding       = 1
AdaptRoundingFixed     = 1
AdaptRndPeriod         = 16

AdaptRndChroma         = 1

AdaptRndWFactorIRef    = 4
AdaptRndWFactorPRef    = 4
AdaptRndWFactorINRef   = 4
AdaptRndWFactorPNRef   = 4

AdaptRndCrWFactorIRef  = 4
AdaptRndCrWFactorPRef  = 4
AdaptRndCrWFactorINRef = 4
AdaptRndCrWFactorPNRef = 4

#####
#Fast Motion Estimation Control Parameters
#####

SearchMode             = 1

UMHexDSR               = 1
UMHexScale             = 3

EPZSPattern            = 2
EPZSDualRefinement     = 3
EPZSFixedPredictors    = 2
EPZSTemporal           = 1
EPZSSpatialMem         = 1
EPZSBlockType          = 1
EPZSMinThresScale      = 0
EPZSMedThresScale      = 1
EPZSMaxThresScale      = 2
EPZSSubPelME           = 1
EPZSSubPelMEBiPred     = 1

```

```

EPZSSubPelThresScale      = 2
EPZSSubPelGrid            = 1

#####
# SEI Parameters
#####

GenerateSEIMessage        = 0
SEIMessageText            = "H.264/AVC Encoder"

UseMVLimits               = 0                # Use MV Limits
SetMVXLimit               = 512              # Horizontal MV Limit (in integer units)
SetMYYLimit               = 512              # Vertical MV Limit (in integer units)

#####
# VUI Parameters
#####
# the variables below do not affect encoding and decoding
# (many are dummy variables but others can be useful when supported by the decoder)

EnableVUISupport          = 0                # Enable VUI Parameters

```

2 Other 4CIF sequences

Listing III.2: Partial configuration file for the *city* sequence coded at 1200 kbps

```

#####
# Files
#####
ReconFile                 = "city_1200kbps_200mtu.yuv"
OutputFile                 = "city_1200kbps_200mtu.264"

#####
# Encoder Control
#####
QPISlice                  = 32
QPPSlice                   = 32

```

Listing III.3: Partial configuration file for the *city* sequence coded at 1500 kbps

```

#####
# Files
#####
ReconFile                 = "city_1500kbps_200mtu.yuv"
OutputFile                 = "city_1500kbps_200mtu.264"

#####
# Encoder Control
#####
QPISlice                  = 31
QPPSlice                   = 31

```

Listing III.4: Partial configuration file for the *crew* sequence coded at 1000 kbps

```

#####
# Files
#####

```

```

InputFile          = "crew_4cif.yuv"

ReconFile          = "crew_1000kbps_200mtu.yuv"
OutputFile         = "crew_1000kbps_200mtu.264"

#####
# Encoder Control
#####
QPISlice           = 36
QPPSlice           = 36

#####
# Error Resilience / Slices
#####

SliceArgument      = 208    # A bug in the encoder prevents the use of 200

```

Listing III.5: Partial configuration file for the *crew* sequence coded at 1200 kbps

```

#####
# Files
#####
InputFile          = "crew_4cif.yuv"

ReconFile          = "crew_1200kbps_200mtu.yuv"
OutputFile         = "crew_1200kbps_200mtu.264"

#####
# Encoder Control
#####
QPISlice           = 35
QPPSlice           = 35

```

Listing III.6: Partial configuration file for the *crew* sequence coded at 1500 kbps

```

#####
# Files
#####
InputFile          = "crew_4cif.yuv"

ReconFile          = "crew_1500kbps_200mtu.yuv"
OutputFile         = "crew_1500kbps_200mtu.264"

#####
# Encoder Control
#####
QPISlice           = 33
QPPSlice           = 33

```

Listing III.7: Partial configuration file for the *harbour* sequence coded at 1000 kbps

```

#####
# Files
#####
InputFile          = "harbour_4cif.yuv"

ReconFile          = "harbour_1000kbps_200mtu.yuv"
OutputFile         = "harbour_1000kbps_200mtu.264"

#####

```

```
# Encoder Control
#####
QPISlice      = 39
QPPSlice      = 39
```

Listing III.8: Partial configuration file for the *harbour* sequence coded at 1200 kbps

```
#####
# Files
#####
InputFile      = "harbour_4cif.yuv"

ReconFile      = "harbour_1200kbps_200mtu.yuv"
OutputFile     = "harbour_1200kbps_200mtu.264"

#####
# Encoder Control
#####
QPISlice      = 38
QPPSlice      = 38
```

Listing III.9: Partial configuration file for the *harbour* sequence coded at 1500 kbps

```
#####
# Files
#####
InputFile      = "harbour_4cif.yuv"

ReconFile      = "harbour_1500kbps_200mtu.yuv"
OutputFile     = "harbour_1500kbps_200mtu.264"

#####
# Encoder Control
#####
QPISlice      = 37
QPPSlice      = 37
```

Listing III.10: Partial configuration file for the *ice* sequence coded at 1000 kbps

```
#####
# Files
#####
InputFile      = "ice_4cif.yuv"          # Input sequence

ReconFile      = "ice_1000kbps_200mtu.yuv"
OutputFile     = "ice_1000kbps_200mtu.264"

#####
# Encoder Control
#####
QPISlice      = 29
QPPSlice      = 29

#####
# Error Resilience / Slices
#####

SliceArgument  = 192    # A bug in the encoder prevents the use of 200
```


Listing III.11: Partial configuration file for the *ice* sequence coded at 1200 kbps

```
#####
# Files
#####
InputFile           = "ice_4cif.yuv"           # Input sequence

ReconFile           = "ice_1200kbps_200mtu.yuv"
OutputFile          = "ice_1200kbps_200mtu.264"

#####
# Encoder Control
#####
QPISlice            = 28
QPPSlice            = 28

#####
# Error Resilience / Slices
#####

SliceArgument       = 192    # A bug in the encoder prevents the use of 200
```

Listing III.12: Partial configuration file for the *ice* sequence coded at 1500 kbps

```
#####
# Files
#####
InputFile           = "ice_4cif.yuv"           # Input sequence

ReconFile           = "ice_1500kbps_200mtu.yuv"
OutputFile          = "ice_1500kbps_200mtu.264"

#####
# Encoder Control
#####
QPISlice            = 26
QPPSlice            = 26
```

Listing III.13: Partial configuration file for the *soccer* sequence coded at 1000 kbps

```
#####
# Files
#####
InputFile           = "soccer_4cif.yuv"

ReconFile           = "soccer_1000kbps_200mtu.yuv"
OutputFile          = "soccer_1000kbps_200mtu.264"

#####
# Encoder Control
#####
QPISlice            = 37
QPPSlice            = 37
```

Listing III.14: Partial configuration file for the *soccer* sequence coded at 1200 kbps

```
#####
# Files
#####
```

```

InputFile          = "soccer_4cif.yuv"

ReconFile          = "soccer_1200kbps_200mtu.yuv"
OutputFile         = "soccer_1200kbps_200mtu.264"

#####
# Encoder Control
#####
QPISlice           = 36
QPPSlice           = 36

```

Listing III.15: Partial configuration file for the *soccer* sequence coded at 1500 kbps

```

#####
# Files
#####
InputFile          = "soccer_4cif.yuv"

ReconFile          = "soccer_1500kbps_200mtu.yuv"
OutputFile         = "soccer_1500kbps_200mtu.264"

#####
# Encoder Control
#####
QPISlice           = 34
QPPSlice           = 34

```

3 NTSC sequences

Listing III.16: Partial configuration file for the *driving* sequence coded at 1000 kbps

```

#####
# Files
#####
InputFile          = "driving_dvd-ntsc.yuv"
SourceWidth        = 720    # Source frame width
SourceHeight       = 480    # Source frame height

ReconFile          = "driving_1000kbps_200mtu.yuv"
OutputFile         = "driving_1000kbps_200mtu.264"

#####
# Encoder Control
#####
QPISlice           = 38
QPPSlice           = 38

```

Listing III.17: Partial configuration file for the *driving* sequence coded at 1200 kbps

```

#####
# Files
#####
InputFile          = "driving_dvd-ntsc.yuv"
SourceWidth        = 720    # Source frame width
SourceHeight       = 480    # Source frame height

ReconFile          = "driving_1200kbps_200mtu.yuv"

```

```

OutputFile          = "driving_1200kbps_200mtu.264"

#####
# Encoder Control
#####
QPISlice            = 37
QPPSlice            = 37

```

Listing III.18: Partial configuration file for the *driving* sequence coded at 1500 kbps

```

#####
# Files
#####
InputFile           = "driving_dvd-ntsc.yuv"
SourceWidth         = 720      # Source frame width
SourceHeight        = 480      # Source frame height

ReconFile            = "driving_1500kbps_200mtu.yuv"
OutputFile           = "driving_1500kbps_200mtu.264"

#####
# Encoder Control
#####
QPISlice            = 36
QPPSlice            = 36

```

Listing III.19: Partial configuration file for the *opening-ceremony* sequence coded at 1000 kbps

```

#####
# Files
#####
InputFile           = "opening-ceremony_dvd-ntsc.yuv"
SourceWidth         = 720      # Source frame width
SourceHeight        = 480      # Source frame height

ReconFile            = "opening-ceremony_1000kbps_200mtu.yuv"
OutputFile           = "opening-ceremony_1000kbps_200mtu.264"

#####
# Encoder Control
#####
QPISlice            = 37
QPPSlice            = 37

```

Listing III.20: Partial configuration file for the *opening-ceremony* sequence coded at 1200 kbps

```

#####
# Files
#####
InputFile           = "opening-ceremony_dvd-ntsc.yuv"
SourceWidth         = 720      # Source frame width
SourceHeight        = 480      # Source frame height

ReconFile            = "opening-ceremony_1200kbps_200mtu.yuv"
OutputFile           = "opening-ceremony_1200kbps_200mtu.264"

```

```
#####
# Encoder Control
#####
QPISlice           = 36
QPPSslice          = 36
#####
```

Listing III.21: Partial configuration file for the *opening-ceremony* sequence coded at 1500 kbps

```
#####
# Files
#####
InputFile           = "opening-ceremony_dvd-ntsc.yuv"
SourceWidth         = 720    # Source frame width
SourceHeight        = 480    # Source frame height

ReconFile           = "opening-ceremony_1500kbps_200mtu.yuv"
OutputFile          = "opening-ceremony_1500kbps_200mtu.264"

#####
# Encoder Control
#####
QPISlice           = 34
QPPSslice          = 34
#####
```

Listing III.22: Partial configuration file for the *whale-show* sequence coded at 1000 kbps

```
#####
# Files
#####
InputFile           = "whale-show_dvd-ntsc.yuv"
SourceWidth         = 720    # Source frame width
SourceHeight        = 480    # Source frame height

ReconFile           = "whale-show_1000kbps_200mtu.yuv"
OutputFile          = "whale-show_1000kbps_200mtu.264"

#####
# Encoder Control
#####
QPISlice           = 43
QPPSslice          = 43
#####
```

Listing III.23: Partial configuration file for the *whale-show* sequence coded at 1200 kbps

```
#####
# Files
#####
InputFile           = "whale-show_dvd-ntsc.yuv"
SourceWidth         = 720    # Source frame width
SourceHeight        = 480    # Source frame height

ReconFile           = "whale-show_1200kbps_200mtu.yuv"
OutputFile          = "whale-show_1200kbps_200mtu.264"

#####
# Encoder Control
#####
```

```
#####
QPISlice           = 42
QPPSlice           = 42
#####
```

Listing III.24: Partial configuration file for the *whale-show* sequence coded at 1500 kbps

```
#####
# Files
#####
InputFile           = "whale-show_dvd-ntsc.yuv"
SourceWidth         = 720    # Source frame width
SourceHeight        = 480    # Source frame height

ReconFile           = "whale-show_1500kbps_200mtu.yuv"
OutputFile          = "whale-show_1500kbps_200mtu.264"

#####
# Encoder Control
#####
QPISlice            = 41
QPPSlice            = 41
#####
```

4 PAL sequence

Listing III.25: Partial configuration file for the *walk* sequence coded at 1000 kbps

```
#####
# Files
#####
InputFile           = "walk_pal.yuv"
SourceWidth         = 720
SourceHeight        = 576

ReconFile           = "walk_1000kbps_200mtu.yuv"
OutputFile          = "walk_1000kbps_200mtu.264"

#####
# Encoder Control
#####
QPISlice            = 42
QPPSlice            = 42

#####
# Error Resilience / Slices
#####
SliceArgument       = 208    # A bug in the encoder prevents the use of 200
#####
```

Listing III.26: Partial configuration file for the *walk* sequence coded at 1200 kbps

```
#####
# Files
#####
InputFile           = "walk_pal.yuv"
SourceWidth         = 720
SourceHeight        = 576
#####
```

```

ReconFile          = "walk_1200kbps_200mtu.yuv"
OutputFile         = "walk_1200kbps_200mtu.264"

#####
# Encoder Control
#####
QPISlice           = 41
QPPSlice           = 41

```

Listing III.27: Partial configuration file for the *walk* sequence coded at 1500 kbps

```

#####
# Files
#####
InputFile          = "walk_pal.yuv"
SourceWidth        = 720
SourceHeight       = 576

ReconFile          = "walk_1500kbps_200mtu.yuv"
OutputFile         = "walk_1500kbps_200mtu.264"

#####
# Encoder Control
#####
QPISlice           = 40
QPPSlice           = 40

```

ANNEX IV

MATLAB NETWORK SIMULATOR

The MATLAB code used to simulate transmission of H.264 slices over an unreliable network is presented here (Listing IV.1). The use of the `comm.LDPCDecoder` object requires the use of MATLAB R2012a. The complementary functions to extract entries (Listing IV.2) from files created with the JM (OutputMode = RTP), and to write LLR values (Listing IV.3) to a file are also given.

Listing IV.1: Unreliable network simulator

```
function h264break(inputfile,outputfile,mtu,rate,snr,frame)
%H264BREAK Corrupt packets associated to frame
% inputfile Complete path to the inputfile
% outputfile Complete path to the outputfile
% mtu Maximum Transmission Unit (in bits)
% snr Channel SNR (in dB)
% frame Index of the frame to corrupt

parmat = sparse(cyclgen(mtu./rate,cyclpoly(mtu./rate,mtu))); % parity-check matrix

hEnc = comm.LDPCEncoder('ParityCheckMatrix',parmat); % channel encoder

hMod = comm.BPSKModulator; % channel modulator

hChan = comm.AWGNChannel( ... % random noise channel
    'NoiseMethod','Signal_to_noise_ratio_(SNR)', ...
    'SNR',snr);

hDemod = comm.BPSKDemodulator(... % channel demodulator
    'DecisionMethod','Approximate_log-likelihood_ratio', ... % use approx LLRs
    'VarianceSource','Property', ... % enable 'Variance' property
    'Variance', 1/10^(hChan.SNR/10));

hDec = comm.LDPCDecoder(... % channel decoder
    'ParityCheckMatrix',parmat,...
    'OutputValue','Information_part',... % output bits individually
    'DecisionMethod','Soft_decision'); % share LLRs

B = h264boundaries(inputfile);
B = B(3:end); % ignore SPS and PPS

in = fopen(inputfile,'r');
out = fopen(outputfile,'w');

for k = 1:B(frame)-1 % good channel conditions
    [h,p]=h264read(in); % fetch data
    p = [p; zeros(mtu-length(p),1)]; % add padding
    encodedData = step(hEnc, logical(p)); % apply FEC
    modSignal = step(hMod, encodedData); % transmission
    demodSignal = step(hDemod, modSignal); % reception
    softDecisions = step(hDec, demodSignal); % remove FEC, keep LLRs
    llrwrite(out,h,softDecisions(1:h(1)*8));
end
```

```

for k = B(frame):B(frame+1)-1
    [h,p]=h264read(in);
    p = [p; zeros(mtu-length(p),1)];
    encodedData = step(hEnc, logical(p));
    modSignal = step(hMod, encodedData);
    receivedSignal = step(hChan, modSignal);
    demodSignal = step(hDemod, receivedSignal);
    softDecisions = step(hDec, demodSignal);
    hardDecisions = softDecisions < 0;
    ind=find(p-hardDecisions,1,'first');
    if ~isempty(ind), h(2) = 0; end
    llrwrite(out,h,softDecisions(1:h(1)*8));
end

while 1
    [h,p]=h264read(in);
    if isempty(h), break, end
    p = [p; zeros(mtu-length(p),1)];
    encodedData = step(hEnc, logical(p));
    modSignal = step(hMod, encodedData);
    demodSignal = step(hDemod, modSignal);
    softDecisions = step(hDec, demodSignal);
    llrwrite(out,h,softDecisions(1:h(1)*8));
end

```

Listing IV.2: H.264 RTP packet extraction (hard decisions)

```

function [h,p]=h264read(fid)
%H264READ Return next RTP packet from H.264 stream (file)

h=fread(fid,2,'uint32',0,'ieee-le');
if isempty(h), p=[]; return, end
p=fread(fid,h(1)*8,'ubit1',0,'ieee-be');

```

Listing IV.3: H.264 RTP packet creation (soft decisions)

```

function llrwrite(fid,h,p)
%LLRWRITE Write LLR values to H.264 stream

fwrite(fid,h,'uint32',0,'ieee-le');
fwrite(fid,p,'double',0,'ieee-le');

```


ANNEX V

EXPERIMENTAL OBSERVATIONS

The detailed experimental observations are presented in Tables V.1, V.2, V.3, for the scenarios at 1000 kbps, 1200 kbps, and 1500 kbps, respectively. The content was used to present the tables and graphs in Chapter 5.

Table V.1 Detailed experimental results for 1000 kbps

Sequence	SNR (dB)	Frame	Run	JM 16.0	STBMA+PDE	SO-MLD
city	4	62	1	23.03	23.03	25.66
city	4	62	2	24.36	25.53	27.31
city	4	62	3	23.76	24.40	24.69
city	4	62	4	23.63	24.20	25.42
city	4	62	5	23.48	26.78	24.18
city	4	62	6	23.34	24.24	24.29
city	4	62	7	23.36	24.62	25.81
city	4	62	8	25.07	28.35	26.89
city	4	62	9	24.31	28.17	26.73
city	4	62	10	23.36	24.62	24.59
city	4	64	1	23.72	23.72	26.00
city	4	64	2	25.01	27.31	27.23
city	4	64	3	24.11	25.11	25.52
city	4	64	4	24.55	28.80	25.57
city	4	64	5	24.52	27.43	27.13
city	4	64	6	24.11	24.78	27.68
city	4	64	7	24.45	29.97	26.72
city	4	64	8	24.13	25.25	27.08
city	4	64	9	25.30	29.40	27.67
city	4	64	10	23.72	23.72	26.57
city	4	77	1	27.48	25.15	29.06
city	4	77	2	27.50	26.21	28.02
city	4	77	3	27.48	27.70	27.86
city	4	77	4	27.61	28.12	28.07
city	4	77	5	27.58	28.93	28.27
city	4	77	6	27.25	27.25	28.12
city	4	77	7	27.68	28.46	28.05

Continued on next page

Table V.1 – continued from previous page

Sequence	SNR (dB)	Frame	Run	JM 16.0	STBMA+PDE	SO-MLD
city	4	77	8	27.46	27.96	27.06
city	4	77	9	27.43	27.60	27.94
city	4	77	10	27.68	27.59	27.96
city	4	78	1	25.93	25.80	26.87
city	4	78	2	25.56	25.61	27.69
city	4	78	3	25.76	27.65	27.59
city	4	78	4	25.18	25.18	26.81
city	4	78	5	25.72	25.26	28.04
city	4	78	6	25.29	27.02	26.60
city	4	78	7	26.04	26.54	28.31
city	4	78	8	25.62	24.57	28.57
city	4	78	9	25.44	25.11	26.99
city	4	78	10	25.80	29.78	27.26
city	4	80	1	25.49	26.74	27.37
city	4	80	2	24.47	26.54	26.31
city	4	80	3	24.82	27.99	27.81
city	4	80	4	24.28	24.28	25.61
city	4	80	5	25.00	27.20	26.52
city	4	80	6	25.33	26.35	27.58
city	4	80	7	25.10	29.29	26.89
city	4	80	8	24.65	24.65	26.66
city	4	80	9	24.63	24.27	26.04
city	4	80	10	25.04	27.50	27.11
city	4	87	1	25.00	26.30	26.33
city	4	87	2	25.18	26.83	26.60
city	4	87	3	25.59	27.03	28.09
city	4	87	4	25.51	27.29	26.68
city	4	87	5	26.09	27.15	28.82
city	4	87	6	25.65	27.31	27.86
city	4	87	7	25.61	27.39	27.79
city	4	87	8	25.16	26.84	26.88
city	4	87	9	25.21	26.14	27.75
city	4	87	10	25.57	27.34	26.70
city	4	90	1	23.96	26.68	26.52
city	4	90	2	24.11	29.19	26.19
city	4	90	3	24.03	25.58	24.91
city	4	90	4	23.83	26.88	26.00
city	4	90	5	23.94	25.91	25.06
city	4	90	6	24.32	27.02	25.75
city	4	90	7	23.91	26.62	26.00
city	4	90	8	23.70	25.10	25.66

Continued on next page

Table V.1 – continued from previous page

Sequence	SNR (dB)	Frame	Run	JM 16.0	STBMA+PDE	SO-MLD
city	5	101	2	27.04	29.49	29.54
city	5	101	3	29.28	31.21	32.07
city	5	101	4	27.73	31.13	30.99
city	5	101	5	26.41	29.69	30.37
city	5	101	6	29.20	31.17	31.31
city	5	101	7	29.50	30.65	31.76
city	5	101	8	27.11	29.99	28.83
city	5	101	9	29.66	31.83	30.85
city	5	101	10	26.33	28.44	29.63
crew	4	65	1	27.60	29.07	29.03
crew	4	65	2	26.66	26.64	26.44
crew	4	65	3	27.29	28.58	27.13
crew	4	65	4	27.58	28.06	28.02
crew	4	65	5	27.34	28.24	27.94
crew	4	65	6	27.41	28.22	28.10
crew	4	65	7	27.03	27.38	25.76
crew	4	65	8	26.71	26.65	26.64
crew	4	65	9	27.50	28.98	28.05
crew	4	65	10	27.06	27.24	28.08
crew	4	67	1	27.01	28.05	27.49
crew	4	67	2	26.85	26.91	27.46
crew	4	67	3	27.09	27.49	28.51
crew	4	67	4	26.86	27.28	27.92
crew	4	67	5	26.77	26.86	27.75
crew	4	67	6	26.71	26.71	26.94
crew	4	67	7	27.27	27.64	28.69
crew	4	67	8	27.18	27.56	27.86
crew	4	67	9	27.46	26.90	28.22
crew	4	67	10	26.53	26.53	26.98
crew	4	68	1	26.91	27.35	27.24
crew	4	68	2	27.49	28.35	28.26
crew	4	68	3	26.80	27.17	27.69
crew	4	68	4	27.33	28.14	27.98
crew	4	68	5	26.58	26.58	27.35
crew	4	68	6	27.17	27.53	27.69
crew	4	68	7	27.14	27.56	27.73
crew	4	68	8	27.24	27.49	28.01
crew	4	68	9	26.68	26.66	27.46
crew	4	68	10	27.69	28.22	29.22
crew	4	74	1	26.13	26.13	27.01
crew	4	74	2	26.95	28.28	28.07

Continued on next page

Table V.1 – continued from previous page

Sequence	SNR (dB)	Frame	Run	JM 16.0	STBMA+PDE	SO-MLD
crew	4	74	3	26.44	26.72	28.29
crew	4	74	4	27.49	28.23	29.29
crew	4	74	5	26.39	27.18	27.78
crew	4	74	6	26.85	27.68	26.96
crew	4	74	7	28.03	29.31	29.92
crew	4	74	8	26.26	26.25	26.92
crew	4	74	9	26.79	27.45	28.21
crew	4	74	10	27.08	28.04	27.96
crew	4	85	1	26.94	26.94	27.16
crew	4	85	2	27.46	27.68	28.17
crew	4	85	3	27.59	27.96	29.17
crew	4	85	4	27.99	28.69	28.94
crew	4	85	5	26.94	26.94	27.94
crew	4	85	6	27.14	27.20	29.44
crew	4	85	7	27.34	27.05	28.23
crew	4	85	8	28.43	28.64	29.54
crew	4	85	9	27.07	26.84	28.30
crew	4	85	10	27.29	27.22	28.23
crew	4	88	1	23.56	23.54	22.93
crew	4	88	2	23.31	23.09	23.95
crew	4	88	3	23.62	23.74	23.89
crew	4	88	4	23.24	23.26	24.07
crew	4	88	5	23.27	23.10	23.11
crew	4	88	6	23.21	23.22	23.14
crew	4	88	7	23.78	23.52	23.98
crew	4	88	8	23.53	23.73	23.60
crew	4	88	9	23.90	24.13	25.22
crew	4	88	10	23.37	23.38	24.12
crew	4	92	1	26.49	26.59	27.00
crew	4	92	2	26.32	26.50	27.20
crew	4	92	3	26.05	25.86	26.75
crew	4	92	4	26.77	27.57	27.72
crew	4	92	5	26.48	27.02	27.41
crew	4	92	6	25.92	25.92	26.61
crew	4	92	7	26.40	26.63	27.03
crew	4	92	8	26.26	26.29	26.79
crew	4	92	9	26.19	26.20	26.85
crew	4	92	10	25.92	25.92	26.28
crew	4	101	1	25.32	25.18	26.04
crew	4	101	2	25.26	23.66	25.72
crew	4	101	3	25.52	25.13	26.94

Continued on next page

Table V.1 – continued from previous page

Sequence	SNR (dB)	Frame	Run	JM 16.0	STBMA+PDE	SO-MLD
crew	4	101	4	26.46	26.80	27.23
crew	4	101	5	24.98	24.85	25.77
crew	4	101	6	25.36	25.53	26.59
crew	4	101	7	25.68	25.39	26.91
crew	4	101	8	25.54	25.68	25.94
crew	4	101	9	26.57	26.97	27.88
crew	4	101	10	25.23	25.18	25.95
crew	4	106	1	22.53	23.01	23.14
crew	4	106	2	22.13	22.25	23.12
crew	4	106	3	22.62	22.91	23.47
crew	4	106	4	22.83	23.19	23.47
crew	4	106	5	22.68	23.10	23.81
crew	4	106	6	22.46	22.76	24.00
crew	4	106	7	22.61	22.74	24.12
crew	4	106	8	23.19	23.55	24.90
crew	4	106	9	22.77	22.65	23.12
crew	4	106	10	22.07	22.28	23.58
crew	4	108	1	25.08	25.16	27.09
crew	4	108	2	25.45	26.35	26.93
crew	4	108	3	24.95	24.75	26.39
crew	4	108	4	25.77	26.26	26.71
crew	4	108	5	25.30	25.77	25.85
crew	4	108	6	25.13	25.20	26.70
crew	4	108	7	25.08	25.18	26.19
crew	4	108	8	25.29	25.62	26.44
crew	4	108	9	25.97	26.50	27.44
crew	4	108	10	25.12	25.57	26.73
crew	5	61	1	22.42	22.45	24.18
crew	5	61	2	22.91	22.96	25.20
crew	5	61	3	22.01	22.04	22.23
crew	5	61	4	22.59	22.63	25.11
crew	5	61	5	22.22	22.25	23.12
crew	5	61	6	22.55	22.58	24.30
crew	5	61	7	22.29	22.32	23.90
crew	5	61	8	23.05	23.09	25.04
crew	5	61	9	23.22	23.26	24.20
crew	5	61	10	22.95	23.00	23.70
crew	5	63	1	28.37	30.52	30.33
crew	5	63	2	28.92	30.70	30.69
crew	5	63	3	27.27	28.65	27.85
crew	5	63	4	28.61	30.31	29.14

Continued on next page

Table V.1 – continued from previous page

Sequence	SNR (dB)	Frame	Run	JM 16.0	STBMA+PDE	SO-MLD
crew	5	63	5	26.41	27.93	28.60
crew	5	63	6	28.11	29.26	28.19
crew	5	63	7	28.01	29.71	29.22
crew	5	63	8	29.28	31.06	30.19
crew	5	63	9	29.63	31.48	31.40
crew	5	63	10	29.59	31.73	31.14
crew	5	65	1	29.02	30.51	30.66
crew	5	65	2	29.42	30.57	30.83
crew	5	65	3	31.00	32.62	31.88
crew	5	65	4	30.52	32.01	32.13
crew	5	65	5	28.34	29.61	30.06
crew	5	65	6	30.56	31.16	30.54
crew	5	65	7	30.05	31.57	31.95
crew	5	65	8	30.11	31.87	30.86
crew	5	65	9	30.19	31.50	30.90
crew	5	65	10	31.24	31.78	31.59
crew	5	66	1	29.38	30.26	30.02
crew	5	66	2	28.14	28.77	29.08
crew	5	66	3	28.44	28.71	29.86
crew	5	66	4	29.17	30.91	29.70
crew	5	66	5	29.67	30.62	30.41
crew	5	66	6	31.41	32.32	32.37
crew	5	66	7	29.37	29.97	30.03
crew	5	66	8	30.78	31.70	31.40
crew	5	66	9	29.77	31.13	30.83
crew	5	66	10	29.24	30.52	30.64
crew	5	70	1	30.90	32.10	32.28
crew	5	70	2	29.23	29.84	30.30
crew	5	70	3	28.75	29.93	29.64
crew	5	70	4	30.73	31.41	32.34
crew	5	70	5	28.60	29.64	28.97
crew	5	70	6	29.28	29.96	29.81
crew	5	70	7	29.00	30.16	30.67
crew	5	70	8	31.36	32.56	32.04
crew	5	70	9	29.89	30.29	30.14
crew	5	70	10	29.73	30.68	30.90
crew	5	73	1	27.71	28.63	29.10
crew	5	73	2	31.01	31.15	32.58
crew	5	73	3	29.77	30.09	30.69
crew	5	73	4	29.81	31.29	30.83
crew	5	73	5	29.10	30.16	29.99

Continued on next page

Table V.1 – continued from previous page

Sequence	SNR (dB)	Frame	Run	JM 16.0	STBMA+PDE	SO-MLD
crew	5	73	6	29.94	30.14	31.95
crew	5	73	7	29.12	30.90	30.52
crew	5	73	8	28.48	29.84	29.45
crew	5	73	9	28.94	30.37	30.27
crew	5	73	10	29.42	30.58	30.62
crew	5	74	1	30.24	31.46	31.45
crew	5	74	2	30.47	31.05	32.16
crew	5	74	3	29.81	30.95	31.17
crew	5	74	4	29.48	30.35	31.76
crew	5	74	5	29.76	31.11	31.00
crew	5	74	6	29.38	31.00	31.44
crew	5	74	7	28.66	30.18	30.01
crew	5	74	8	31.74	32.59	32.97
crew	5	74	9	28.44	29.74	29.27
crew	5	74	10	29.20	30.56	30.71
crew	5	78	1	30.39	31.32	30.93
crew	5	78	2	28.07	29.64	30.10
crew	5	78	3	28.75	30.49	29.94
crew	5	78	4	28.60	30.10	30.15
crew	5	78	5	29.55	30.36	30.94
crew	5	78	6	29.35	30.89	31.98
crew	5	78	7	29.24	30.90	31.04
crew	5	78	8	29.89	31.32	31.97
crew	5	78	9	29.47	31.06	31.19
crew	5	78	10	29.50	30.15	31.22
crew	5	79	1	29.18	30.11	30.69
crew	5	79	2	30.32	31.24	30.98
crew	5	79	3	30.00	31.10	31.40
crew	5	79	4	29.70	30.32	30.43
crew	5	79	5	30.05	31.24	31.38
crew	5	79	6	29.38	30.56	30.48
crew	5	79	7	30.09	30.70	31.35
crew	5	79	8	30.95	31.98	31.73
crew	5	79	9	30.82	31.57	30.53
crew	5	79	10	28.80	29.96	30.99
crew	5	80	1	29.41	29.99	29.76
crew	5	80	2	29.87	30.87	31.18
crew	5	80	3	29.45	30.51	30.82
crew	5	80	4	29.29	30.16	30.54
crew	5	80	5	28.32	28.78	29.54
crew	5	80	6	29.69	30.85	30.74

Continued on next page

Table V.1 – continued from previous page

Sequence	SNR (dB)	Frame	Run	JM 16.0	STBMA+PDE	SO-MLD
harbour	4	66	3	24.76	24.98	25.37
harbour	4	66	4	24.84	24.88	25.57
harbour	4	66	5	24.56	24.77	25.85
harbour	4	66	6	24.97	25.49	25.86
harbour	4	66	7	24.80	24.92	25.46
harbour	4	66	8	25.02	25.18	26.19
harbour	4	66	9	24.75	24.89	25.07
harbour	4	66	10	25.00	25.19	25.86
harbour	4	68	1	25.06	25.09	24.74
harbour	4	68	2	25.58	25.27	25.73
harbour	4	68	3	25.21	24.51	25.47
harbour	4	68	4	25.00	24.65	25.00
harbour	4	68	5	25.26	25.33	25.36
harbour	4	68	6	25.26	24.90	24.81
harbour	4	68	7	25.28	24.61	25.36
harbour	4	68	8	25.47	24.67	25.72
harbour	4	68	9	25.30	24.89	25.14
harbour	4	68	10	25.26	24.90	24.86
harbour	4	73	1	22.98	22.98	24.34
harbour	4	73	2	23.14	23.38	23.74
harbour	4	73	3	23.40	24.63	24.34
harbour	4	73	4	23.30	23.86	24.27
harbour	4	73	5	23.15	24.72	23.23
harbour	4	73	6	23.70	25.51	25.13
harbour	4	73	7	23.61	25.06	24.76
harbour	4	73	8	23.12	23.89	24.58
harbour	4	73	9	23.85	24.89	25.52
harbour	4	73	10	23.22	23.86	23.58
harbour	4	76	1	25.76	25.83	24.94
harbour	4	76	2	25.52	25.51	25.28
harbour	4	76	3	25.33	25.46	25.35
harbour	4	76	4	25.53	23.24	24.86
harbour	4	76	5	25.43	24.22	25.41
harbour	4	76	6	25.74	25.86	23.90
harbour	4	76	7	25.63	25.83	25.31
harbour	4	76	8	25.36	25.12	25.43
harbour	4	76	9	25.26	25.26	24.81
harbour	4	76	10	25.41	25.60	25.04
harbour	4	85	1	24.40	25.49	25.12
harbour	4	85	2	24.14	24.77	24.35
harbour	4	85	3	23.92	24.15	25.34

Continued on next page

Table V.1 – continued from previous page

Sequence	SNR (dB)	Frame	Run	JM 16.0	STBMA+PDE	SO-MLD
harbour	4	101	5	20.89	23.23	22.78
harbour	4	101	6	20.84	26.09	24.30
harbour	4	101	7	20.45	23.05	22.59
harbour	4	101	8	19.37	19.37	21.34
harbour	4	101	9	19.84	22.88	22.43
harbour	4	101	10	19.80	21.66	21.56
harbour	4	102	1	25.87	22.71	26.01
harbour	4	102	2	25.59	25.58	25.12
harbour	4	102	3	25.67	25.16	26.16
harbour	4	102	4	25.53	25.46	25.74
harbour	4	102	5	25.60	25.46	25.85
harbour	4	102	6	26.00	25.72	25.90
harbour	4	102	7	25.86	25.51	25.84
harbour	4	102	8	25.79	25.71	25.88
harbour	4	102	9	26.29	25.63	26.27
harbour	4	102	10	25.57	21.13	25.18
harbour	5	66	1	26.88	27.33	27.49
harbour	5	66	2	25.66	26.09	26.46
harbour	5	66	3	26.55	26.97	27.28
harbour	5	66	4	25.98	26.14	26.88
harbour	5	66	5	25.60	26.02	26.67
harbour	5	66	6	26.41	26.89	26.87
harbour	5	66	7	26.98	27.31	27.44
harbour	5	66	8	27.28	27.59	27.73
harbour	5	66	9	26.11	26.59	26.95
harbour	5	66	10	26.77	27.13	27.17
harbour	5	68	1	26.16	25.84	26.40
harbour	5	68	2	27.08	26.90	26.93
harbour	5	68	3	26.12	26.28	26.60
harbour	5	68	4	26.93	24.98	26.00
harbour	5	68	5	26.70	24.96	26.78
harbour	5	68	6	26.99	27.07	27.11
harbour	5	68	7	27.29	27.37	27.85
harbour	5	68	8	26.91	26.15	27.85
harbour	5	68	9	26.17	26.13	26.22
harbour	5	68	10	26.43	26.45	26.48
harbour	5	73	1	24.23	25.58	26.10
harbour	5	73	2	25.21	26.64	27.12
harbour	5	73	3	25.77	26.98	26.75
harbour	5	73	4	25.28	26.41	25.99
harbour	5	73	5	25.65	26.47	27.58

Continued on next page

Table V.1 – continued from previous page

Sequence	SNR (dB)	Frame	Run	JM 16.0	STBMA+PDE	SO-MLD
harbour	5	96	7	21.21	26.99	23.96
harbour	5	96	8	23.02	25.77	25.55
harbour	5	96	9	20.66	24.96	24.55
harbour	5	96	10	23.70	27.53	25.19
harbour	5	99	1	24.26	27.13	25.60
harbour	5	99	2	24.45	26.94	25.03
harbour	5	99	3	24.61	26.40	27.06
harbour	5	99	4	24.84	26.69	26.04
harbour	5	99	5	23.31	26.12	25.79
harbour	5	99	6	25.28	27.63	27.16
harbour	5	99	7	23.58	24.51	26.02
harbour	5	99	8	24.28	27.00	26.12
harbour	5	99	9	23.22	25.92	25.15
harbour	5	99	10	24.59	26.94	26.82
harbour	5	101	1	22.56	27.20	25.94
harbour	5	101	2	23.02	25.65	24.75
harbour	5	101	3	23.70	27.12	25.77
harbour	5	101	4	21.62	26.74	25.31
harbour	5	101	5	24.60	26.14	25.58
harbour	5	101	6	22.85	27.10	26.66
harbour	5	101	7	24.20	27.25	25.91
harbour	5	101	8	22.14	25.23	24.53
harbour	5	101	9	21.24	24.39	24.62
harbour	5	101	10	24.28	27.46	25.28
harbour	5	102	1	27.17	27.12	27.33
harbour	5	102	2	26.64	26.62	26.95
harbour	5	102	3	26.82	26.80	27.15
harbour	5	102	4	27.59	27.59	27.64
harbour	5	102	5	26.63	26.69	26.90
harbour	5	102	6	27.03	26.99	27.26
harbour	5	102	7	27.17	27.16	27.55
harbour	5	102	8	26.95	27.02	27.29
harbour	5	102	9	27.10	27.11	27.29
harbour	5	102	10	26.43	26.49	26.81
ice	4	62	1	25.38	27.44	27.90
ice	4	62	2	25.55	25.69	28.27
ice	4	62	3	23.82	23.84	26.40
ice	4	62	4	24.07	24.21	25.94
ice	4	62	5	24.06	24.28	25.17
ice	4	62	6	24.75	25.74	26.84
ice	4	62	7	24.32	25.03	27.36

Continued on next page

Table V.1 – continued from previous page

Sequence	SNR (dB)	Frame	Run	JM 16.0	STBMA+PDE	SO-MLD
ice	4	62	8	23.96	24.24	26.21
ice	4	62	9	26.14	26.85	29.58
ice	4	62	10	24.09	23.99	26.64
ice	4	69	1	24.85	25.50	26.76
ice	4	69	2	24.51	24.22	26.05
ice	4	69	3	24.17	24.08	25.49
ice	4	69	4	24.26	24.25	25.23
ice	4	69	5	24.30	24.64	25.31
ice	4	69	6	25.13	26.25	25.84
ice	4	69	7	24.94	25.36	26.12
ice	4	69	8	23.99	24.09	25.17
ice	4	69	9	24.54	24.63	26.17
ice	4	69	10	24.32	24.45	25.59
ice	4	75	1	25.78	26.24	28.84
ice	4	75	2	25.82	25.34	27.62
ice	4	75	3	25.76	24.92	27.47
ice	4	75	4	25.80	26.62	28.93
ice	4	75	5	25.36	25.82	27.81
ice	4	75	6	26.29	25.90	29.64
ice	4	75	7	25.81	25.61	28.16
ice	4	75	8	25.56	26.15	27.76
ice	4	75	9	24.79	24.79	26.41
ice	4	75	10	25.96	27.13	29.79
ice	4	78	1	25.08	25.59	27.51
ice	4	78	2	24.80	25.01	26.39
ice	4	78	3	26.19	27.68	29.36
ice	4	78	4	25.17	25.00	27.85
ice	4	78	5	25.29	25.71	27.82
ice	4	78	6	24.99	25.14	26.45
ice	4	78	7	25.36	26.32	26.96
ice	4	78	8	25.18	25.77	26.56
ice	4	78	9	24.83	23.84	26.89
ice	4	78	10	25.30	26.13	29.61
ice	4	85	1	25.19	24.46	27.05
ice	4	85	2	26.16	25.31	28.28
ice	4	85	3	25.25	24.95	27.74
ice	4	85	4	25.52	24.61	27.57
ice	4	85	5	26.02	26.22	27.66
ice	4	85	6	26.24	25.72	30.04
ice	4	85	7	26.48	27.95	29.41
ice	4	85	8	25.41	25.58	26.99

Continued on next page

Table V.1 – continued from previous page

Sequence	SNR (dB)	Frame	Run	JM 16.0	STBMA+PDE	SO-MLD
ice	4	85	9	25.45	25.62	28.15
ice	4	85	10	25.52	26.16	27.31
ice	4	89	1	24.68	25.79	26.31
ice	4	89	2	24.71	26.62	27.33
ice	4	89	3	25.19	26.45	26.94
ice	4	89	4	24.49	26.00	27.28
ice	4	89	5	25.84	27.57	28.32
ice	4	89	6	24.77	26.24	27.35
ice	4	89	7	24.23	25.39	26.29
ice	4	89	8	24.90	26.05	26.18
ice	4	89	9	25.14	26.73	27.29
ice	4	89	10	24.35	25.41	26.21
ice	4	94	1	24.22	26.50	27.99
ice	4	94	2	24.28	24.95	26.28
ice	4	94	3	24.19	24.29	27.50
ice	4	94	4	24.34	24.45	27.12
ice	4	94	5	24.49	27.99	27.00
ice	4	94	6	23.97	23.70	27.17
ice	4	94	7	24.22	26.50	27.80
ice	4	94	8	25.09	27.40	28.93
ice	4	94	9	24.82	25.82	27.06
ice	4	94	10	25.62	29.89	29.56
ice	4	96	1	24.40	26.47	27.93
ice	4	96	2	25.22	27.98	28.81
ice	4	96	3	24.41	25.25	27.12
ice	4	96	4	25.58	26.96	28.84
ice	4	96	5	25.27	28.10	29.16
ice	4	96	6	24.60	26.87	28.27
ice	4	96	7	24.77	26.97	28.20
ice	4	96	8	24.44	25.72	26.75
ice	4	96	9	24.04	24.06	25.89
ice	4	96	10	24.72	26.95	27.27
ice	4	98	1	23.70	24.92	26.74
ice	4	98	2	23.74	24.22	25.98
ice	4	98	3	24.11	25.10	25.74
ice	4	98	4	24.57	26.71	26.64
ice	4	98	5	23.90	25.61	26.94
ice	4	98	6	23.66	24.81	26.49
ice	4	98	7	24.29	25.75	26.45
ice	4	98	8	25.20	27.98	29.04
ice	4	98	9	24.73	25.73	26.85

Continued on next page

Table V.1 – continued from previous page

Sequence	SNR (dB)	Frame	Run	JM 16.0	STBMA+PDE	SO-MLD
ice	5	78	1	27.66	30.23	31.37
ice	5	78	2	27.55	30.28	31.91
ice	5	78	3	29.58	32.93	35.84
ice	5	78	4	32.27	36.31	35.38
ice	5	78	5	29.23	31.92	31.56
ice	5	78	6	28.46	30.20	31.82
ice	5	78	7	27.72	28.96	30.40
ice	5	78	8	28.63	31.58	32.81
ice	5	78	9	29.15	32.19	32.58
ice	5	78	10	28.24	30.60	32.28
ice	5	85	1	28.13	30.74	31.30
ice	5	85	2	30.21	32.22	32.84
ice	5	85	3	29.35	31.84	32.19
ice	5	85	4	31.98	33.32	34.31
ice	5	85	5	28.77	30.98	30.65
ice	5	85	6	30.33	33.26	34.20
ice	5	85	7	31.77	32.44	35.67
ice	5	85	8	28.97	31.51	32.95
ice	5	85	9	27.35	28.61	31.19
ice	5	85	10	31.71	34.13	35.02
ice	5	89	1	27.37	31.17	32.25
ice	5	89	2	28.57	29.90	31.83
ice	5	89	3	28.79	31.08	31.10
ice	5	89	4	27.23	29.52	29.91
ice	5	89	5	29.44	32.28	32.10
ice	5	89	6	27.34	31.07	31.47
ice	5	89	7	27.73	29.14	30.44
ice	5	89	8	30.66	34.25	36.13
ice	5	89	9	29.73	30.52	32.39
ice	5	89	10	28.47	30.45	32.64
ice	5	94	1	27.73	30.07	32.92
ice	5	94	2	28.14	31.94	32.07
ice	5	94	3	30.17	32.77	34.53
ice	5	94	4	28.54	31.59	30.70
ice	5	94	5	26.97	31.11	30.53
ice	5	94	6	28.24	30.72	34.15
ice	5	94	7	30.16	31.18	36.13
ice	5	94	8	26.66	30.67	31.39
ice	5	94	9	28.08	32.15	31.06
ice	5	94	10	28.32	34.48	32.90
ice	5	96	1	26.88	31.52	31.23

Continued on next page

Table V.1 – continued from previous page

Sequence	SNR (dB)	Frame	Run	JM 16.0	STBMA+PDE	SO-MLD
ice	5	96	2	27.47	31.08	31.26
ice	5	96	3	28.25	29.74	32.28
ice	5	96	4	29.63	34.96	34.68
ice	5	96	5	27.91	30.56	31.65
ice	5	96	6	29.38	31.60	30.33
ice	5	96	7	28.02	30.81	33.88
ice	5	96	8	27.74	30.02	31.01
ice	5	96	9	27.63	31.46	30.77
ice	5	96	10	26.92	29.39	31.49
ice	5	98	1	26.00	29.47	30.27
ice	5	98	2	26.38	28.09	29.83
ice	5	98	3	26.18	30.31	29.39
ice	5	98	4	28.35	30.17	30.42
ice	5	98	5	25.29	29.55	30.01
ice	5	98	6	27.53	31.86	30.33
ice	5	98	7	28.29	31.71	31.59
ice	5	98	8	27.34	32.44	32.86
ice	5	98	9	27.22	30.68	30.64
ice	5	98	10	27.99	31.39	34.42
ice	5	100	1	28.67	33.88	34.75
ice	5	100	2	26.41	30.28	32.60
ice	5	100	3	25.75	29.64	29.82
ice	5	100	4	29.18	32.84	34.01
ice	5	100	5	26.25	30.51	30.37
ice	5	100	6	29.30	33.66	34.93
ice	5	100	7	29.80	32.36	33.42
ice	5	100	8	28.42	31.55	31.80
ice	5	100	9	27.33	31.34	30.24
ice	5	100	10	26.78	30.31	29.95
opening-ceremony	4	65	1	26.39	26.06	26.51
opening-ceremony	4	65	2	26.23	26.23	26.25
opening-ceremony	4	65	3	26.52	26.90	26.46
opening-ceremony	4	65	4	26.27	26.27	26.34
opening-ceremony	4	65	5	26.23	26.23	26.16
opening-ceremony	4	65	6	26.31	26.28	25.74
opening-ceremony	4	65	7	26.36	26.31	26.35
opening-ceremony	4	65	8	26.41	26.24	26.04
opening-ceremony	4	65	9	26.33	26.29	26.73
opening-ceremony	4	65	10	26.66	26.37	25.54
opening-ceremony	4	67	1	26.48	26.99	27.09
opening-ceremony	4	67	2	26.58	26.07	26.95

Continued on next page

Table V.1 – continued from previous page

Sequence	SNR (dB)	Frame	Run	JM 16.0	STBMA+PDE	SO-MLD
opening-ceremony	4	108	5	26.81	26.77	26.58
opening-ceremony	4	108	6	26.31	26.23	26.70
opening-ceremony	4	108	7	26.31	26.17	23.74
opening-ceremony	4	108	8	26.30	26.09	26.37
opening-ceremony	4	108	9	26.29	26.21	26.02
opening-ceremony	4	108	10	26.46	26.44	26.25
opening-ceremony	5	65	1	27.21	27.50	27.52
opening-ceremony	5	65	2	26.60	26.69	27.03
opening-ceremony	5	65	3	27.39	27.66	27.18
opening-ceremony	5	65	4	26.79	27.18	27.15
opening-ceremony	5	65	5	27.29	27.54	27.60
opening-ceremony	5	65	6	27.13	26.87	26.89
opening-ceremony	5	65	7	27.52	27.60	27.72
opening-ceremony	5	65	8	26.82	26.87	26.99
opening-ceremony	5	65	9	26.91	26.99	27.34
opening-ceremony	5	65	10	27.25	27.56	27.50
opening-ceremony	5	67	1	27.50	27.60	27.71
opening-ceremony	5	67	2	27.24	27.23	27.39
opening-ceremony	5	67	3	27.03	27.33	27.30
opening-ceremony	5	67	4	26.88	27.38	27.37
opening-ceremony	5	67	5	27.61	27.59	27.62
opening-ceremony	5	67	6	27.15	27.23	27.37
opening-ceremony	5	67	7	27.26	27.19	25.59
opening-ceremony	5	67	8	27.71	27.71	27.65
opening-ceremony	5	67	9	26.97	27.16	27.25
opening-ceremony	5	67	10	27.26	27.43	27.55
opening-ceremony	5	68	1	27.49	27.38	27.54
opening-ceremony	5	68	2	27.38	27.37	27.63
opening-ceremony	5	68	3	27.14	27.27	27.36
opening-ceremony	5	68	4	27.06	27.38	27.46
opening-ceremony	5	68	5	27.05	27.15	27.01
opening-ceremony	5	68	6	26.98	27.00	27.25
opening-ceremony	5	68	7	27.33	27.38	27.03
opening-ceremony	5	68	8	27.45	27.44	27.52
opening-ceremony	5	68	9	26.96	27.08	27.23
opening-ceremony	5	68	10	26.78	26.81	26.86
opening-ceremony	5	74	1	27.35	27.18	27.32
opening-ceremony	5	74	2	26.62	26.67	26.93
opening-ceremony	5	74	3	26.71	26.68	27.17
opening-ceremony	5	74	4	26.91	27.11	27.11
opening-ceremony	5	74	5	27.33	27.22	27.59

Continued on next page

Table V.1 – continued from previous page

Sequence	SNR (dB)	Frame	Run	JM 16.0	STBMA+PDE	SO-MLD
opening-ceremony	5	101	7	26.82	26.77	26.68
opening-ceremony	5	101	8	27.49	27.43	27.10
opening-ceremony	5	101	9	26.96	26.31	27.14
opening-ceremony	5	101	10	27.03	26.34	26.79
opening-ceremony	5	106	1	27.15	27.38	26.65
opening-ceremony	5	106	2	27.13	27.12	27.51
opening-ceremony	5	106	3	26.91	26.82	26.99
opening-ceremony	5	106	4	27.39	27.48	27.63
opening-ceremony	5	106	5	27.05	27.02	26.81
opening-ceremony	5	106	6	27.29	27.47	26.88
opening-ceremony	5	106	7	27.33	27.34	27.45
opening-ceremony	5	106	8	27.13	27.29	27.60
opening-ceremony	5	106	9	26.77	27.04	26.56
opening-ceremony	5	106	10	26.93	27.10	27.23
opening-ceremony	5	108	1	26.87	27.01	27.25
opening-ceremony	5	108	2	27.00	27.16	27.20
opening-ceremony	5	108	3	26.77	26.88	27.33
opening-ceremony	5	108	4	27.29	27.38	27.42
opening-ceremony	5	108	5	27.40	27.43	27.50
opening-ceremony	5	108	6	27.21	27.17	27.27
opening-ceremony	5	108	7	27.14	27.21	27.25
opening-ceremony	5	108	8	27.04	26.96	26.91
opening-ceremony	5	108	9	26.84	26.60	26.86
opening-ceremony	5	108	10	26.96	27.16	27.21
soccer	4	61	1	23.38	23.39	23.47
soccer	4	61	2	22.68	22.69	21.69
soccer	4	61	3	22.92	22.93	22.40
soccer	4	61	4	22.71	22.72	23.33
soccer	4	61	5	23.27	23.28	23.90
soccer	4	61	6	23.04	23.05	23.74
soccer	4	61	7	22.85	22.86	22.75
soccer	4	61	8	23.02	23.02	22.55
soccer	4	61	9	22.77	22.77	23.23
soccer	4	61	10	23.08	23.08	24.04
soccer	4	66	1	21.95	22.89	24.00
soccer	4	66	2	21.86	22.82	23.75
soccer	4	66	3	23.17	24.12	25.85
soccer	4	66	4	21.91	21.91	23.37
soccer	4	66	5	22.43	22.63	24.85
soccer	4	66	6	21.84	22.73	23.73
soccer	4	66	7	22.62	23.65	24.60

Continued on next page

Table V.1 – continued from previous page

Sequence	SNR (dB)	Frame	Run	JM 16.0	STBMA+PDE	SO-MLD
soccer	4	91	9	21.78	21.79	22.80
soccer	4	91	10	21.53	21.54	21.54
soccer	4	92	1	23.33	23.35	24.29
soccer	4	92	2	23.87	24.21	25.27
soccer	4	92	3	22.32	22.35	22.26
soccer	4	92	4	23.33	23.53	24.55
soccer	4	92	5	22.84	23.67	23.38
soccer	4	92	6	23.15	23.97	25.66
soccer	4	92	7	22.23	22.22	22.94
soccer	4	92	8	22.32	22.35	23.69
soccer	4	92	9	23.52	23.49	25.07
soccer	4	92	10	23.11	22.80	24.34
soccer	4	96	1	22.51	22.59	24.44
soccer	4	96	2	22.39	21.76	23.53
soccer	4	96	3	22.35	20.29	22.99
soccer	4	96	4	23.44	21.28	24.25
soccer	4	96	5	22.52	22.77	24.79
soccer	4	96	6	23.11	23.52	24.90
soccer	4	96	7	22.74	22.42	24.34
soccer	4	96	8	22.40	20.34	23.84
soccer	4	96	9	22.90	22.92	23.81
soccer	4	96	10	23.40	23.71	25.02
soccer	4	97	1	22.31	22.60	24.42
soccer	4	97	2	22.71	22.45	23.24
soccer	4	97	3	21.92	21.92	22.79
soccer	4	97	4	22.07	20.44	22.70
soccer	4	97	5	22.07	20.44	23.87
soccer	4	97	6	22.34	21.97	23.67
soccer	4	97	7	22.25	21.86	24.48
soccer	4	97	8	22.32	21.41	23.21
soccer	4	97	9	22.10	21.09	24.20
soccer	4	97	10	22.57	21.09	23.37
soccer	4	98	1	21.76	21.20	22.40
soccer	4	98	2	22.11	22.46	23.70
soccer	4	98	3	22.06	21.91	23.28
soccer	4	98	4	22.18	22.38	23.58
soccer	4	98	5	22.05	21.35	23.27
soccer	4	98	6	22.18	22.38	22.94
soccer	4	98	7	22.35	20.91	22.76
soccer	4	98	8	21.50	21.50	22.53
soccer	4	98	9	22.25	21.53	23.52

Continued on next page

Table V.1 – continued from previous page

Sequence	SNR (dB)	Frame	Run	JM 16.0	STBMA+PDE	SO-MLD
soccer	5	80	1	25.30	26.42	26.36
soccer	5	80	2	24.60	25.72	25.85
soccer	5	80	3	24.74	25.88	27.62
soccer	5	80	4	24.70	26.31	26.72
soccer	5	80	5	24.53	26.09	26.44
soccer	5	80	6	25.36	27.09	27.57
soccer	5	80	7	25.01	25.00	26.51
soccer	5	80	8	25.46	27.05	27.39
soccer	5	80	9	23.95	24.84	26.10
soccer	5	80	10	25.58	25.22	26.98
soccer	5	91	1	24.55	24.56	26.31
soccer	5	91	2	24.75	24.77	26.89
soccer	5	91	3	24.10	24.12	25.68
soccer	5	91	4	23.97	23.98	25.27
soccer	5	91	5	24.11	24.12	25.97
soccer	5	91	6	24.73	24.75	25.06
soccer	5	91	7	23.00	23.00	24.25
soccer	5	91	8	24.75	24.76	26.05
soccer	5	91	9	25.77	25.78	27.15
soccer	5	91	10	24.03	24.04	26.33
soccer	5	92	1	26.80	28.50	28.49
soccer	5	92	2	26.58	28.79	29.34
soccer	5	92	3	27.43	28.33	28.70
soccer	5	92	4	25.44	26.15	28.45
soccer	5	92	5	24.55	25.75	25.22
soccer	5	92	6	28.00	29.28	30.20
soccer	5	92	7	25.76	26.80	27.82
soccer	5	92	8	25.95	26.12	28.01
soccer	5	92	9	27.62	27.59	29.62
soccer	5	92	10	28.46	29.58	30.56
soccer	5	96	1	24.20	24.23	27.57
soccer	5	96	2	24.96	25.41	25.14
soccer	5	96	3	24.35	25.14	26.40
soccer	5	96	4	27.42	28.85	28.84
soccer	5	96	5	24.60	25.80	27.38
soccer	5	96	6	24.58	23.94	27.64
soccer	5	96	7	24.20	24.62	27.89
soccer	5	96	8	23.50	23.53	25.32
soccer	5	96	9	26.56	27.03	28.81
soccer	5	96	10	28.03	30.28	30.22
soccer	5	97	1	25.74	25.91	27.70

Continued on next page

Table V.1 – continued from previous page

Sequence	SNR (dB)	Frame	Run	JM 16.0	STBMA+PDE	SO-MLD
soccer	5	97	2	25.43	25.64	28.04
soccer	5	97	3	25.81	27.11	29.28
soccer	5	97	4	26.69	27.79	28.59
soccer	5	97	5	26.15	27.36	28.68
soccer	5	97	6	25.66	26.97	28.25
soccer	5	97	7	24.65	24.76	27.52
soccer	5	97	8	24.79	24.71	27.13
soccer	5	97	9	25.28	24.98	26.84
soccer	5	97	10	24.33	23.91	25.12
soccer	5	98	1	24.56	25.86	26.84
soccer	5	98	2	26.41	27.58	27.43
soccer	5	98	3	26.52	25.46	26.65
soccer	5	98	4	24.67	25.62	27.08
soccer	5	98	5	24.25	24.33	26.99
soccer	5	98	6	27.42	29.07	29.13
soccer	5	98	7	25.03	25.52	26.15
soccer	5	98	8	26.09	27.66	27.67
soccer	5	98	9	25.70	26.62	26.66
soccer	5	98	10	24.54	26.77	27.43
walk	4	61	1	16.47	16.47	17.95
walk	4	61	2	15.60	15.61	17.32
walk	4	61	3	16.06	16.06	18.29
walk	4	61	4	16.17	16.16	18.53
walk	4	61	5	15.50	15.51	17.74
walk	4	61	6	15.39	15.39	16.99
walk	4	61	7	15.77	15.77	18.64
walk	4	61	8	16.59	16.59	18.71
walk	4	61	9	15.55	15.56	16.50
walk	4	61	10	15.36	15.36	17.39
walk	4	62	1	14.28	15.96	15.49
walk	4	62	2	13.30	13.26	13.59
walk	4	62	3	14.16	16.07	15.35
walk	4	62	4	14.08	17.38	15.99
walk	4	62	5	14.56	17.25	17.63
walk	4	62	6	13.34	13.22	13.50
walk	4	62	7	13.48	13.65	14.18
walk	4	62	8	13.51	14.64	14.42
walk	4	62	9	14.29	15.50	15.88
walk	4	62	10	13.97	14.68	15.49
walk	4	65	1	17.30	17.62	19.45
walk	4	65	2	16.83	16.83	20.75

Continued on next page

Table V.1 – continued from previous page

Sequence	SNR (dB)	Frame	Run	JM 16.0	STBMA+PDE	SO-MLD
walk	4	65	3	17.53	17.77	21.64
walk	4	65	4	17.39	18.63	20.07
walk	4	65	5	17.30	17.64	21.96
walk	4	65	6	16.83	16.83	20.17
walk	4	65	7	17.63	17.97	19.54
walk	4	65	8	17.13	17.29	19.17
walk	4	65	9	17.14	17.11	19.22
walk	4	65	10	18.03	18.74	22.65
walk	4	73	1	16.65	19.62	21.25
walk	4	73	2	15.81	17.32	18.89
walk	4	73	3	16.54	17.38	18.36
walk	4	73	4	15.49	15.89	18.04
walk	4	73	5	15.38	15.38	20.69
walk	4	73	6	15.95	17.84	18.87
walk	4	73	7	16.16	18.32	18.83
walk	4	73	8	16.29	18.40	19.34
walk	4	73	9	15.47	16.06	18.41
walk	4	73	10	16.67	19.52	20.79
walk	4	76	1	14.74	16.79	18.07
walk	4	76	2	14.71	18.14	19.50
walk	4	76	3	14.96	17.18	17.64
walk	4	76	4	15.23	17.13	18.23
walk	4	76	5	14.99	17.07	17.94
walk	4	76	6	15.33	16.68	17.73
walk	4	76	7	15.00	18.33	17.09
walk	4	76	8	14.57	16.95	16.82
walk	4	76	9	14.61	16.10	17.83
walk	4	76	10	15.13	16.93	18.23
walk	4	79	1	18.28	21.30	21.38
walk	4	79	2	16.38	16.85	18.74
walk	4	79	3	16.46	17.73	17.89
walk	4	79	4	16.76	18.33	20.98
walk	4	79	5	17.01	21.34	19.01
walk	4	79	6	16.64	17.16	19.96
walk	4	79	7	17.30	20.66	20.41
walk	4	79	8	17.27	18.27	21.28
walk	4	79	9	18.08	19.78	20.00
walk	4	79	10	16.65	18.50	19.42
walk	4	82	1	17.01	17.55	21.03
walk	4	82	2	16.96	19.54	19.89
walk	4	82	3	17.23	20.52	20.49

Continued on next page

Table V.1 – continued from previous page

Sequence	SNR (dB)	Frame	Run	JM 16.0	STBMA+PDE	SO-MLD
walk	5	61	5	18.92	18.93	20.61
walk	5	61	6	17.30	17.30	19.67
walk	5	61	7	20.06	20.07	22.43
walk	5	61	8	18.92	18.92	23.72
walk	5	61	9	18.83	18.84	21.99
walk	5	61	10	19.26	19.27	22.03
walk	5	62	1	18.73	22.15	21.21
walk	5	62	2	16.38	18.87	18.05
walk	5	62	3	17.81	20.66	20.20
walk	5	62	4	19.72	23.57	22.49
walk	5	62	5	16.76	20.47	20.11
walk	5	62	6	17.05	20.27	18.67
walk	5	62	7	20.82	24.34	24.26
walk	5	62	8	19.69	22.69	22.79
walk	5	62	9	19.31	22.04	21.73
walk	5	62	10	15.44	16.47	17.38
walk	5	65	1	19.78	20.74	21.78
walk	5	65	2	18.43	19.44	23.19
walk	5	65	3	22.47	23.96	25.14
walk	5	65	4	18.84	20.20	20.73
walk	5	65	5	18.73	19.34	23.72
walk	5	65	6	21.13	22.29	23.80
walk	5	65	7	19.54	20.23	22.10
walk	5	65	8	21.29	23.19	27.32
walk	5	65	9	19.72	21.30	26.05
walk	5	65	10	21.28	22.51	27.13
walk	5	73	1	17.61	21.37	24.50
walk	5	73	2	17.56	21.89	19.56
walk	5	73	3	19.37	23.57	20.90
walk	5	73	4	17.78	24.43	21.62
walk	5	73	5	21.83	25.06	27.00
walk	5	73	6	18.63	20.66	22.70
walk	5	73	7	19.97	24.39	24.03
walk	5	73	8	22.93	25.66	25.15
walk	5	73	9	18.24	20.41	23.26
walk	5	73	10	19.76	23.04	24.61
walk	5	76	1	16.92	22.41	19.67
walk	5	76	2	18.26	24.42	22.64
walk	5	76	3	18.60	24.00	24.96
walk	5	76	4	19.78	25.33	22.72
walk	5	76	5	17.43	23.39	23.01

Continued on next page

Table V.1 – continued from previous page

Sequence	SNR (dB)	Frame	Run	JM 16.0	STBMA+PDE	SO-MLD
walk	5	84	7	21.14	24.12	25.80
walk	5	84	8	22.57	23.95	24.92
walk	5	84	9	20.06	21.35	23.18
walk	5	84	10	21.63	22.45	23.67
walk	5	90	1	18.80	21.75	23.52
walk	5	90	2	20.56	22.16	24.71
walk	5	90	3	20.57	22.83	23.36
walk	5	90	4	19.98	21.91	24.24
walk	5	90	5	21.34	24.54	23.97
walk	5	90	6	19.12	22.40	23.39
walk	5	90	7	19.38	21.61	22.52
walk	5	90	8	20.32	24.55	23.54
walk	5	90	9	20.69	23.87	22.97
walk	5	90	10	22.87	25.46	24.87
whale-show	4	65	1	22.19	22.08	22.29
whale-show	4	65	2	22.16	22.32	21.91
whale-show	4	65	3	22.58	22.31	22.82
whale-show	4	65	4	22.09	22.05	22.48
whale-show	4	65	5	22.00	21.98	22.52
whale-show	4	65	6	22.11	22.08	21.98
whale-show	4	65	7	22.09	21.88	22.15
whale-show	4	65	8	22.10	22.08	22.21
whale-show	4	65	9	22.30	22.27	22.01
whale-show	4	65	10	22.43	22.21	22.82
whale-show	4	67	1	22.48	22.33	22.37
whale-show	4	67	2	22.36	22.29	22.53
whale-show	4	67	3	22.56	22.44	22.64
whale-show	4	67	4	22.25	22.24	22.06
whale-show	4	67	5	22.48	22.23	22.55
whale-show	4	67	6	22.60	22.23	22.58
whale-show	4	67	7	22.17	22.17	21.64
whale-show	4	67	8	22.43	22.37	22.39
whale-show	4	67	9	22.92	22.66	22.91
whale-show	4	67	10	22.52	22.40	22.73
whale-show	4	68	1	22.47	22.43	22.82
whale-show	4	68	2	22.29	22.20	22.26
whale-show	4	68	3	22.53	22.46	22.85
whale-show	4	68	4	22.44	22.37	22.37
whale-show	4	68	5	22.40	22.38	22.20
whale-show	4	68	6	22.30	22.28	22.51
whale-show	4	68	7	22.52	22.43	22.50

Continued on next page

Table V.1 – continued from previous page

Sequence	SNR (dB)	Frame	Run	JM 16.0	STBMA+PDE	SO-MLD
whale-show	5	88	1	23.07	23.11	23.48
whale-show	5	88	2	22.97	23.04	23.09
whale-show	5	88	3	22.53	22.66	23.25
whale-show	5	88	4	22.45	22.52	22.86
whale-show	5	88	5	23.00	23.08	23.14
whale-show	5	88	6	22.62	22.61	23.10
whale-show	5	88	7	23.37	23.44	23.41
whale-show	5	88	8	22.60	22.68	23.06
whale-show	5	88	9	23.43	23.29	23.49
whale-show	5	88	10	23.42	23.47	23.25
whale-show	5	92	1	24.07	24.07	24.21
whale-show	5	92	2	24.15	24.16	24.22
whale-show	5	92	3	23.46	23.45	23.66
whale-show	5	92	4	23.94	23.93	24.07
whale-show	5	92	5	24.05	23.83	24.25
whale-show	5	92	6	23.28	23.20	23.41
whale-show	5	92	7	23.28	23.18	23.39
whale-show	5	92	8	23.57	23.41	23.68
whale-show	5	92	9	23.54	23.38	23.76
whale-show	5	92	10	23.60	23.51	23.73
whale-show	5	101	1	23.01	23.06	23.28
whale-show	5	101	2	23.30	23.36	23.22
whale-show	5	101	3	23.21	23.13	23.38
whale-show	5	101	4	22.75	22.82	23.06
whale-show	5	101	5	23.13	23.20	23.46
whale-show	5	101	6	22.98	22.96	23.17
whale-show	5	101	7	23.10	23.02	23.11
whale-show	5	101	8	22.86	22.75	23.15
whale-show	5	101	9	23.03	23.00	23.14
whale-show	5	101	10	22.81	22.64	22.82
whale-show	5	106	1	22.54	22.61	22.73
whale-show	5	106	2	23.34	23.36	23.41
whale-show	5	106	3	23.10	23.17	23.20
whale-show	5	106	4	23.08	23.06	23.15
whale-show	5	106	5	22.87	22.80	23.03
whale-show	5	106	6	22.98	22.98	23.11
whale-show	5	106	7	22.53	22.46	22.54
whale-show	5	106	8	22.55	22.57	22.73
whale-show	5	106	9	23.00	23.05	22.99
whale-show	5	106	10	22.95	23.04	22.98
whale-show	5	108	1	22.90	22.92	23.07

Continued on next page

Table V.1 – continued from previous page

Sequence	SNR (dB)	Frame	Run	JM 16.0	STBMA+PDE	SO-MLD
whale-show	5	108	2	23.23	23.26	23.37
whale-show	5	108	3	22.88	22.83	23.06
whale-show	5	108	4	22.94	22.94	23.08
whale-show	5	108	5	23.10	23.25	23.41
whale-show	5	108	6	22.96	23.06	23.13
whale-show	5	108	7	23.27	23.26	23.23
whale-show	5	108	8	23.03	23.11	23.28
whale-show	5	108	9	23.00	23.07	23.36
whale-show	5	108	10	22.87	22.81	23.01

Table V.2 Detailed experimental results for 1200 kbps

Sequence	SNR (dB)	Frame	Run	JM 16.0	STBMA+PDE	SO-MLD
city	4	62	1	23.16	24.04	24.13
city	4	62	2	23.71	27.16	26.95
city	4	62	3	23.40	24.44	26.76
city	4	62	4	24.18	26.14	26.88
city	4	62	5	23.86	26.57	27.64
city	4	62	6	24.47	26.93	27.59
city	4	62	7	24.79	27.85	27.79
city	4	62	8	24.10	27.06	27.05
city	4	62	9	24.92	27.13	27.81
city	4	62	10	23.92	25.76	26.39
city	4	66	1	24.67	27.12	27.70
city	4	66	2	25.28	26.15	29.63
city	4	66	3	25.43	29.31	28.20
city	4	66	4	24.86	28.64	26.55
city	4	66	5	25.14	28.72	27.19
city	4	66	6	24.27	24.27	27.27
city	4	66	7	24.47	24.64	27.27
city	4	66	8	24.68	27.70	27.83
city	4	66	9	24.58	26.99	27.38
city	4	66	10	24.63	25.00	28.38
city	4	71	1	24.44	25.09	26.13
city	4	71	2	25.29	25.51	28.40

Continued on next page

Table V.2 – continued from previous page

Sequence	SNR (dB)	Frame	Run	JM 16.0	STBMA+PDE	SO-MLD
city	4	84	4	25.03	26.53	27.08
city	4	84	5	24.32	24.43	26.25
city	4	84	6	24.33	24.71	26.19
city	4	84	7	24.42	26.14	26.17
city	4	84	8	25.53	28.02	29.05
city	4	84	9	24.73	27.23	24.61
city	4	84	10	24.64	26.78	27.75
city	4	88	1	24.65	25.06	25.29
city	4	88	2	24.82	26.66	27.23
city	4	88	3	24.54	28.42	26.66
city	4	88	4	24.15	24.15	26.38
city	4	88	5	24.39	26.67	24.91
city	4	88	6	24.81	28.99	25.66
city	4	88	7	24.41	24.98	25.82
city	4	88	8	24.98	27.14	28.07
city	4	88	9	25.85	29.80	27.11
city	4	88	10	24.76	25.09	25.88
city	4	95	1	24.26	25.99	26.51
city	4	95	2	24.55	27.34	27.51
city	4	95	3	24.42	27.73	26.37
city	4	95	4	24.75	28.36	28.14
city	4	95	5	24.44	27.62	27.22
city	4	95	6	24.79	27.89	26.94
city	4	95	7	23.94	23.94	25.58
city	4	95	8	24.29	25.42	27.55
city	4	95	9	24.39	28.24	25.19
city	4	95	10	24.73	26.30	26.57
city	4	101	1	24.78	28.47	26.96
city	4	101	2	25.31	27.53	27.55
city	4	101	3	25.00	28.18	27.60
city	4	101	4	25.03	28.25	26.76
city	4	101	5	24.75	25.11	24.84
city	4	101	6	25.11	28.17	26.74
city	4	101	7	25.88	30.43	28.89
city	4	101	8	24.58	24.82	26.24
city	4	101	9	24.74	28.51	28.26
city	4	101	10	24.71	27.68	25.24
city	5	66	1	26.51	29.99	29.72
city	5	66	2	26.21	29.54	30.98
city	5	66	3	27.25	29.97	32.30
city	5	66	4	27.59	32.03	28.93

Continued on next page

Table V.2 – continued from previous page

Sequence	SNR (dB)	Frame	Run	JM 16.0	STBMA+PDE	SO-MLD
city	5	66	5	26.57	31.87	29.83
city	5	66	6	27.50	31.05	30.27
city	5	66	7	28.16	31.25	30.67
city	5	66	8	28.96	32.03	32.37
city	5	66	9	28.65	31.52	30.63
city	5	66	10	27.44	32.10	30.51
city	5	68	1	29.80	31.40	32.68
city	5	68	2	27.20	31.14	30.39
city	5	68	3	27.05	29.71	30.30
city	5	68	4	28.81	32.38	31.50
city	5	68	5	27.40	31.53	31.25
city	5	68	6	30.86	32.15	32.54
city	5	68	7	28.49	31.82	31.31
city	5	68	8	26.37	29.54	27.76
city	5	68	9	29.11	32.35	30.67
city	5	68	10	30.87	31.50	32.34
city	5	71	1	28.22	31.28	31.04
city	5	71	2	26.42	29.22	30.55
city	5	71	3	26.42	30.49	29.83
city	5	71	4	28.78	31.46	30.68
city	5	71	5	26.57	31.43	29.44
city	5	71	6	26.63	30.60	29.97
city	5	71	7	29.94	32.73	32.76
city	5	71	8	26.62	30.21	29.09
city	5	71	9	28.23	32.46	31.69
city	5	71	10	28.48	31.60	31.67
city	5	72	1	27.91	30.87	29.38
city	5	72	2	29.74	31.42	32.19
city	5	72	3	27.18	31.71	30.49
city	5	72	4	26.60	28.42	28.50
city	5	72	5	26.23	30.57	28.07
city	5	72	6	28.62	32.21	29.77
city	5	72	7	28.22	31.88	30.56
city	5	72	8	26.72	31.36	28.78
city	5	72	9	28.12	31.79	30.30
city	5	72	10	26.98	31.00	29.63
city	5	75	1	27.85	29.91	30.31
city	5	75	2	28.53	30.85	30.36
city	5	75	3	28.66	31.57	31.95
city	5	75	4	27.19	30.84	29.92
city	5	75	5	28.35	31.62	30.71

Continued on next page

Table V.2 – continued from previous page

Sequence	SNR (dB)	Frame	Run	JM 16.0	STBMA+PDE	SO-MLD
city	5	95	7	27.24	31.76	29.85
city	5	95	8	26.84	31.36	30.25
city	5	95	9	27.74	31.67	29.33
city	5	95	10	27.56	31.86	30.18
city	5	101	1	27.38	31.72	31.15
city	5	101	2	28.46	32.08	31.55
city	5	101	3	28.56	31.52	31.71
city	5	101	4	26.55	31.21	30.26
city	5	101	5	27.99	31.03	29.98
city	5	101	6	29.41	32.11	30.88
city	5	101	7	28.10	31.05	30.18
city	5	101	8	28.14	31.32	31.15
city	5	101	9	28.17	31.41	31.22
city	5	101	10	27.74	31.43	29.58
crew	4	61	1	19.87	19.88	21.02
crew	4	61	2	19.65	19.66	21.07
crew	4	61	3	19.55	19.55	20.03
crew	4	61	4	20.16	20.17	22.12
crew	4	61	5	19.43	19.44	19.86
crew	4	61	6	19.84	19.84	19.79
crew	4	61	7	19.65	19.65	20.45
crew	4	61	8	20.01	20.02	20.54
crew	4	61	9	19.50	19.51	20.49
crew	4	61	10	19.79	19.80	21.39
crew	4	62	1	20.12	20.27	21.47
crew	4	62	2	19.31	19.41	19.60
crew	4	62	3	20.17	20.28	21.04
crew	4	62	4	19.75	19.80	20.35
crew	4	62	5	19.42	19.31	20.49
crew	4	62	6	19.95	20.15	20.37
crew	4	62	7	19.60	19.79	20.63
crew	4	62	8	19.31	19.32	18.93
crew	4	62	9	20.01	20.18	21.05
crew	4	62	10	19.72	19.81	21.51
crew	4	65	1	27.87	28.97	29.40
crew	4	65	2	27.60	28.34	28.67
crew	4	65	3	27.35	28.55	28.69
crew	4	65	4	27.30	27.11	28.90
crew	4	65	5	26.90	26.61	27.28
crew	4	65	6	27.39	27.89	28.98
crew	4	65	7	27.55	27.53	28.85

Continued on next page

Table V.2 – continued from previous page

Sequence	SNR (dB)	Frame	Run	JM 16.0	STBMA+PDE	SO-MLD
crew	4	65	8	27.04	27.62	28.04
crew	4	65	9	27.10	27.48	28.76
crew	4	65	10	28.16	28.48	29.31
crew	4	77	1	26.54	26.84	28.28
crew	4	77	2	26.72	27.21	27.88
crew	4	77	3	26.11	26.11	27.42
crew	4	77	4	26.86	27.32	28.31
crew	4	77	5	26.94	27.99	28.41
crew	4	77	6	27.61	29.27	29.25
crew	4	77	7	26.37	26.66	27.65
crew	4	77	8	27.86	29.10	30.25
crew	4	77	9	26.32	26.91	28.27
crew	4	77	10	27.01	28.25	29.23
crew	4	86	1	27.71	27.77	26.20
crew	4	86	2	27.27	27.30	28.15
crew	4	86	3	27.15	27.15	26.19
crew	4	86	4	27.84	28.53	28.15
crew	4	86	5	27.35	27.23	28.64
crew	4	86	6	27.31	27.30	26.14
crew	4	86	7	27.90	28.70	29.31
crew	4	86	8	27.26	27.08	28.10
crew	4	86	9	28.94	29.62	29.89
crew	4	86	10	27.69	28.36	28.23
crew	4	88	1	23.52	23.72	24.37
crew	4	88	2	23.81	24.13	24.98
crew	4	88	3	23.70	23.52	24.69
crew	4	88	4	23.44	23.75	24.38
crew	4	88	5	23.84	23.84	24.76
crew	4	88	6	23.69	23.89	24.34
crew	4	88	7	23.69	23.79	23.67
crew	4	88	8	23.36	23.24	23.48
crew	4	88	9	23.88	24.05	25.18
crew	4	88	10	23.97	24.26	24.00
crew	4	91	1	23.95	23.97	25.59
crew	4	91	2	23.64	23.65	23.25
crew	4	91	3	24.09	24.10	24.21
crew	4	91	4	24.00	24.03	24.47
crew	4	91	5	23.84	23.86	23.87
crew	4	91	6	23.77	23.78	24.29
crew	4	91	7	23.88	23.90	22.48
crew	4	91	8	23.76	23.77	24.62

Continued on next page

Table V.2 – continued from previous page

Sequence	SNR (dB)	Frame	Run	JM 16.0	STBMA+PDE	SO-MLD
crew	4	91	9	24.17	24.19	25.01
crew	4	91	10	23.73	23.74	23.98
crew	4	94	1	26.66	27.17	27.61
crew	4	94	2	26.59	26.97	28.16
crew	4	94	3	26.61	27.03	27.73
crew	4	94	4	26.69	26.99	28.06
crew	4	94	5	26.90	27.09	28.41
crew	4	94	6	26.73	27.19	28.72
crew	4	94	7	26.83	27.60	28.85
crew	4	94	8	27.28	28.71	28.85
crew	4	94	9	26.88	27.30	27.98
crew	4	94	10	27.09	27.76	28.08
crew	4	95	1	27.01	27.75	28.39
crew	4	95	2	26.84	27.20	28.02
crew	4	95	3	27.03	27.43	28.21
crew	4	95	4	27.47	28.17	28.29
crew	4	95	5	26.89	27.52	27.69
crew	4	95	6	26.90	27.45	27.81
crew	4	95	7	26.87	26.82	27.93
crew	4	95	8	27.76	28.32	28.77
crew	4	95	9	26.63	26.01	27.85
crew	4	95	10	27.10	27.93	27.93
crew	4	97	1	27.57	28.71	29.93
crew	4	97	2	26.32	26.32	27.78
crew	4	97	3	26.62	26.93	27.79
crew	4	97	4	26.80	26.78	28.44
crew	4	97	5	26.81	27.12	29.19
crew	4	97	6	27.81	28.64	29.36
crew	4	97	7	26.38	26.42	26.63
crew	4	97	8	26.94	27.36	28.64
crew	4	97	9	26.61	26.93	27.65
crew	4	97	10	26.97	27.49	27.94
crew	5	65	1	28.76	30.81	30.25
crew	5	65	2	31.77	32.60	32.67
crew	5	65	3	29.22	30.99	31.19
crew	5	65	4	30.11	31.55	32.15
crew	5	65	5	30.51	30.96	32.16
crew	5	65	6	30.96	31.97	32.36
crew	5	65	7	29.06	31.14	29.36
crew	5	65	8	29.73	30.64	31.32
crew	5	65	9	30.60	31.85	31.52

Continued on next page

Table V.2 – continued from previous page

Sequence	SNR (dB)	Frame	Run	JM 16.0	STBMA+PDE	SO-MLD
crew	5	80	1	29.99	30.29	31.19
crew	5	80	2	30.85	32.38	32.39
crew	5	80	3	31.11	32.12	32.27
crew	5	80	4	29.94	30.25	30.69
crew	5	80	5	31.03	32.07	32.16
crew	5	80	6	28.80	29.40	30.65
crew	5	80	7	30.51	31.80	31.69
crew	5	80	8	29.61	30.66	31.62
crew	5	80	9	29.86	31.23	31.58
crew	5	80	10	30.71	31.78	31.97
crew	5	84	1	29.34	30.63	31.67
crew	5	84	2	28.82	29.04	31.20
crew	5	84	3	30.77	31.90	32.51
crew	5	84	4	29.69	30.81	31.70
crew	5	84	5	28.98	30.19	30.34
crew	5	84	6	31.09	31.78	32.19
crew	5	84	7	28.69	29.93	31.42
crew	5	84	8	29.56	30.54	32.26
crew	5	84	9	30.79	31.62	31.75
crew	5	84	10	29.86	31.06	30.81
crew	5	87	1	30.53	32.07	32.14
crew	5	87	2	30.84	32.06	31.71
crew	5	87	3	28.39	29.73	29.58
crew	5	87	4	28.68	29.83	31.53
crew	5	87	5	29.99	31.31	31.78
crew	5	87	6	31.24	32.27	32.77
crew	5	87	7	30.24	31.40	32.25
crew	5	87	8	28.48	29.59	29.65
crew	5	87	9	29.69	31.10	30.80
crew	5	87	10	29.82	30.45	32.28
crew	5	93	1	29.28	30.83	30.78
crew	5	93	2	29.96	31.29	31.37
crew	5	93	3	29.49	31.03	30.88
crew	5	93	4	28.30	29.64	29.75
crew	5	93	5	27.74	28.85	29.26
crew	5	93	6	28.04	28.54	29.27
crew	5	93	7	29.98	31.85	31.15
crew	5	93	8	29.24	29.94	30.69
crew	5	93	9	30.21	31.27	30.81
crew	5	93	10	29.10	30.66	30.29
crew	5	99	1	29.86	31.05	30.70

Continued on next page

Table V.2 – continued from previous page

Sequence	SNR (dB)	Frame	Run	JM 16.0	STBMA+PDE	SO-MLD
driving	5	62	5	21.98	26.75	25.81
driving	5	62	6	22.43	25.16	25.84
driving	5	62	7	21.57	24.81	26.61
driving	5	62	8	21.62	25.03	25.20
driving	5	62	9	21.78	26.05	26.48
driving	5	62	10	22.40	25.91	27.57
driving	5	63	1	23.45	25.34	27.61
driving	5	63	2	24.35	26.47	27.04
driving	5	63	3	22.31	25.76	25.37
driving	5	63	4	22.92	25.25	27.57
driving	5	63	5	21.69	24.32	24.91
driving	5	63	6	22.37	26.18	26.88
driving	5	63	7	22.38	24.61	24.74
driving	5	63	8	21.44	24.24	25.69
driving	5	63	9	25.05	28.43	27.01
driving	5	63	10	21.14	23.11	24.39
driving	5	70	1	22.73	25.76	24.07
driving	5	70	2	23.73	26.76	25.60
driving	5	70	3	22.08	24.31	25.93
driving	5	70	4	22.14	25.80	23.76
driving	5	70	5	22.37	25.08	25.51
driving	5	70	6	22.49	25.99	27.01
driving	5	70	7	23.04	26.53	27.24
driving	5	70	8	23.59	25.49	25.37
driving	5	70	9	22.63	25.25	25.50
driving	5	70	10	22.85	26.83	25.66
driving	5	71	1	25.10	26.89	26.54
driving	5	71	2	23.64	26.82	26.41
driving	5	71	3	25.74	28.23	27.82
driving	5	71	4	23.87	24.85	25.57
driving	5	71	5	23.64	26.67	26.35
driving	5	71	6	24.59	26.91	26.35
driving	5	71	7	23.66	26.63	24.94
driving	5	71	8	25.35	26.86	27.71
driving	5	71	9	23.38	25.97	26.35
driving	5	71	10	25.37	26.86	27.99
driving	5	80	1	25.05	28.76	29.35
driving	5	80	2	23.98	27.99	26.09
driving	5	80	3	23.23	26.00	25.50
driving	5	80	4	22.76	24.42	24.05
driving	5	80	5	25.54	27.35	27.00

Continued on next page

Table V.2 – continued from previous page

Sequence	SNR (dB)	Frame	Run	JM 16.0	STBMA+PDE	SO-MLD
driving	5	92	7	20.82	24.81	24.68
driving	5	92	8	25.05	27.57	28.05
driving	5	92	9	21.71	25.00	23.22
driving	5	92	10	22.60	26.54	23.60
harbour	4	64	1	24.75	24.48	25.44
harbour	4	64	2	24.90	25.25	25.62
harbour	4	64	3	24.53	25.24	24.92
harbour	4	64	4	25.38	26.12	25.49
harbour	4	64	5	24.90	25.17	25.50
harbour	4	64	6	24.93	25.16	24.89
harbour	4	64	7	24.90	25.22	25.77
harbour	4	64	8	24.76	24.50	25.07
harbour	4	64	9	24.75	24.44	25.40
harbour	4	64	10	25.07	25.32	25.83
harbour	4	65	1	24.30	24.25	24.96
harbour	4	65	2	24.63	25.68	24.94
harbour	4	65	3	24.13	24.31	24.53
harbour	4	65	4	24.66	24.95	25.31
harbour	4	65	5	24.12	25.12	24.43
harbour	4	65	6	24.84	25.77	25.60
harbour	4	65	7	24.32	24.55	24.75
harbour	4	65	8	24.56	25.31	25.09
harbour	4	65	9	24.72	25.54	25.24
harbour	4	65	10	24.69	25.89	25.17
harbour	4	70	1	25.26	25.22	25.49
harbour	4	70	2	24.88	24.63	25.39
harbour	4	70	3	24.84	24.82	25.80
harbour	4	70	4	24.90	25.00	25.36
harbour	4	70	5	25.23	24.71	25.95
harbour	4	70	6	25.51	25.56	25.83
harbour	4	70	7	24.79	24.25	25.18
harbour	4	70	8	25.33	24.67	25.68
harbour	4	70	9	24.76	24.84	24.90
harbour	4	70	10	24.66	23.77	24.49
harbour	4	73	1	23.73	24.50	25.74
harbour	4	73	2	23.52	24.37	24.20
harbour	4	73	3	23.86	25.16	25.18
harbour	4	73	4	23.89	26.09	25.07
harbour	4	73	5	23.22	23.33	24.76
harbour	4	73	6	23.70	26.03	25.10
harbour	4	73	7	23.44	24.59	25.34

Continued on next page

Table V.2 – continued from previous page

Sequence	SNR (dB)	Frame	Run	JM 16.0	STBMA+PDE	SO-MLD
harbour	4	85	9	24.23	23.41	25.35
harbour	4	85	10	24.32	25.42	25.17
harbour	4	87	1	25.60	25.91	25.54
harbour	4	87	2	25.56	25.13	25.86
harbour	4	87	3	25.74	25.81	26.43
harbour	4	87	4	25.37	25.46	25.59
harbour	4	87	5	25.40	25.77	25.88
harbour	4	87	6	25.57	26.10	25.59
harbour	4	87	7	25.79	25.83	26.11
harbour	4	87	8	26.06	26.22	26.53
harbour	4	87	9	25.49	25.62	25.52
harbour	4	87	10	25.97	26.21	26.43
harbour	4	88	1	25.58	25.52	25.72
harbour	4	88	2	24.85	24.85	25.24
harbour	4	88	3	25.38	25.79	25.47
harbour	4	88	4	25.54	25.88	26.09
harbour	4	88	5	24.85	24.85	25.18
harbour	4	88	6	24.85	24.85	25.65
harbour	4	88	7	25.25	25.36	25.88
harbour	4	88	8	25.40	25.20	25.90
harbour	4	88	9	25.11	25.38	24.84
harbour	4	88	10	25.38	25.76	25.82
harbour	5	65	1	26.11	26.91	26.95
harbour	5	65	2	27.14	27.57	27.98
harbour	5	65	3	27.29	28.35	28.36
harbour	5	65	4	26.32	27.04	27.61
harbour	5	65	5	26.48	27.32	27.47
harbour	5	65	6	26.12	27.04	27.33
harbour	5	65	7	27.13	27.95	27.62
harbour	5	65	8	26.65	27.39	27.52
harbour	5	65	9	25.98	26.69	26.66
harbour	5	65	10	27.33	27.92	28.08
harbour	5	67	1	26.43	28.00	27.31
harbour	5	67	2	24.93	26.82	27.01
harbour	5	67	3	25.62	27.24	27.55
harbour	5	67	4	24.77	26.66	26.43
harbour	5	67	5	25.03	26.59	26.28
harbour	5	67	6	24.56	26.77	25.54
harbour	5	67	7	24.41	26.91	25.80
harbour	5	67	8	24.79	25.94	25.98
harbour	5	67	9	24.41	26.91	26.46

Continued on next page

Table V.2 – continued from previous page

Sequence	SNR (dB)	Frame	Run	JM 16.0	STBMA+PDE	SO-MLD
harbour	5	67	10	26.05	27.74	27.69
harbour	5	68	1	27.38	27.19	27.54
harbour	5	68	2	26.88	26.55	26.65
harbour	5	68	3	27.19	26.47	26.93
harbour	5	68	4	27.82	27.28	28.36
harbour	5	68	5	26.57	26.53	26.82
harbour	5	68	6	27.53	27.79	27.90
harbour	5	68	7	26.88	26.85	27.03
harbour	5	68	8	26.11	26.05	26.03
harbour	5	68	9	26.63	25.85	27.26
harbour	5	68	10	27.09	26.96	27.44
harbour	5	74	1	25.13	26.10	27.15
harbour	5	74	2	26.02	27.81	27.30
harbour	5	74	3	24.88	26.18	26.76
harbour	5	74	4	25.78	27.02	27.60
harbour	5	74	5	25.99	27.61	27.85
harbour	5	74	6	25.71	26.83	26.31
harbour	5	74	7	25.65	26.70	26.48
harbour	5	74	8	26.13	27.50	27.42
harbour	5	74	9	25.66	27.43	27.26
harbour	5	74	10	25.92	27.15	27.25
harbour	5	85	1	25.40	26.70	26.89
harbour	5	85	2	26.09	27.56	26.83
harbour	5	85	3	27.58	28.48	28.05
harbour	5	85	4	26.25	27.00	26.84
harbour	5	85	5	26.70	27.55	27.43
harbour	5	85	6	25.88	27.08	27.00
harbour	5	85	7	26.58	27.86	27.42
harbour	5	85	8	26.65	27.33	27.29
harbour	5	85	9	25.61	26.82	27.05
harbour	5	85	10	26.69	27.77	26.87
harbour	5	88	1	26.59	26.61	26.68
harbour	5	88	2	26.05	26.15	27.18
harbour	5	88	3	26.60	27.00	27.24
harbour	5	88	4	27.06	27.65	27.68
harbour	5	88	5	27.12	27.65	27.54
harbour	5	88	6	26.68	27.03	27.48
harbour	5	88	7	26.64	27.30	27.76
harbour	5	88	8	26.15	26.60	27.14
harbour	5	88	9	26.80	27.11	27.54
harbour	5	88	10	26.87	27.47	27.27

Continued on next page

Table V.2 – continued from previous page

Sequence	SNR (dB)	Frame	Run	JM 16.0	STBMA+PDE	SO-MLD
harbour	5	92	1	28.38	28.67	28.53
harbour	5	92	2	27.29	27.66	28.06
harbour	5	92	3	27.86	28.42	28.73
harbour	5	92	4	27.45	27.73	28.10
harbour	5	92	5	25.81	26.72	26.79
harbour	5	92	6	26.20	26.33	25.83
harbour	5	92	7	27.16	27.89	28.02
harbour	5	92	8	27.94	28.44	27.96
harbour	5	92	9	27.45	27.99	28.56
harbour	5	92	10	26.16	26.89	27.11
harbour	5	101	1	22.49	27.43	26.69
harbour	5	101	2	22.98	27.61	25.65
harbour	5	101	3	22.82	26.47	25.79
harbour	5	101	4	23.61	27.82	26.43
harbour	5	101	5	23.00	27.26	25.69
harbour	5	101	6	22.66	25.39	25.29
harbour	5	101	7	22.00	24.58	24.49
harbour	5	101	8	22.87	27.35	26.30
harbour	5	101	9	22.96	27.82	25.60
harbour	5	101	10	23.60	26.81	26.21
harbour	5	106	1	24.39	27.37	25.20
harbour	5	106	2	24.45	27.42	27.16
harbour	5	106	3	23.59	26.92	25.78
harbour	5	106	4	25.15	27.61	25.99
harbour	5	106	5	24.42	27.07	26.32
harbour	5	106	6	24.56	26.74	25.74
harbour	5	106	7	25.21	26.91	27.33
harbour	5	106	8	24.16	25.43	26.45
harbour	5	106	9	24.48	27.06	27.05
harbour	5	106	10	25.46	27.16	27.53
harbour	5	108	1	25.37	27.90	27.55
harbour	5	108	2	23.35	27.40	26.09
harbour	5	108	3	23.11	25.89	25.01
harbour	5	108	4	23.43	26.15	25.57
harbour	5	108	5	25.21	27.65	26.86
harbour	5	108	6	23.57	27.10	26.97
harbour	5	108	7	24.06	27.02	26.81
harbour	5	108	8	25.62	27.96	27.28
harbour	5	108	9	23.93	26.05	25.66
harbour	5	108	10	23.93	26.89	25.92
ice	4	63	1	24.17	24.63	26.20

Continued on next page

Table V.2 – continued from previous page

Sequence	SNR (dB)	Frame	Run	JM 16.0	STBMA+PDE	SO-MLD
ice	4	63	2	24.21	24.88	26.40
ice	4	63	3	24.34	25.25	25.86
ice	4	63	4	24.38	24.42	26.51
ice	4	63	5	24.43	26.01	26.32
ice	4	63	6	24.58	26.24	28.56
ice	4	63	7	24.10	23.74	26.18
ice	4	63	8	24.28	24.95	25.74
ice	4	63	9	24.50	25.57	26.69
ice	4	63	10	24.89	25.72	26.79
ice	4	64	1	23.98	24.95	27.07
ice	4	64	2	24.31	24.49	27.46
ice	4	64	3	25.38	27.58	28.88
ice	4	64	4	24.00	24.53	26.32
ice	4	64	5	23.75	24.04	25.37
ice	4	64	6	23.96	23.60	25.77
ice	4	64	7	24.51	24.75	27.02
ice	4	64	8	24.99	25.98	28.42
ice	4	64	9	24.33	26.12	26.64
ice	4	64	10	24.10	25.05	26.37
ice	4	67	1	24.93	26.01	27.77
ice	4	67	2	23.93	24.79	25.62
ice	4	67	3	24.08	23.83	25.48
ice	4	67	4	23.93	23.67	26.09
ice	4	67	5	24.43	24.77	26.59
ice	4	67	6	24.04	24.54	26.30
ice	4	67	7	24.13	24.12	25.81
ice	4	67	8	24.84	25.24	27.63
ice	4	67	9	23.67	23.34	25.40
ice	4	67	10	24.35	24.82	25.89
ice	4	70	1	24.85	25.61	26.68
ice	4	70	2	24.97	25.56	26.93
ice	4	70	3	24.64	25.23	25.96
ice	4	70	4	24.78	24.58	26.87
ice	4	70	5	24.52	24.88	25.64
ice	4	70	6	24.46	24.76	25.67
ice	4	70	7	24.14	23.80	25.93
ice	4	70	8	24.74	25.03	25.60
ice	4	70	9	24.08	24.01	25.11
ice	4	70	10	24.59	24.46	26.22
ice	4	72	1	24.90	25.36	26.53
ice	4	72	2	25.50	24.53	27.31

Continued on next page

Table V.2 – continued from previous page

Sequence	SNR (dB)	Frame	Run	JM 16.0	STBMA+PDE	SO-MLD
ice	4	72	3	25.37	25.96	27.21
ice	4	72	4	24.75	24.12	25.98
ice	4	72	5	24.88	25.29	25.85
ice	4	72	6	25.33	25.81	26.78
ice	4	72	7	25.44	25.81	27.43
ice	4	72	8	24.79	25.13	26.64
ice	4	72	9	24.92	24.43	25.67
ice	4	72	10	25.57	25.85	27.16
ice	4	78	1	25.17	26.75	28.62
ice	4	78	2	25.45	25.95	28.68
ice	4	78	3	24.89	24.86	26.55
ice	4	78	4	25.17	25.50	28.12
ice	4	78	5	25.34	26.76	29.22
ice	4	78	6	25.08	26.27	27.97
ice	4	78	7	25.06	24.77	26.92
ice	4	78	8	25.95	27.06	28.12
ice	4	78	9	26.05	27.62	28.01
ice	4	78	10	25.64	27.64	28.71
ice	4	85	1	25.46	25.02	27.92
ice	4	85	2	25.20	25.21	27.07
ice	4	85	3	25.61	25.69	28.33
ice	4	85	4	26.01	27.61	28.70
ice	4	85	5	25.72	26.80	28.40
ice	4	85	6	25.24	25.02	27.25
ice	4	85	7	25.13	25.20	28.41
ice	4	85	8	25.85	26.11	29.97
ice	4	85	9	25.24	24.29	27.50
ice	4	85	10	25.25	25.19	27.77
ice	4	86	1	24.94	25.64	28.00
ice	4	86	2	26.75	27.43	30.03
ice	4	86	3	25.38	26.36	28.49
ice	4	86	4	25.54	25.30	28.27
ice	4	86	5	25.39	26.27	29.23
ice	4	86	6	25.42	26.65	28.03
ice	4	86	7	24.85	25.38	26.90
ice	4	86	8	25.82	27.44	28.07
ice	4	86	9	25.41	25.77	27.32
ice	4	86	10	25.09	26.27	27.61
ice	4	93	1	24.95	28.08	27.60
ice	4	93	2	25.03	27.62	29.29
ice	4	93	3	24.93	26.80	26.40

Continued on next page

Table V.2 – continued from previous page

Sequence	SNR (dB)	Frame	Run	JM 16.0	STBMA+PDE	SO-MLD
ice	4	93	4	24.41	26.07	26.70
ice	4	93	5	24.37	26.11	26.57
ice	4	93	6	24.91	27.58	26.58
ice	4	93	7	24.01	23.54	28.10
ice	4	93	8	24.66	27.73	28.86
ice	4	93	9	24.74	25.52	26.09
ice	4	93	10	24.46	26.72	26.41
ice	4	99	1	23.79	23.81	26.09
ice	4	99	2	24.13	25.97	27.26
ice	4	99	3	25.16	26.99	28.41
ice	4	99	4	23.78	24.23	26.28
ice	4	99	5	24.26	24.27	26.73
ice	4	99	6	24.24	24.75	25.58
ice	4	99	7	24.35	25.25	27.93
ice	4	99	8	24.17	26.62	27.27
ice	4	99	9	24.07	24.97	27.03
ice	4	99	10	24.70	28.46	27.38
ice	5	66	1	26.20	30.25	29.44
ice	5	66	2	27.55	30.30	30.66
ice	5	66	3	26.99	28.81	30.34
ice	5	66	4	30.19	32.47	34.22
ice	5	66	5	28.96	32.12	32.57
ice	5	66	6	29.59	35.15	36.35
ice	5	66	7	26.62	28.51	29.73
ice	5	66	8	28.63	31.46	32.22
ice	5	66	9	27.32	29.78	29.03
ice	5	66	10	29.05	35.14	34.38
ice	5	67	1	26.32	27.99	30.34
ice	5	67	2	28.28	30.37	35.11
ice	5	67	3	27.29	31.75	30.82
ice	5	67	4	27.81	30.35	32.57
ice	5	67	5	27.40	30.19	31.00
ice	5	67	6	27.93	30.49	32.32
ice	5	67	7	31.68	34.21	34.45
ice	5	67	8	31.47	34.08	35.86
ice	5	67	9	26.72	27.84	30.81
ice	5	67	10	27.56	29.17	32.40
ice	5	73	1	32.10	33.73	33.37
ice	5	73	2	26.54	27.62	29.23
ice	5	73	3	29.89	31.48	33.02
ice	5	73	4	28.32	31.24	32.28

Continued on next page

Table V.2 – continued from previous page

Sequence	SNR (dB)	Frame	Run	JM 16.0	STBMA+PDE	SO-MLD
ice	5	73	5	28.94	30.78	33.20
ice	5	73	6	28.60	31.43	31.05
ice	5	73	7	31.01	31.96	32.12
ice	5	73	8	31.00	33.18	34.75
ice	5	73	9	30.09	33.18	33.25
ice	5	73	10	29.51	31.96	33.96
ice	5	76	1	28.94	31.52	32.72
ice	5	76	2	28.36	31.74	32.54
ice	5	76	3	28.76	31.63	32.98
ice	5	76	4	27.64	30.02	31.34
ice	5	76	5	28.24	30.69	31.53
ice	5	76	6	28.24	30.93	30.30
ice	5	76	7	27.40	29.82	30.81
ice	5	76	8	27.57	28.64	29.76
ice	5	76	9	28.29	32.17	33.60
ice	5	76	10	29.58	32.52	35.63
ice	5	84	1	28.86	31.41	32.55
ice	5	84	2	28.12	29.62	30.72
ice	5	84	3	30.36	31.78	32.68
ice	5	84	4	29.76	31.69	31.95
ice	5	84	5	30.31	32.76	32.59
ice	5	84	6	30.16	32.08	34.06
ice	5	84	7	28.51	30.80	32.29
ice	5	84	8	30.89	32.92	32.44
ice	5	84	9	30.50	32.12	32.12
ice	5	84	10	29.85	31.57	32.51
ice	5	89	1	27.58	30.31	31.29
ice	5	89	2	27.58	30.16	31.28
ice	5	89	3	27.34	29.12	30.07
ice	5	89	4	26.52	29.13	30.00
ice	5	89	5	29.30	34.86	33.48
ice	5	89	6	27.90	29.40	30.45
ice	5	89	7	29.07	33.85	33.02
ice	5	89	8	26.57	30.24	30.60
ice	5	89	9	27.83	28.38	28.75
ice	5	89	10	27.80	32.39	31.59
ice	5	91	1	27.20	27.21	27.88
ice	5	91	2	28.60	28.62	28.64
ice	5	91	3	27.48	27.50	29.89
ice	5	91	4	27.44	27.45	30.07
ice	5	91	5	29.54	29.54	32.34

Continued on next page

Table V.2 – continued from previous page

Sequence	SNR (dB)	Frame	Run	JM 16.0	STBMA+PDE	SO-MLD
ice	5	91	6	27.61	27.63	29.54
ice	5	91	7	28.54	28.55	30.21
ice	5	91	8	29.45	29.46	32.84
ice	5	91	9	28.14	28.16	23.27
ice	5	91	10	28.91	28.93	30.98
ice	5	96	1	28.87	31.74	32.91
ice	5	96	2	27.45	32.01	30.37
ice	5	96	3	30.48	35.40	35.66
ice	5	96	4	27.79	31.40	31.36
ice	5	96	5	30.87	34.69	34.12
ice	5	96	6	27.90	31.88	30.92
ice	5	96	7	28.48	31.99	30.58
ice	5	96	8	29.36	32.08	30.41
ice	5	96	9	27.99	32.08	30.55
ice	5	96	10	28.24	32.31	31.43
ice	5	97	1	27.94	31.49	31.47
ice	5	97	2	30.08	32.85	32.98
ice	5	97	3	26.90	31.90	31.35
ice	5	97	4	27.46	32.19	30.69
ice	5	97	5	29.60	35.17	33.61
ice	5	97	6	28.54	33.18	32.12
ice	5	97	7	29.59	31.70	34.13
ice	5	97	8	27.22	30.46	32.04
ice	5	97	9	28.17	31.42	32.11
ice	5	97	10	27.99	32.65	29.70
ice	5	99	1	28.31	31.55	31.11
ice	5	99	2	27.99	30.26	30.50
ice	5	99	3	27.22	31.12	32.32
ice	5	99	4	26.42	31.24	34.66
ice	5	99	5	25.18	27.63	29.29
ice	5	99	6	26.97	32.34	29.68
ice	5	99	7	27.26	32.43	34.21
ice	5	99	8	29.10	33.90	35.33
ice	5	99	9	27.63	31.44	30.26
ice	5	99	10	28.31	32.87	34.85
opening-ceremony	4	65	1	26.92	26.01	26.70
opening-ceremony	4	65	2	27.06	27.15	27.21
opening-ceremony	4	65	3	26.60	26.60	26.75
opening-ceremony	4	65	4	26.74	26.69	26.81
opening-ceremony	4	65	5	26.64	26.64	26.32
opening-ceremony	4	65	6	26.60	26.60	26.38

Continued on next page

Table V.2 – continued from previous page

Sequence	SNR (dB)	Frame	Run	JM 16.0	STBMA+PDE	SO-MLD
opening-ceremony	4	65	7	26.78	26.99	26.46
opening-ceremony	4	65	8	27.01	27.01	27.27
opening-ceremony	4	65	9	26.71	26.71	26.93
opening-ceremony	4	65	10	26.96	25.91	26.78
opening-ceremony	4	67	1	26.79	26.79	26.73
opening-ceremony	4	67	2	26.57	26.29	26.15
opening-ceremony	4	67	3	26.80	26.79	26.61
opening-ceremony	4	67	4	26.77	26.66	27.06
opening-ceremony	4	67	5	26.57	26.59	26.44
opening-ceremony	4	67	6	26.62	26.51	26.26
opening-ceremony	4	67	7	26.98	26.78	26.98
opening-ceremony	4	67	8	26.82	25.60	27.00
opening-ceremony	4	67	9	26.76	25.76	25.49
opening-ceremony	4	67	10	26.57	26.57	25.15
opening-ceremony	4	68	1	26.59	23.68	26.55
opening-ceremony	4	68	2	26.69	25.91	27.03
opening-ceremony	4	68	3	26.81	26.71	26.63
opening-ceremony	4	68	4	26.85	26.28	26.55
opening-ceremony	4	68	5	26.85	26.76	26.59
opening-ceremony	4	68	6	26.66	26.60	26.92
opening-ceremony	4	68	7	26.76	25.53	26.78
opening-ceremony	4	68	8	27.16	27.41	27.53
opening-ceremony	4	68	9	26.90	21.22	27.04
opening-ceremony	4	68	10	26.54	26.54	26.55
opening-ceremony	4	74	1	26.78	26.80	26.92
opening-ceremony	4	74	2	26.81	26.61	27.11
opening-ceremony	4	74	3	27.17	26.58	27.19
opening-ceremony	4	74	4	26.69	26.75	27.10
opening-ceremony	4	74	5	26.85	26.76	26.61
opening-ceremony	4	74	6	26.61	26.61	25.92
opening-ceremony	4	74	7	26.97	27.14	26.29
opening-ceremony	4	74	8	26.72	26.59	27.11
opening-ceremony	4	74	9	26.72	26.80	26.69
opening-ceremony	4	74	10	26.71	26.71	27.44
opening-ceremony	4	85	1	26.87	26.38	26.27
opening-ceremony	4	85	2	26.90	26.39	25.68
opening-ceremony	4	85	3	26.64	26.59	26.81
opening-ceremony	4	85	4	26.98	26.73	27.00
opening-ceremony	4	85	5	26.50	26.50	25.46
opening-ceremony	4	85	6	26.63	26.03	26.61
opening-ceremony	4	85	7	26.64	26.03	26.23

Continued on next page

Table V.2 – continued from previous page

Sequence	SNR (dB)	Frame	Run	JM 16.0	STBMA+PDE	SO-MLD
opening-ceremony	4	106	9	26.83	26.81	27.10
opening-ceremony	4	106	10	26.66	26.67	27.06
opening-ceremony	4	108	1	26.59	26.45	26.92
opening-ceremony	4	108	2	26.75	26.55	26.76
opening-ceremony	4	108	3	26.82	26.68	27.19
opening-ceremony	4	108	4	26.78	26.81	27.04
opening-ceremony	4	108	5	26.66	26.66	26.73
opening-ceremony	4	108	6	26.62	26.56	26.90
opening-ceremony	4	108	7	26.76	26.75	27.47
opening-ceremony	4	108	8	26.82	26.78	27.33
opening-ceremony	4	108	9	26.55	26.55	26.52
opening-ceremony	4	108	10	26.60	26.54	26.44
opening-ceremony	5	64	1	27.26	26.79	27.52
opening-ceremony	5	64	2	27.95	28.04	28.24
opening-ceremony	5	64	3	27.96	28.04	27.92
opening-ceremony	5	64	4	27.19	26.97	27.43
opening-ceremony	5	64	5	27.63	27.72	27.83
opening-ceremony	5	64	6	27.23	26.01	27.21
opening-ceremony	5	64	7	28.26	28.28	28.44
opening-ceremony	5	64	8	28.06	27.84	28.19
opening-ceremony	5	64	9	27.46	26.76	27.86
opening-ceremony	5	64	10	27.58	27.72	27.66
opening-ceremony	5	67	1	27.96	28.13	28.12
opening-ceremony	5	67	2	27.58	27.99	28.06
opening-ceremony	5	67	3	28.01	28.17	27.97
opening-ceremony	5	67	4	28.24	28.09	28.15
opening-ceremony	5	67	5	27.47	27.54	27.70
opening-ceremony	5	67	6	27.51	27.08	27.91
opening-ceremony	5	67	7	27.54	27.79	27.85
opening-ceremony	5	67	8	27.47	27.77	27.92
opening-ceremony	5	67	9	27.38	27.51	27.48
opening-ceremony	5	67	10	26.92	27.17	27.08
opening-ceremony	5	73	1	27.32	27.41	27.65
opening-ceremony	5	73	2	27.62	27.01	27.48
opening-ceremony	5	73	3	27.51	27.96	28.04
opening-ceremony	5	73	4	27.95	27.55	27.90
opening-ceremony	5	73	5	27.49	27.96	27.95
opening-ceremony	5	73	6	27.68	27.37	27.88
opening-ceremony	5	73	7	27.06	26.64	26.10
opening-ceremony	5	73	8	27.45	27.62	27.66
opening-ceremony	5	73	9	27.14	26.67	27.51

Continued on next page

Table V.2 – continued from previous page

Sequence	SNR (dB)	Frame	Run	JM 16.0	STBMA+PDE	SO-MLD
opening-ceremony	5	73	10	27.46	27.94	27.93
opening-ceremony	5	76	1	27.51	27.25	25.63
opening-ceremony	5	76	2	27.89	28.06	27.93
opening-ceremony	5	76	3	27.89	28.10	28.17
opening-ceremony	5	76	4	27.64	27.64	25.46
opening-ceremony	5	76	5	27.53	27.74	27.79
opening-ceremony	5	76	6	27.48	27.85	27.85
opening-ceremony	5	76	7	27.38	27.04	27.74
opening-ceremony	5	76	8	27.92	27.97	26.04
opening-ceremony	5	76	9	27.54	27.62	27.72
opening-ceremony	5	76	10	27.72	27.94	28.10
opening-ceremony	5	78	1	27.31	27.49	27.60
opening-ceremony	5	78	2	27.14	27.59	27.48
opening-ceremony	5	78	3	27.16	27.52	27.72
opening-ceremony	5	78	4	27.57	27.64	27.79
opening-ceremony	5	78	5	26.77	26.88	26.81
opening-ceremony	5	78	6	27.37	27.46	27.60
opening-ceremony	5	78	7	27.06	27.36	26.89
opening-ceremony	5	78	8	27.34	27.03	27.25
opening-ceremony	5	78	9	27.32	27.31	27.53
opening-ceremony	5	78	10	27.08	27.05	27.15
opening-ceremony	5	80	1	27.27	26.76	26.59
opening-ceremony	5	80	2	27.30	27.47	27.66
opening-ceremony	5	80	3	26.78	26.79	26.48
opening-ceremony	5	80	4	27.23	27.69	26.92
opening-ceremony	5	80	5	27.21	27.45	27.93
opening-ceremony	5	80	6	27.68	27.67	27.70
opening-ceremony	5	80	7	27.54	27.64	27.54
opening-ceremony	5	80	8	27.41	27.41	27.88
opening-ceremony	5	80	9	27.19	27.17	27.59
opening-ceremony	5	80	10	27.60	27.58	27.49
opening-ceremony	5	84	1	27.55	27.79	27.85
opening-ceremony	5	84	2	27.54	26.77	25.45
opening-ceremony	5	84	3	27.52	27.74	27.76
opening-ceremony	5	84	4	27.49	26.73	26.85
opening-ceremony	5	84	5	27.82	27.94	26.53
opening-ceremony	5	84	6	27.58	27.80	25.46
opening-ceremony	5	84	7	27.30	27.60	25.45
opening-ceremony	5	84	8	27.75	27.85	27.68
opening-ceremony	5	84	9	27.64	27.80	27.84
opening-ceremony	5	84	10	27.38	27.64	27.71

Continued on next page

Table V.2 – continued from previous page

Sequence	SNR (dB)	Frame	Run	JM 16.0	STBMA+PDE	SO-MLD
opening-ceremony	5	85	1	27.28	27.37	27.49
opening-ceremony	5	85	2	27.47	27.01	27.53
opening-ceremony	5	85	3	27.83	27.77	27.96
opening-ceremony	5	85	4	27.15	27.50	27.44
opening-ceremony	5	85	5	27.78	27.97	27.98
opening-ceremony	5	85	6	27.00	26.96	27.61
opening-ceremony	5	85	7	27.72	27.83	27.80
opening-ceremony	5	85	8	27.60	27.53	27.29
opening-ceremony	5	85	9	27.28	27.43	27.52
opening-ceremony	5	85	10	27.59	27.83	27.64
opening-ceremony	5	93	1	28.28	28.49	28.59
opening-ceremony	5	93	2	27.85	26.64	27.65
opening-ceremony	5	93	3	27.83	27.64	27.70
opening-ceremony	5	93	4	27.68	27.56	27.86
opening-ceremony	5	93	5	27.91	28.09	28.14
opening-ceremony	5	93	6	27.71	27.97	28.09
opening-ceremony	5	93	7	27.32	27.46	27.41
opening-ceremony	5	93	8	28.34	28.56	28.63
opening-ceremony	5	93	9	28.33	27.99	28.11
opening-ceremony	5	93	10	28.26	28.45	28.33
opening-ceremony	5	98	1	27.61	27.58	27.78
opening-ceremony	5	98	2	27.29	27.24	27.42
opening-ceremony	5	98	3	27.88	27.94	27.92
opening-ceremony	5	98	4	27.87	28.07	28.23
opening-ceremony	5	98	5	27.88	28.30	28.13
opening-ceremony	5	98	6	27.42	27.80	27.95
opening-ceremony	5	98	7	27.84	28.10	28.07
opening-ceremony	5	98	8	27.29	27.40	27.35
opening-ceremony	5	98	9	27.35	27.41	27.23
opening-ceremony	5	98	10	27.40	27.63	27.83
soccer	4	62	1	22.43	22.71	24.61
soccer	4	62	2	22.19	23.30	23.64
soccer	4	62	3	24.13	26.29	26.41
soccer	4	62	4	22.58	23.29	23.59
soccer	4	62	5	23.99	26.56	26.14
soccer	4	62	6	22.79	23.59	26.49
soccer	4	62	7	22.01	22.01	24.80
soccer	4	62	8	22.66	23.19	24.41
soccer	4	62	9	22.44	22.04	25.10
soccer	4	62	10	23.51	24.42	26.02
soccer	4	63	1	23.14	24.28	25.67

Continued on next page

Table V.2 – continued from previous page

Sequence	SNR (dB)	Frame	Run	JM 16.0	STBMA+PDE	SO-MLD
soccer	4	81	3	22.48	21.08	24.70
soccer	4	81	4	22.38	22.43	24.09
soccer	4	81	5	22.84	23.60	24.48
soccer	4	81	6	22.33	22.31	23.77
soccer	4	81	7	23.27	23.86	24.48
soccer	4	81	8	22.40	22.97	25.12
soccer	4	81	9	22.66	22.33	24.22
soccer	4	81	10	23.94	23.49	25.63
soccer	4	83	1	22.71	22.58	25.02
soccer	4	83	2	22.93	23.16	24.14
soccer	4	83	3	22.62	22.38	25.71
soccer	4	83	4	23.79	21.80	25.90
soccer	4	83	5	23.91	21.88	26.35
soccer	4	83	6	22.91	22.94	25.25
soccer	4	83	7	22.69	22.78	24.70
soccer	4	83	8	22.94	20.27	24.65
soccer	4	83	9	23.55	23.63	24.80
soccer	4	83	10	22.53	20.83	23.57
soccer	4	87	1	21.14	21.14	22.65
soccer	4	87	2	22.30	23.31	24.71
soccer	4	87	3	21.46	21.44	23.00
soccer	4	87	4	21.59	21.73	22.91
soccer	4	87	5	21.99	22.74	23.87
soccer	4	87	6	21.73	21.90	23.61
soccer	4	87	7	21.73	21.67	23.13
soccer	4	87	8	21.14	21.14	22.68
soccer	4	87	9	21.67	20.76	23.36
soccer	4	87	10	21.14	21.14	22.81
soccer	4	91	1	21.45	21.46	22.31
soccer	4	91	2	21.51	21.51	22.16
soccer	4	91	3	22.08	22.08	22.73
soccer	4	91	4	21.57	21.57	21.85
soccer	4	91	5	21.24	21.24	20.98
soccer	4	91	6	21.01	21.01	21.65
soccer	4	91	7	21.50	21.50	23.06
soccer	4	91	8	21.48	21.49	21.74
soccer	4	91	9	20.94	20.94	21.43
soccer	4	91	10	21.55	21.55	21.41
soccer	4	92	1	22.58	22.93	23.63
soccer	4	92	2	21.99	21.99	22.50
soccer	4	92	3	22.36	22.50	23.71

Continued on next page

Table V.2 – continued from previous page

Sequence	SNR (dB)	Frame	Run	JM 16.0	STBMA+PDE	SO-MLD
soccer	5	74	5	25.82	27.65	28.06
soccer	5	74	6	23.67	25.27	26.53
soccer	5	74	7	25.97	26.73	27.35
soccer	5	74	8	26.12	27.77	28.16
soccer	5	74	9	25.35	24.54	27.46
soccer	5	74	10	25.98	27.16	27.17
soccer	5	85	1	25.18	25.82	27.85
soccer	5	85	2	26.08	26.48	27.96
soccer	5	85	3	26.95	27.25	28.39
soccer	5	85	4	24.18	23.88	27.07
soccer	5	85	5	24.53	25.62	26.85
soccer	5	85	6	25.40	25.29	27.81
soccer	5	85	7	25.99	26.79	28.16
soccer	5	85	8	25.34	26.07	26.88
soccer	5	85	9	24.14	24.85	26.09
soccer	5	85	10	25.17	26.21	26.65
soccer	5	88	1	26.38	28.44	28.63
soccer	5	88	2	24.24	25.57	25.58
soccer	5	88	3	25.04	26.59	27.29
soccer	5	88	4	23.37	23.43	26.57
soccer	5	88	5	24.09	25.86	26.64
soccer	5	88	6	25.65	26.84	27.42
soccer	5	88	7	26.55	28.51	28.04
soccer	5	88	8	26.79	28.03	28.44
soccer	5	88	9	25.30	27.32	28.22
soccer	5	88	10	24.68	26.26	27.52
soccer	5	92	1	25.93	26.49	27.27
soccer	5	92	2	25.40	25.73	27.62
soccer	5	92	3	23.75	25.00	25.47
soccer	5	92	4	24.58	25.87	27.23
soccer	5	92	5	24.32	25.32	26.93
soccer	5	92	6	27.21	28.59	29.53
soccer	5	92	7	25.36	27.53	27.23
soccer	5	92	8	24.80	27.01	26.86
soccer	5	92	9	26.57	26.90	28.22
soccer	5	92	10	25.98	27.15	27.54
soccer	5	101	1	23.64	26.12	27.68
soccer	5	101	2	24.37	27.27	29.06
soccer	5	101	3	22.97	27.05	27.14
soccer	5	101	4	24.07	27.40	28.17
soccer	5	101	5	22.99	26.03	27.65

Continued on next page

Table V.2 – continued from previous page

Sequence	SNR (dB)	Frame	Run	JM 16.0	STBMA+PDE	SO-MLD
soccer	5	101	6	23.39	27.06	27.04
soccer	5	101	7	23.09	27.32	27.05
soccer	5	101	8	23.54	26.42	26.97
soccer	5	101	9	23.89	26.69	30.07
soccer	5	101	10	26.47	29.14	29.39
soccer	5	106	1	21.41	26.83	26.24
soccer	5	106	2	22.36	26.97	26.19
soccer	5	106	3	20.39	27.14	23.64
soccer	5	106	4	25.20	28.51	27.42
soccer	5	106	5	23.66	28.86	27.40
soccer	5	106	6	21.42	26.46	25.97
soccer	5	106	7	21.22	24.80	24.05
soccer	5	106	8	22.84	29.84	28.96
soccer	5	106	9	21.23	26.36	25.02
soccer	5	106	10	22.14	26.07	24.80
soccer	5	108	1	20.47	24.48	23.74
soccer	5	108	2	20.27	23.81	22.92
soccer	5	108	3	19.70	23.23	22.08
soccer	5	108	4	22.34	26.49	25.85
soccer	5	108	5	21.36	24.30	23.12
soccer	5	108	6	20.47	23.59	23.96
soccer	5	108	7	18.83	21.10	20.39
soccer	5	108	8	20.75	24.19	22.71
soccer	5	108	9	19.66	22.12	22.35
soccer	5	108	10	19.77	22.69	23.84
walk	4	65	1	17.71	18.01	20.98
walk	4	65	2	18.09	19.75	21.27
walk	4	65	3	17.20	17.93	19.67
walk	4	65	4	16.77	16.77	18.75
walk	4	65	5	17.14	17.07	21.33
walk	4	65	6	17.96	18.97	20.87
walk	4	65	7	17.53	17.92	21.14
walk	4	65	8	17.26	17.45	19.60
walk	4	65	9	16.98	16.89	20.38
walk	4	65	10	17.54	17.45	19.79
walk	4	68	1	18.54	20.17	22.39
walk	4	68	2	19.19	22.46	21.63
walk	4	68	3	18.99	20.23	21.16
walk	4	68	4	20.24	22.37	22.07
walk	4	68	5	18.73	18.97	21.23
walk	4	68	6	19.59	21.36	22.86

Continued on next page

Table V.2 – continued from previous page

Sequence	SNR (dB)	Frame	Run	JM 16.0	STBMA+PDE	SO-MLD
walk	4	68	7	18.61	21.21	21.34
walk	4	68	8	18.36	18.85	21.75
walk	4	68	9	19.67	21.96	20.85
walk	4	68	10	19.06	19.99	23.16
walk	4	69	1	17.91	19.92	23.11
walk	4	69	2	17.03	17.03	20.77
walk	4	69	3	17.27	17.95	20.29
walk	4	69	4	17.85	19.21	20.23
walk	4	69	5	18.16	21.03	23.08
walk	4	69	6	18.01	18.86	21.92
walk	4	69	7	17.38	17.85	23.13
walk	4	69	8	17.03	17.03	21.36
walk	4	69	9	17.49	18.21	21.69
walk	4	69	10	17.71	20.38	20.36
walk	4	70	1	18.37	21.63	21.59
walk	4	70	2	18.21	20.87	19.82
walk	4	70	3	17.35	17.83	21.09
walk	4	70	4	17.53	18.42	20.62
walk	4	70	5	17.60	18.85	21.61
walk	4	70	6	17.12	17.50	18.62
walk	4	70	7	19.65	22.27	22.20
walk	4	70	8	17.61	19.78	21.20
walk	4	70	9	17.48	18.81	20.99
walk	4	70	10	18.09	19.49	19.83
walk	4	77	1	13.77	14.94	15.29
walk	4	77	2	13.50	14.71	17.85
walk	4	77	3	14.89	19.10	17.59
walk	4	77	4	14.65	16.18	17.36
walk	4	77	5	14.42	17.69	18.72
walk	4	77	6	14.02	18.08	17.68
walk	4	77	7	14.33	17.07	17.34
walk	4	77	8	13.79	14.70	15.65
walk	4	77	9	13.85	17.79	16.18
walk	4	77	10	13.67	15.45	15.74
walk	4	80	1	14.50	20.84	19.85
walk	4	80	2	14.46	22.23	17.15
walk	4	80	3	14.25	16.99	18.58
walk	4	80	4	14.08	14.95	17.07
walk	4	80	5	14.42	21.26	17.41
walk	4	80	6	15.15	20.07	18.01
walk	4	80	7	14.61	20.59	18.30

Continued on next page

Table V.2 – continued from previous page

Sequence	SNR (dB)	Frame	Run	JM 16.0	STBMA+PDE	SO-MLD
walk	4	99	9	14.75	15.34	17.73
walk	4	99	10	14.40	14.84	17.07
walk	5	62	1	18.08	21.14	20.92
walk	5	62	2	16.25	17.77	17.33
walk	5	62	3	16.31	20.61	18.80
walk	5	62	4	19.75	24.13	21.66
walk	5	62	5	17.38	21.20	18.96
walk	5	62	6	18.10	21.47	20.14
walk	5	62	7	18.36	21.52	20.19
walk	5	62	8	17.30	20.95	19.67
walk	5	62	9	17.51	20.29	19.14
walk	5	62	10	21.16	26.04	23.67
walk	5	64	1	17.04	21.60	22.11
walk	5	64	2	17.09	21.41	20.94
walk	5	64	3	17.98	23.72	21.56
walk	5	64	4	17.29	22.57	21.15
walk	5	64	5	16.66	19.66	21.59
walk	5	64	6	18.26	21.94	23.26
walk	5	64	7	18.28	22.89	21.52
walk	5	64	8	16.86	21.56	21.52
walk	5	64	9	16.46	18.70	19.24
walk	5	64	10	17.66	23.52	21.64
walk	5	66	1	21.21	23.58	25.22
walk	5	66	2	24.05	26.89	27.34
walk	5	66	3	21.34	23.32	24.27
walk	5	66	4	21.79	24.78	24.57
walk	5	66	5	20.12	22.35	23.19
walk	5	66	6	20.54	21.69	25.65
walk	5	66	7	21.14	21.99	24.30
walk	5	66	8	20.87	23.23	23.56
walk	5	66	9	21.49	24.92	26.13
walk	5	66	10	20.59	22.26	22.83
walk	5	68	1	22.04	23.80	26.29
walk	5	68	2	20.41	23.71	26.98
walk	5	68	3	20.69	24.36	25.91
walk	5	68	4	24.02	25.33	27.07
walk	5	68	5	22.62	24.91	23.73
walk	5	68	6	22.47	24.60	27.10
walk	5	68	7	24.49	26.62	27.44
walk	5	68	8	22.20	24.71	26.04
walk	5	68	9	21.53	24.15	24.28

Continued on next page

Table V.2 – continued from previous page

Sequence	SNR (dB)	Frame	Run	JM 16.0	STBMA+PDE	SO-MLD
walk	5	91	1	20.09	20.10	21.71
walk	5	91	2	19.67	19.69	21.59
walk	5	91	3	20.16	20.18	22.76
walk	5	91	4	18.45	18.46	19.85
walk	5	91	5	19.10	19.11	22.36
walk	5	91	6	20.22	20.23	23.14
walk	5	91	7	20.15	20.17	23.21
walk	5	91	8	18.99	19.01	21.69
walk	5	91	9	19.04	19.05	19.13
walk	5	91	10	19.15	19.17	22.31
walk	5	93	1	21.83	25.77	25.85
walk	5	93	2	20.07	21.98	22.36
walk	5	93	3	20.39	22.40	24.07
walk	5	93	4	21.72	25.95	27.01
walk	5	93	5	22.29	22.65	25.10
walk	5	93	6	22.17	23.12	23.38
walk	5	93	7	21.16	25.51	25.39
walk	5	93	8	20.22	21.71	22.74
walk	5	93	9	19.25	22.54	21.82
walk	5	93	10	21.82	26.42	26.26
whale-show	4	65	1	22.29	22.26	22.60
whale-show	4	65	2	22.49	22.65	22.90
whale-show	4	65	3	22.46	22.54	22.72
whale-show	4	65	4	22.39	22.27	22.69
whale-show	4	65	5	22.40	22.16	22.24
whale-show	4	65	6	22.46	22.55	22.55
whale-show	4	65	7	22.57	22.59	22.69
whale-show	4	65	8	22.41	22.25	22.80
whale-show	4	65	9	22.39	22.34	22.12
whale-show	4	65	10	22.36	22.44	22.66
whale-show	4	67	1	22.46	22.44	22.59
whale-show	4	67	2	22.92	22.78	23.14
whale-show	4	67	3	22.64	22.46	22.89
whale-show	4	67	4	22.75	22.63	23.09
whale-show	4	67	5	22.81	22.59	23.04
whale-show	4	67	6	22.46	22.47	22.62
whale-show	4	67	7	22.47	22.44	22.51
whale-show	4	67	8	22.81	22.76	23.17
whale-show	4	67	9	22.46	22.47	22.57
whale-show	4	67	10	22.87	22.72	23.10
whale-show	4	68	1	22.49	22.44	22.76

Continued on next page

Table V.2 – continued from previous page

Sequence	SNR (dB)	Frame	Run	JM 16.0	STBMA+PDE	SO-MLD
whale-show	4	92	4	22.86	22.87	23.45
whale-show	4	92	5	23.00	23.02	23.33
whale-show	4	92	6	22.90	22.88	23.63
whale-show	4	92	7	22.88	22.88	23.37
whale-show	4	92	8	22.88	22.93	23.42
whale-show	4	92	9	23.03	23.07	23.08
whale-show	4	92	10	22.88	22.92	23.59
whale-show	4	101	1	22.41	22.33	22.46
whale-show	4	101	2	22.43	22.10	22.54
whale-show	4	101	3	22.23	22.23	22.04
whale-show	4	101	4	22.56	22.49	22.93
whale-show	4	101	5	22.29	22.10	22.48
whale-show	4	101	6	22.31	22.27	22.44
whale-show	4	101	7	22.33	22.32	22.59
whale-show	4	101	8	22.21	22.18	22.02
whale-show	4	101	9	22.23	22.29	22.44
whale-show	4	101	10	22.69	22.71	22.81
whale-show	4	106	1	22.41	22.39	22.39
whale-show	4	106	2	22.05	22.04	21.91
whale-show	4	106	3	21.99	21.91	22.63
whale-show	4	106	4	22.06	22.06	22.28
whale-show	4	106	5	22.34	22.35	22.63
whale-show	4	106	6	22.20	22.22	22.27
whale-show	4	106	7	22.03	22.03	22.13
whale-show	4	106	8	22.31	22.30	22.45
whale-show	4	106	9	22.53	22.57	23.10
whale-show	4	106	10	22.48	22.52	22.77
whale-show	4	108	1	22.36	22.16	22.76
whale-show	4	108	2	22.30	22.30	22.55
whale-show	4	108	3	22.38	22.45	22.41
whale-show	4	108	4	22.85	22.84	23.02
whale-show	4	108	5	22.09	22.09	22.64
whale-show	4	108	6	22.40	22.27	22.71
whale-show	4	108	7	22.37	22.37	22.87
whale-show	4	108	8	22.34	21.98	22.33
whale-show	4	108	9	22.24	22.23	22.62
whale-show	4	108	10	22.48	22.37	22.80
whale-show	5	69	1	23.78	23.77	23.99
whale-show	5	69	2	23.24	23.16	23.63
whale-show	5	69	3	23.26	23.23	23.16
whale-show	5	69	4	23.59	23.56	23.58

Continued on next page

Table V.2 – continued from previous page

Sequence	SNR (dB)	Frame	Run	JM 16.0	STBMA+PDE	SO-MLD
whale-show	5	69	5	23.17	23.21	23.44
whale-show	5	69	6	23.89	23.83	23.93
whale-show	5	69	7	23.57	23.53	24.13
whale-show	5	69	8	23.40	23.33	23.47
whale-show	5	69	9	24.06	23.98	24.19
whale-show	5	69	10	23.83	23.77	24.16
whale-show	5	74	1	23.75	23.73	23.93
whale-show	5	74	2	23.32	23.31	23.75
whale-show	5	74	3	23.22	23.13	23.48
whale-show	5	74	4	24.15	24.07	24.12
whale-show	5	74	5	23.42	23.33	23.88
whale-show	5	74	6	23.82	23.83	24.09
whale-show	5	74	7	23.52	23.36	23.81
whale-show	5	74	8	23.23	23.21	23.48
whale-show	5	74	9	23.21	22.93	23.34
whale-show	5	74	10	23.29	23.25	23.37
whale-show	5	79	1	23.28	23.15	23.57
whale-show	5	79	2	23.54	23.48	23.69
whale-show	5	79	3	23.44	23.46	23.74
whale-show	5	79	4	23.57	23.54	23.96
whale-show	5	79	5	24.00	23.75	24.04
whale-show	5	79	6	23.15	22.88	23.38
whale-show	5	79	7	23.30	22.86	23.63
whale-show	5	79	8	22.99	22.70	23.33
whale-show	5	79	9	23.63	23.57	23.82
whale-show	5	79	10	23.79	23.73	24.12
whale-show	5	81	1	23.43	23.48	23.49
whale-show	5	81	2	23.67	23.69	23.80
whale-show	5	81	3	23.23	23.16	23.86
whale-show	5	81	4	23.08	22.81	23.64
whale-show	5	81	5	23.22	23.17	23.80
whale-show	5	81	6	23.58	23.61	23.85
whale-show	5	81	7	22.96	22.69	23.11
whale-show	5	81	8	23.62	23.57	23.99
whale-show	5	81	9	23.56	23.52	23.70
whale-show	5	81	10	23.08	23.07	23.80
whale-show	5	82	1	23.06	23.08	23.38
whale-show	5	82	2	23.53	23.51	23.39
whale-show	5	82	3	22.90	22.77	23.45
whale-show	5	82	4	23.53	23.50	23.74
whale-show	5	82	5	23.13	23.20	23.39

Continued on next page

Table V.2 – continued from previous page

Sequence	SNR (dB)	Frame	Run	JM 16.0	STBMA+PDE	SO-MLD
whale-show	5	82	6	22.74	22.73	23.30
whale-show	5	82	7	23.08	23.10	23.54
whale-show	5	82	8	23.18	23.31	23.55
whale-show	5	82	9	23.37	23.41	23.39
whale-show	5	82	10	23.32	23.41	22.97
whale-show	5	83	1	23.40	23.57	23.66
whale-show	5	83	2	22.94	22.88	23.82
whale-show	5	83	3	23.93	23.95	24.21
whale-show	5	83	4	22.89	23.11	23.56
whale-show	5	83	5	23.13	23.60	24.01
whale-show	5	83	6	22.88	22.84	23.70
whale-show	5	83	7	23.25	23.55	23.67
whale-show	5	83	8	23.38	23.65	23.99
whale-show	5	83	9	22.91	23.31	23.75
whale-show	5	83	10	23.38	23.50	23.75
whale-show	5	85	1	23.10	23.27	23.44
whale-show	5	85	2	23.17	23.20	23.94
whale-show	5	85	3	23.55	23.64	24.17
whale-show	5	85	4	23.16	23.30	23.55
whale-show	5	85	5	23.38	23.57	23.73
whale-show	5	85	6	23.35	23.43	23.59
whale-show	5	85	7	22.99	23.14	23.61
whale-show	5	85	8	23.20	23.21	23.63
whale-show	5	85	9	23.54	23.47	23.93
whale-show	5	85	10	23.37	23.59	23.57
whale-show	5	87	1	23.23	23.26	23.60
whale-show	5	87	2	23.37	23.36	23.76
whale-show	5	87	3	23.36	23.30	23.80
whale-show	5	87	4	23.13	23.07	23.61
whale-show	5	87	5	23.93	23.98	24.15
whale-show	5	87	6	23.37	23.35	23.64
whale-show	5	87	7	23.32	23.38	23.75
whale-show	5	87	8	23.22	23.16	23.54
whale-show	5	87	9	23.48	23.54	23.72
whale-show	5	87	10	24.07	24.07	24.21
whale-show	5	88	1	22.75	22.71	23.06
whale-show	5	88	2	23.14	23.32	23.45
whale-show	5	88	3	23.29	23.29	23.55
whale-show	5	88	4	23.07	23.18	23.50
whale-show	5	88	5	23.48	23.54	23.89
whale-show	5	88	6	23.32	23.39	23.75

Continued on next page

Table V.2 – continued from previous page

Sequence	SNR (dB)	Frame	Run	JM 16.0	STBMA+PDE	SO-MLD
whale-show	5	88	7	23.10	23.20	23.43
whale-show	5	88	8	23.84	23.83	24.07
whale-show	5	88	9	22.92	22.93	23.44
whale-show	5	88	10	22.79	22.81	22.98
whale-show	5	89	1	22.99	22.99	23.75
whale-show	5	89	2	23.25	23.38	23.57
whale-show	5	89	3	22.91	23.12	23.74
whale-show	5	89	4	23.40	23.46	23.76
whale-show	5	89	5	23.06	23.22	23.64
whale-show	5	89	6	23.13	23.25	23.71
whale-show	5	89	7	22.80	22.85	23.81
whale-show	5	89	8	22.81	22.92	23.69
whale-show	5	89	9	23.40	23.52	23.93
whale-show	5	89	10	22.61	22.78	23.54

Table V.3 Detailed experimental results for 1500 kbps

Sequence	SNR (dB)	Frame	Run	JM 16.0	STBMA+PDE	SO-MLD
city	4	65	1	24.00	25.72	25.66
city	4	65	2	24.13	26.80	25.41
city	4	65	3	23.83	26.58	25.71
city	4	65	4	23.69	25.64	25.30
city	4	65	5	24.40	26.91	26.41
city	4	65	6	23.98	24.82	26.45
city	4	65	7	24.34	28.56	25.53
city	4	65	8	24.46	25.79	25.74
city	4	65	9	24.34	28.35	25.70
city	4	65	10	24.37	27.87	25.52
city	4	67	1	24.64	24.99	26.70
city	4	67	2	24.68	25.23	26.54
city	4	67	3	25.07	26.77	28.25
city	4	67	4	25.03	29.24	28.15
city	4	67	5	24.78	25.55	26.28
city	4	67	6	25.12	29.07	27.07
city	4	67	7	24.81	25.63	27.00

Continued on next page

Table V.3 – continued from previous page

Sequence	SNR (dB)	Frame	Run	JM 16.0	STBMA+PDE	SO-MLD
city	4	67	8	24.88	26.97	27.17
city	4	67	9	26.00	29.60	27.48
city	4	67	10	25.22	28.09	28.00
city	4	68	1	25.41	29.93	27.94
city	4	68	2	24.90	26.76	29.22
city	4	68	3	25.03	25.90	28.40
city	4	68	4	24.87	25.81	27.84
city	4	68	5	25.48	29.98	28.43
city	4	68	6	25.30	28.74	29.83
city	4	68	7	24.88	25.55	28.50
city	4	68	8	25.17	28.26	28.52
city	4	68	9	25.22	26.78	28.18
city	4	68	10	25.39	27.29	29.06
city	4	74	1	25.93	27.93	27.68
city	4	74	2	25.08	25.30	26.84
city	4	74	3	26.21	29.84	28.21
city	4	74	4	25.40	24.04	26.67
city	4	74	5	25.98	29.90	26.95
city	4	74	6	25.62	25.38	26.75
city	4	74	7	25.77	27.39	27.52
city	4	74	8	25.63	27.09	26.07
city	4	74	9	26.00	27.24	27.63
city	4	74	10	26.53	28.87	29.66
city	4	85	1	24.42	27.36	27.82
city	4	85	2	24.97	29.47	26.69
city	4	85	3	24.37	28.64	25.90
city	4	85	4	23.66	24.24	24.78
city	4	85	5	23.34	23.34	24.82
city	4	85	6	24.12	27.02	25.98
city	4	85	7	24.63	29.42	26.91
city	4	85	8	24.12	27.73	25.87
city	4	85	9	23.44	23.72	24.26
city	4	85	10	23.96	28.51	25.88
city	4	88	1	24.97	28.43	27.88
city	4	88	2	24.64	25.88	27.18
city	4	88	3	24.74	25.91	26.16
city	4	88	4	24.91	27.11	26.51
city	4	88	5	24.40	26.70	25.35
city	4	88	6	24.60	28.00	27.37
city	4	88	7	25.89	29.32	27.77
city	4	88	8	24.42	27.15	26.51

Continued on next page

Table V.3 – continued from previous page

Sequence	SNR (dB)	Frame	Run	JM 16.0	STBMA+PDE	SO-MLD
city	4	108	10	24.41	25.39	27.74
city	5	61	1	26.18	26.21	26.88
city	5	61	2	25.63	25.65	25.39
city	5	61	3	27.19	27.22	27.81
city	5	61	4	25.80	25.82	25.82
city	5	61	5	26.53	26.55	27.95
city	5	61	6	26.30	26.32	27.50
city	5	61	7	26.26	26.28	25.76
city	5	61	8	25.91	25.93	26.75
city	5	61	9	26.43	26.45	27.39
city	5	61	10	26.31	26.34	26.83
city	5	65	1	29.06	32.34	31.18
city	5	65	2	28.01	32.63	29.77
city	5	65	3	27.98	31.92	29.62
city	5	65	4	26.94	31.00	29.83
city	5	65	5	27.28	32.41	30.47
city	5	65	6	27.36	32.03	29.75
city	5	65	7	26.34	31.43	29.91
city	5	65	8	27.88	32.50	30.83
city	5	65	9	26.83	31.19	29.55
city	5	65	10	28.55	32.11	31.18
city	5	77	1	30.54	32.06	31.55
city	5	77	2	29.91	31.51	30.90
city	5	77	3	29.15	30.47	30.56
city	5	77	4	29.96	31.36	31.74
city	5	77	5	30.22	30.86	30.71
city	5	77	6	30.29	32.05	31.77
city	5	77	7	30.26	32.21	31.12
city	5	77	8	29.87	31.73	31.16
city	5	77	9	30.58	32.23	31.54
city	5	77	10	29.22	30.73	30.66
city	5	80	1	27.55	31.51	30.12
city	5	80	2	28.78	32.71	31.17
city	5	80	3	26.97	31.12	28.82
city	5	80	4	27.37	31.30	30.31
city	5	80	5	26.74	31.74	28.89
city	5	80	6	27.59	31.03	30.76
city	5	80	7	27.91	31.20	29.41
city	5	80	8	27.60	31.42	28.79
city	5	80	9	27.13	31.79	29.47
city	5	80	10	28.41	32.19	31.10

Continued on next page

Table V.3 – continued from previous page

Sequence	SNR (dB)	Frame	Run	JM 16.0	STBMA+PDE	SO-MLD
city	5	106	2	28.78	32.28	31.34
city	5	106	3	28.96	30.76	31.90
city	5	106	4	26.50	31.88	30.21
city	5	106	5	27.70	31.98	31.51
city	5	106	6	28.96	31.48	31.74
city	5	106	7	28.79	32.72	31.87
city	5	106	8	25.79	31.60	29.70
city	5	106	9	28.34	31.21	30.59
city	5	106	10	26.33	31.71	31.76
city	5	108	1	30.24	33.56	31.92
city	5	108	2	26.50	31.28	30.19
city	5	108	3	26.78	31.71	29.30
city	5	108	4	26.21	31.57	28.91
city	5	108	5	27.46	31.75	29.28
city	5	108	6	28.83	33.34	31.82
city	5	108	7	26.82	32.26	30.02
city	5	108	8	26.62	32.21	29.60
city	5	108	9	27.12	30.53	31.82
city	5	108	10	27.37	32.96	31.16
crew	4	62	1	19.60	19.65	21.45
crew	4	62	2	19.54	19.55	21.33
crew	4	62	3	19.40	19.25	20.31
crew	4	62	4	19.39	19.39	20.97
crew	4	62	5	19.66	19.59	19.95
crew	4	62	6	19.57	19.53	20.51
crew	4	62	7	19.72	19.82	20.73
crew	4	62	8	19.20	19.21	21.23
crew	4	62	9	19.80	19.75	21.08
crew	4	62	10	19.61	19.49	21.57
crew	4	72	1	27.07	27.51	28.14
crew	4	72	2	26.95	26.99	26.72
crew	4	72	3	27.41	28.11	28.43
crew	4	72	4	27.20	28.01	28.35
crew	4	72	5	27.00	27.34	27.43
crew	4	72	6	27.22	28.19	27.97
crew	4	72	7	26.99	27.56	28.16
crew	4	72	8	27.97	28.94	28.77
crew	4	72	9	27.04	27.56	27.34
crew	4	72	10	26.65	27.40	27.16
crew	4	75	1	26.24	26.73	26.54
crew	4	75	2	26.60	27.09	28.40

Continued on next page

Table V.3 – continued from previous page

Sequence	SNR (dB)	Frame	Run	JM 16.0	STBMA+PDE	SO-MLD
crew	4	75	3	26.46	27.81	27.85
crew	4	75	4	27.29	28.81	29.22
crew	4	75	5	26.49	27.66	28.80
crew	4	75	6	26.60	27.11	28.21
crew	4	75	7	26.39	27.01	28.05
crew	4	75	8	26.87	28.21	28.59
crew	4	75	9	27.00	28.50	28.70
crew	4	75	10	26.65	27.16	28.73
crew	4	76	1	27.04	28.73	29.18
crew	4	76	2	27.05	28.65	28.62
crew	4	76	3	26.41	26.67	28.20
crew	4	76	4	26.13	26.12	27.57
crew	4	76	5	27.09	28.07	28.27
crew	4	76	6	26.41	26.43	28.11
crew	4	76	7	26.49	27.14	27.97
crew	4	76	8	26.70	28.05	29.55
crew	4	76	9	26.54	26.95	28.84
crew	4	76	10	26.46	27.40	27.46
crew	4	79	1	26.84	27.60	28.37
crew	4	79	2	27.36	27.23	29.35
crew	4	79	3	27.71	28.61	29.75
crew	4	79	4	27.66	27.76	29.52
crew	4	79	5	27.35	27.98	29.28
crew	4	79	6	26.84	26.85	28.88
crew	4	79	7	27.37	27.91	29.10
crew	4	79	8	27.78	28.75	28.37
crew	4	79	9	27.98	29.06	30.08
crew	4	79	10	27.28	27.89	28.39
crew	4	81	1	27.53	28.38	29.29
crew	4	81	2	26.85	26.98	29.15
crew	4	81	3	27.17	27.55	28.30
crew	4	81	4	27.74	28.35	29.72
crew	4	81	5	27.14	27.65	28.90
crew	4	81	6	27.64	28.37	28.77
crew	4	81	7	27.40	26.69	28.48
crew	4	81	8	27.14	27.37	28.35
crew	4	81	9	27.89	28.85	29.41
crew	4	81	10	27.65	28.27	29.62
crew	4	82	1	27.09	27.33	28.14
crew	4	82	2	26.93	27.23	27.65
crew	4	82	3	26.73	26.83	28.68

Continued on next page

Table V.3 – continued from previous page

Sequence	SNR (dB)	Frame	Run	JM 16.0	STBMA+PDE	SO-MLD
crew	4	82	4	27.24	27.72	28.69
crew	4	82	5	27.20	27.96	28.58
crew	4	82	6	26.60	26.56	28.68
crew	4	82	7	27.54	27.46	29.16
crew	4	82	8	27.11	26.59	29.14
crew	4	82	9	26.39	26.39	27.41
crew	4	82	10	27.43	27.94	28.91
crew	4	83	1	27.06	27.94	28.21
crew	4	83	2	26.37	26.37	28.15
crew	4	83	3	27.60	28.78	28.92
crew	4	83	4	26.81	26.98	28.81
crew	4	83	5	26.47	26.42	28.33
crew	4	83	6	27.25	28.11	29.44
crew	4	83	7	26.74	27.07	28.28
crew	4	83	8	27.00	27.96	29.13
crew	4	83	9	26.82	27.15	28.33
crew	4	83	10	27.32	28.93	29.79
crew	4	84	1	27.14	27.77	28.29
crew	4	84	2	27.19	27.80	28.32
crew	4	84	3	27.80	28.28	29.48
crew	4	84	4	26.75	26.99	27.54
crew	4	84	5	26.72	26.72	29.33
crew	4	84	6	27.02	26.74	29.43
crew	4	84	7	26.59	26.65	27.48
crew	4	84	8	26.99	27.27	27.88
crew	4	84	9	27.07	27.38	29.46
crew	4	84	10	27.05	27.22	28.83
crew	4	90	1	23.57	23.58	24.13
crew	4	90	2	23.77	24.00	23.63
crew	4	90	3	24.02	23.89	24.45
crew	4	90	4	24.08	24.43	24.64
crew	4	90	5	23.78	24.02	24.61
crew	4	90	6	24.23	24.43	24.63
crew	4	90	7	23.75	23.67	24.22
crew	4	90	8	23.83	24.02	24.69
crew	4	90	9	23.87	23.38	23.99
crew	4	90	10	24.01	24.25	24.68
crew	5	72	1	30.13	32.38	31.12
crew	5	72	2	31.42	32.96	31.35
crew	5	72	3	29.97	31.73	30.80
crew	5	72	4	28.61	29.69	30.86

Continued on next page

Table V.3 – continued from previous page

Sequence	SNR (dB)	Frame	Run	JM 16.0	STBMA+PDE	SO-MLD
crew	5	72	5	29.05	30.79	30.18
crew	5	72	6	29.59	30.99	30.44
crew	5	72	7	30.51	32.60	31.94
crew	5	72	8	28.85	30.09	30.16
crew	5	72	9	30.73	32.42	32.51
crew	5	72	10	31.41	32.96	33.07
crew	5	74	1	29.09	29.78	30.80
crew	5	74	2	29.56	32.36	31.84
crew	5	74	3	28.25	29.70	31.33
crew	5	74	4	29.08	31.19	31.07
crew	5	74	5	31.82	33.50	32.91
crew	5	74	6	29.87	31.41	32.15
crew	5	74	7	28.31	30.75	31.29
crew	5	74	8	29.47	30.96	31.97
crew	5	74	9	30.10	32.08	31.99
crew	5	74	10	30.65	32.82	32.76
crew	5	75	1	30.20	32.19	31.74
crew	5	75	2	30.29	32.22	33.07
crew	5	75	3	31.29	33.56	33.49
crew	5	75	4	30.55	32.37	33.46
crew	5	75	5	28.61	30.37	31.73
crew	5	75	6	31.42	32.75	32.05
crew	5	75	7	29.16	30.79	31.17
crew	5	75	8	29.24	31.48	32.03
crew	5	75	9	28.72	30.92	31.10
crew	5	75	10	31.67	33.88	33.53
crew	5	87	1	30.40	31.51	32.97
crew	5	87	2	29.46	31.40	30.82
crew	5	87	3	30.65	32.53	32.50
crew	5	87	4	30.01	32.26	32.86
crew	5	87	5	30.12	31.24	31.40
crew	5	87	6	29.71	31.22	33.00
crew	5	87	7	30.87	32.33	32.99
crew	5	87	8	29.72	31.31	31.38
crew	5	87	9	29.50	31.14	30.98
crew	5	87	10	30.14	31.57	33.02
crew	5	89	1	27.84	28.42	28.15
crew	5	89	2	26.87	27.50	28.67
crew	5	89	3	26.14	26.45	27.71
crew	5	89	4	25.91	26.22	27.83
crew	5	89	5	25.73	26.16	27.14

Continued on next page

Table V.3 – continued from previous page

Sequence	SNR (dB)	Frame	Run	JM 16.0	STBMA+PDE	SO-MLD
crew	5	89	6	27.11	27.60	29.21
crew	5	89	7	28.02	28.39	29.30
crew	5	89	8	26.59	27.25	28.51
crew	5	89	9	27.09	27.44	29.55
crew	5	89	10	26.46	26.81	28.27
crew	5	93	1	29.10	30.33	30.49
crew	5	93	2	29.51	31.30	30.66
crew	5	93	3	29.04	29.85	30.11
crew	5	93	4	29.60	31.21	31.51
crew	5	93	5	30.03	31.78	31.97
crew	5	93	6	29.56	31.43	30.38
crew	5	93	7	29.70	31.03	31.34
crew	5	93	8	29.22	30.52	31.36
crew	5	93	9	29.24	30.80	30.49
crew	5	93	10	28.80	30.73	30.57
crew	5	96	1	29.75	31.18	32.06
crew	5	96	2	30.11	31.31	31.39
crew	5	96	3	29.84	31.70	32.03
crew	5	96	4	31.08	32.66	33.48
crew	5	96	5	30.68	32.45	32.66
crew	5	96	6	30.51	31.43	32.35
crew	5	96	7	29.60	31.19	31.91
crew	5	96	8	31.13	32.50	32.97
crew	5	96	9	29.08	30.52	30.73
crew	5	96	10	31.09	32.20	32.51
crew	5	98	1	29.74	31.61	30.43
crew	5	98	2	29.84	31.94	31.76
crew	5	98	3	28.99	30.34	30.99
crew	5	98	4	29.15	31.65	31.02
crew	5	98	5	30.24	31.87	31.61
crew	5	98	6	29.62	31.89	31.01
crew	5	98	7	28.48	30.55	30.70
crew	5	98	8	30.37	32.44	32.73
crew	5	98	9	28.60	30.49	31.78
crew	5	98	10	29.50	31.00	30.57
crew	5	99	1	29.62	31.46	31.09
crew	5	99	2	29.24	31.26	30.15
crew	5	99	3	29.09	30.80	31.24
crew	5	99	4	28.56	30.24	30.96
crew	5	99	5	29.15	31.22	30.42
crew	5	99	6	29.06	30.72	31.35

Continued on next page

Table V.3 – continued from previous page

Sequence	SNR (dB)	Frame	Run	JM 16.0	STBMA+PDE	SO-MLD
driving	4	74	8	19.56	20.61	22.29
driving	4	74	9	20.12	22.47	24.10
driving	4	74	10	19.39	21.76	22.23
driving	4	77	1	20.75	21.90	23.04
driving	4	77	2	20.39	20.92	22.48
driving	4	77	3	20.82	21.57	23.47
driving	4	77	4	21.07	21.65	22.42
driving	4	77	5	21.61	21.15	23.99
driving	4	77	6	21.45	22.97	24.14
driving	4	77	7	20.93	22.54	24.04
driving	4	77	8	20.65	21.70	22.95
driving	4	77	9	20.64	20.34	22.94
driving	4	77	10	20.70	21.46	21.46
driving	4	79	1	20.58	21.66	23.37
driving	4	79	2	20.47	20.35	22.15
driving	4	79	3	21.07	23.25	22.62
driving	4	79	4	21.17	21.75	23.35
driving	4	79	5	20.15	19.22	22.16
driving	4	79	6	20.88	22.20	23.18
driving	4	79	7	20.88	21.60	23.38
driving	4	79	8	20.48	19.89	23.00
driving	4	79	9	20.91	22.68	23.32
driving	4	79	10	20.77	22.06	23.19
driving	4	84	1	20.66	22.63	24.02
driving	4	84	2	20.54	23.25	22.99
driving	4	84	3	20.82	22.74	22.75
driving	4	84	4	20.19	20.40	22.53
driving	4	84	5	20.35	21.62	22.11
driving	4	84	6	20.54	20.34	22.72
driving	4	84	7	21.06	23.15	23.34
driving	4	84	8	20.82	22.86	23.43
driving	4	84	9	19.74	20.76	21.14
driving	4	84	10	20.41	21.50	22.64
driving	4	89	1	21.38	22.23	23.40
driving	4	89	2	20.88	16.74	22.13
driving	4	89	3	21.06	18.25	22.61
driving	4	89	4	22.45	23.97	24.26
driving	4	89	5	21.03	21.37	23.72
driving	4	89	6	21.23	19.77	22.89
driving	4	89	7	20.86	21.40	22.97
driving	4	89	8	20.86	20.72	22.40

Continued on next page

Table V.3 – continued from previous page

Sequence	SNR (dB)	Frame	Run	JM 16.0	STBMA+PDE	SO-MLD
driving	5	62	10	23.06	28.12	24.30
driving	5	65	1	25.56	28.37	28.35
driving	5	65	2	23.80	26.33	25.99
driving	5	65	3	21.96	24.13	23.47
driving	5	65	4	24.76	27.77	27.01
driving	5	65	5	25.22	26.82	26.28
driving	5	65	6	22.94	25.85	24.68
driving	5	65	7	23.49	26.77	27.62
driving	5	65	8	22.93	26.39	24.77
driving	5	65	9	24.32	27.51	26.41
driving	5	65	10	22.79	25.97	24.46
driving	5	67	1	22.27	25.77	26.15
driving	5	67	2	22.25	26.96	25.79
driving	5	67	3	23.46	27.21	28.63
driving	5	67	4	22.23	26.99	27.63
driving	5	67	5	24.17	28.45	26.34
driving	5	67	6	22.69	26.16	27.09
driving	5	67	7	22.28	25.89	26.69
driving	5	67	8	23.25	27.79	26.68
driving	5	67	9	22.07	26.24	25.09
driving	5	67	10	21.06	25.30	24.42
driving	5	68	1	21.96	26.12	24.12
driving	5	68	2	23.36	27.53	28.31
driving	5	68	3	22.66	26.78	24.58
driving	5	68	4	22.56	27.46	25.05
driving	5	68	5	22.50	26.64	25.98
driving	5	68	6	21.18	25.70	24.05
driving	5	68	7	21.46	24.80	24.62
driving	5	68	8	22.69	27.38	25.33
driving	5	68	9	21.82	25.39	25.54
driving	5	68	10	22.37	26.23	25.48
driving	5	77	1	24.18	26.47	27.54
driving	5	77	2	26.61	28.90	28.69
driving	5	77	3	22.73	25.33	27.95
driving	5	77	4	24.26	27.41	28.23
driving	5	77	5	22.46	23.96	26.56
driving	5	77	6	23.78	27.85	25.61
driving	5	77	7	22.77	25.29	26.12
driving	5	77	8	23.85	27.19	26.31
driving	5	77	9	24.46	27.55	26.04
driving	5	77	10	24.66	27.09	26.23

Continued on next page

Table V.3 – continued from previous page

Sequence	SNR (dB)	Frame	Run	JM 16.0	STBMA+PDE	SO-MLD
driving	5	90	2	23.89	27.94	27.96
driving	5	90	3	23.68	27.38	27.16
driving	5	90	4	22.89	25.96	25.08
driving	5	90	5	23.32	26.90	26.95
driving	5	90	6	23.24	27.47	25.55
driving	5	90	7	23.57	27.22	26.32
driving	5	90	8	23.23	25.53	27.59
driving	5	90	9	24.90	28.46	27.64
driving	5	90	10	22.21	25.49	25.96
harbour	4	65	1	24.55	25.30	25.05
harbour	4	65	2	24.72	25.53	25.77
harbour	4	65	3	24.44	25.68	25.23
harbour	4	65	4	24.57	25.13	25.31
harbour	4	65	5	24.70	25.20	25.17
harbour	4	65	6	24.55	25.11	25.17
harbour	4	65	7	24.13	24.13	25.13
harbour	4	65	8	24.69	26.03	25.23
harbour	4	65	9	24.61	24.92	25.69
harbour	4	65	10	24.51	25.24	25.35
harbour	4	67	1	22.47	23.32	24.00
harbour	4	67	2	23.12	25.23	24.39
harbour	4	67	3	23.24	24.44	25.47
harbour	4	67	4	22.72	25.16	24.19
harbour	4	67	5	23.11	25.43	24.87
harbour	4	67	6	23.10	25.41	24.92
harbour	4	67	7	23.33	25.34	24.95
harbour	4	67	8	23.26	25.26	25.02
harbour	4	67	9	22.46	22.93	23.75
harbour	4	67	10	23.21	25.37	25.29
harbour	4	68	1	25.38	25.45	25.49
harbour	4	68	2	26.07	25.19	26.33
harbour	4	68	3	25.63	25.33	25.54
harbour	4	68	4	25.68	24.10	25.84
harbour	4	68	5	25.86	24.63	26.24
harbour	4	68	6	25.58	25.80	26.22
harbour	4	68	7	25.60	25.36	25.34
harbour	4	68	8	25.69	24.48	26.22
harbour	4	68	9	26.20	25.13	25.81
harbour	4	68	10	25.87	25.09	25.66
harbour	4	74	1	23.58	24.22	25.46
harbour	4	74	2	24.08	25.10	26.29

Continued on next page

Table V.3 – continued from previous page

Sequence	SNR (dB)	Frame	Run	JM 16.0	STBMA+PDE	SO-MLD
harbour	4	101	4	19.94	21.93	21.59
harbour	4	101	5	19.75	22.88	21.79
harbour	4	101	6	20.00	22.15	22.41
harbour	4	101	7	20.03	22.69	22.55
harbour	4	101	8	20.25	24.13	22.70
harbour	4	101	9	20.06	21.68	22.06
harbour	4	101	10	19.72	21.00	21.71
harbour	4	106	1	21.69	24.10	23.62
harbour	4	106	2	22.15	24.44	23.51
harbour	4	106	3	21.55	23.46	24.46
harbour	4	106	4	22.20	24.63	24.18
harbour	4	106	5	22.42	24.91	24.44
harbour	4	106	6	21.83	24.29	23.89
harbour	4	106	7	22.28	25.00	24.61
harbour	4	106	8	22.77	26.66	24.85
harbour	4	106	9	21.78	24.25	23.06
harbour	4	106	10	22.17	25.75	24.49
harbour	4	108	1	21.27	23.33	23.14
harbour	4	108	2	21.32	24.51	23.86
harbour	4	108	3	21.77	26.35	25.31
harbour	4	108	4	22.21	25.63	25.61
harbour	4	108	5	21.39	22.40	24.05
harbour	4	108	6	21.43	25.30	23.53
harbour	4	108	7	21.08	21.82	22.59
harbour	4	108	8	21.69	26.61	24.69
harbour	4	108	9	22.10	26.48	25.01
harbour	4	108	10	21.58	25.40	23.23
harbour	5	61	1	24.06	24.10	25.34
harbour	5	61	2	24.46	24.50	24.18
harbour	5	61	3	23.91	23.95	24.93
harbour	5	61	4	24.04	24.08	24.50
harbour	5	61	5	24.29	24.33	24.32
harbour	5	61	6	24.27	24.31	25.28
harbour	5	61	7	24.20	24.23	24.70
harbour	5	61	8	25.27	25.31	25.46
harbour	5	61	9	23.81	23.84	24.39
harbour	5	61	10	23.94	23.97	24.27
harbour	5	63	1	27.60	28.02	28.09
harbour	5	63	2	26.83	27.23	27.22
harbour	5	63	3	27.32	27.62	28.08
harbour	5	63	4	27.80	28.21	28.81

Continued on next page

Table V.3 – continued from previous page

Sequence	SNR (dB)	Frame	Run	JM 16.0	STBMA+PDE	SO-MLD
harbour	5	78	6	25.47	28.54	27.36
harbour	5	78	7	24.69	27.73	26.65
harbour	5	78	8	25.84	27.43	28.13
harbour	5	78	9	25.87	28.31	27.28
harbour	5	78	10	25.98	28.54	28.37
harbour	5	82	1	28.83	28.78	29.07
harbour	5	82	2	28.26	28.24	28.93
harbour	5	82	3	28.62	28.67	28.73
harbour	5	82	4	28.59	28.62	28.68
harbour	5	82	5	28.25	28.21	28.76
harbour	5	82	6	28.66	28.56	29.23
harbour	5	82	7	28.27	28.38	28.91
harbour	5	82	8	27.99	28.10	28.29
harbour	5	82	9	27.74	27.53	27.88
harbour	5	82	10	28.79	28.91	28.97
harbour	5	91	1	26.67	26.70	24.87
harbour	5	91	2	26.95	26.98	24.41
harbour	5	91	3	26.69	26.72	23.23
harbour	5	91	4	26.85	26.88	25.29
harbour	5	91	5	26.26	26.29	24.50
harbour	5	91	6	26.82	26.85	24.78
harbour	5	91	7	27.18	27.21	25.57
harbour	5	91	8	26.39	26.41	24.42
harbour	5	91	9	26.98	27.00	25.48
harbour	5	91	10	26.85	26.88	25.41
harbour	5	96	1	22.44	25.14	26.59
harbour	5	96	2	22.44	28.04	25.23
harbour	5	96	3	23.57	28.76	27.02
harbour	5	96	4	21.71	26.26	25.38
harbour	5	96	5	22.54	28.26	26.62
harbour	5	96	6	21.74	27.72	25.07
harbour	5	96	7	23.23	28.55	26.63
harbour	5	96	8	21.31	26.15	25.26
harbour	5	96	9	22.36	27.67	25.23
harbour	5	96	10	21.60	23.39	25.05
harbour	5	108	1	24.47	27.54	26.54
harbour	5	108	2	25.36	28.69	27.79
harbour	5	108	3	25.44	28.10	27.51
harbour	5	108	4	23.43	27.48	26.60
harbour	5	108	5	25.42	28.96	28.12
harbour	5	108	6	25.12	28.00	27.99

Continued on next page

Table V.3 – continued from previous page

Sequence	SNR (dB)	Frame	Run	JM 16.0	STBMA+PDE	SO-MLD
ice	4	85	8	25.45	25.79	28.06
ice	4	85	9	25.98	25.98	28.12
ice	4	85	10	25.23	24.71	27.62
ice	4	88	1	25.18	27.20	27.41
ice	4	88	2	24.58	25.77	26.14
ice	4	88	3	24.89	26.08	27.09
ice	4	88	4	24.82	26.02	28.38
ice	4	88	5	24.60	24.82	27.77
ice	4	88	6	24.85	25.41	27.01
ice	4	88	7	24.95	25.92	27.11
ice	4	88	8	25.12	25.89	28.36
ice	4	88	9	25.00	26.48	27.02
ice	4	88	10	24.93	25.95	27.99
ice	4	91	1	24.66	24.66	23.00
ice	4	91	2	24.70	24.70	24.73
ice	4	91	3	25.05	25.05	25.87
ice	4	91	4	24.82	24.82	26.14
ice	4	91	5	24.56	24.56	24.89
ice	4	91	6	24.67	24.67	25.26
ice	4	91	7	25.19	25.19	24.83
ice	4	91	8	24.64	24.64	21.52
ice	4	91	9	24.70	24.71	23.79
ice	4	91	10	24.81	24.81	22.16
ice	4	93	1	24.66	27.14	28.92
ice	4	93	2	24.35	26.95	28.36
ice	4	93	3	24.01	23.84	26.20
ice	4	93	4	24.07	25.13	25.12
ice	4	93	5	25.09	28.13	28.73
ice	4	93	6	24.21	26.06	26.60
ice	4	93	7	25.17	28.28	29.26
ice	4	93	8	24.50	26.64	27.58
ice	4	93	9	24.56	26.73	27.04
ice	4	93	10	24.48	26.68	28.09
ice	4	95	1	23.85	24.97	27.00
ice	4	95	2	24.14	26.41	25.42
ice	4	95	3	23.90	24.54	26.64
ice	4	95	4	24.56	26.06	27.41
ice	4	95	5	24.46	25.94	27.16
ice	4	95	6	24.70	25.87	28.87
ice	4	95	7	24.10	26.46	25.75
ice	4	95	8	24.20	25.49	27.05

Continued on next page

Table V.3 – continued from previous page

Sequence	SNR (dB)	Frame	Run	JM 16.0	STBMA+PDE	SO-MLD
ice	4	95	9	24.08	24.72	26.70
ice	4	95	10	24.11	25.60	27.16
ice	4	100	1	24.33	25.14	29.02
ice	4	100	2	24.14	23.35	26.81
ice	4	100	3	24.76	25.84	29.78
ice	4	100	4	24.27	26.24	27.41
ice	4	100	5	24.65	27.47	28.45
ice	4	100	6	24.69	26.65	28.00
ice	4	100	7	24.74	27.13	29.05
ice	4	100	8	23.90	23.81	28.71
ice	4	100	9	24.76	26.63	29.08
ice	4	100	10	24.29	24.34	27.19
ice	4	101	1	24.74	26.13	26.53
ice	4	101	2	24.85	26.48	27.76
ice	4	101	3	24.54	26.89	29.65
ice	4	101	4	24.30	27.10	27.38
ice	4	101	5	24.36	27.07	27.11
ice	4	101	6	24.29	26.34	28.19
ice	4	101	7	25.32	28.39	28.26
ice	4	101	8	24.50	26.40	28.69
ice	4	101	9	25.04	28.79	28.46
ice	4	101	10	24.92	26.59	28.03
ice	5	66	1	27.56	31.41	32.21
ice	5	66	2	29.65	33.56	35.27
ice	5	66	3	26.70	28.96	29.14
ice	5	66	4	27.81	31.60	31.25
ice	5	66	5	27.06	30.14	32.05
ice	5	66	6	27.65	32.33	31.14
ice	5	66	7	29.63	33.88	33.63
ice	5	66	8	28.97	31.90	33.66
ice	5	66	9	30.64	33.75	35.45
ice	5	66	10	25.97	28.49	29.82
ice	5	70	1	28.51	30.10	31.79
ice	5	70	2	27.81	31.77	31.14
ice	5	70	3	28.18	31.16	30.83
ice	5	70	4	26.73	29.81	30.83
ice	5	70	5	28.20	30.61	32.51
ice	5	70	6	28.32	31.87	32.80
ice	5	70	7	26.81	28.57	29.92
ice	5	70	8	27.37	31.14	30.99
ice	5	70	9	31.31	33.51	35.50

Continued on next page

Table V.3 – continued from previous page

Sequence	SNR (dB)	Frame	Run	JM 16.0	STBMA+PDE	SO-MLD
ice	5	88	1	28.80	32.17	34.95
ice	5	88	2	27.48	31.09	30.30
ice	5	88	3	28.21	31.15	33.15
ice	5	88	4	31.00	33.03	32.60
ice	5	88	5	27.32	30.42	31.25
ice	5	88	6	28.06	31.11	33.36
ice	5	88	7	28.93	31.13	31.77
ice	5	88	8	28.72	33.04	32.50
ice	5	88	9	29.65	31.87	32.68
ice	5	88	10	27.70	30.99	30.86
ice	5	92	1	27.99	31.28	33.00
ice	5	92	2	29.39	32.25	32.41
ice	5	92	3	26.29	31.61	30.10
ice	5	92	4	26.39	31.65	32.69
ice	5	92	5	28.04	33.72	30.36
ice	5	92	6	27.39	32.07	31.60
ice	5	92	7	28.92	33.98	31.04
ice	5	92	8	29.33	33.06	31.10
ice	5	92	9	30.02	36.25	35.32
ice	5	92	10	28.50	32.13	31.78
ice	5	94	1	26.55	31.70	29.26
ice	5	94	2	29.50	33.52	32.49
ice	5	94	3	28.41	30.94	32.38
ice	5	94	4	28.33	31.33	30.81
ice	5	94	5	28.92	32.43	31.39
ice	5	94	6	25.45	28.10	29.56
ice	5	94	7	27.88	31.41	32.84
ice	5	94	8	28.38	33.30	32.30
ice	5	94	9	27.65	32.95	31.61
ice	5	94	10	26.97	30.60	29.61
ice	5	96	1	26.81	30.41	30.85
ice	5	96	2	27.39	30.05	32.04
ice	5	96	3	29.07	34.15	34.65
ice	5	96	4	29.27	34.10	32.94
ice	5	96	5	28.80	30.40	30.79
ice	5	96	6	28.17	31.76	30.73
ice	5	96	7	29.76	32.83	32.28
ice	5	96	8	26.74	29.73	30.43
ice	5	96	9	30.19	33.07	34.22
ice	5	96	10	27.23	29.76	31.73
opening-ceremony	4	61	1	27.94	27.89	21.01

Continued on next page

Table V.3 – continued from previous page

Sequence	SNR (dB)	Frame	Run	JM 16.0	STBMA+PDE	SO-MLD
opening-ceremony	4	61	2	27.78	27.75	20.47
opening-ceremony	4	61	3	27.67	27.65	20.83
opening-ceremony	4	61	4	27.70	27.67	20.35
opening-ceremony	4	61	5	27.69	27.65	20.21
opening-ceremony	4	61	6	27.99	27.97	21.31
opening-ceremony	4	61	7	27.72	27.70	20.05
opening-ceremony	4	61	8	27.83	27.81	20.98
opening-ceremony	4	61	9	27.80	27.77	20.22
opening-ceremony	4	61	10	27.56	27.56	20.70
opening-ceremony	4	65	1	27.88	27.50	28.06
opening-ceremony	4	65	2	27.86	27.45	28.31
opening-ceremony	4	65	3	27.78	27.98	28.28
opening-ceremony	4	65	4	27.92	27.66	28.30
opening-ceremony	4	65	5	27.75	27.39	27.92
opening-ceremony	4	65	6	27.85	27.87	28.26
opening-ceremony	4	65	7	27.67	27.58	27.89
opening-ceremony	4	65	8	27.82	27.86	27.26
opening-ceremony	4	65	9	27.70	27.51	27.89
opening-ceremony	4	65	10	27.76	27.38	27.88
opening-ceremony	4	71	1	27.68	27.80	27.40
opening-ceremony	4	71	2	27.66	27.36	27.60
opening-ceremony	4	71	3	27.71	27.14	27.85
opening-ceremony	4	71	4	28.13	28.22	27.69
opening-ceremony	4	71	5	27.72	27.09	27.86
opening-ceremony	4	71	6	28.00	28.04	28.24
opening-ceremony	4	71	7	27.71	27.81	27.70
opening-ceremony	4	71	8	27.63	27.62	27.94
opening-ceremony	4	71	9	27.60	27.56	27.75
opening-ceremony	4	71	10	27.62	27.56	27.79
opening-ceremony	4	77	1	27.52	27.46	27.78
opening-ceremony	4	77	2	27.46	22.97	27.54
opening-ceremony	4	77	3	27.55	27.62	27.59
opening-ceremony	4	77	4	27.72	27.64	27.87
opening-ceremony	4	77	5	27.49	27.35	27.50
opening-ceremony	4	77	6	27.28	27.26	27.18
opening-ceremony	4	77	7	27.29	27.09	27.58
opening-ceremony	4	77	8	27.56	27.64	26.88
opening-ceremony	4	77	9	27.30	27.03	27.44
opening-ceremony	4	77	10	27.32	27.30	27.82
opening-ceremony	4	78	1	27.48	27.17	27.56
opening-ceremony	4	78	2	27.68	27.33	27.44

Continued on next page

Table V.3 – continued from previous page

Sequence	SNR (dB)	Frame	Run	JM 16.0	STBMA+PDE	SO-MLD
opening-ceremony	4	78	3	27.30	26.37	27.25
opening-ceremony	4	78	4	27.37	27.44	28.03
opening-ceremony	4	78	5	27.64	27.65	27.94
opening-ceremony	4	78	6	27.46	27.31	28.06
opening-ceremony	4	78	7	27.33	27.29	26.82
opening-ceremony	4	78	8	27.69	27.81	28.29
opening-ceremony	4	78	9	27.45	27.37	27.74
opening-ceremony	4	78	10	27.51	27.56	27.51
opening-ceremony	4	86	1	27.62	27.46	27.20
opening-ceremony	4	86	2	27.60	27.27	27.11
opening-ceremony	4	86	3	27.85	28.24	27.89
opening-ceremony	4	86	4	27.94	27.78	28.12
opening-ceremony	4	86	5	27.56	27.41	27.71
opening-ceremony	4	86	6	27.76	27.57	28.06
opening-ceremony	4	86	7	27.93	27.58	27.73
opening-ceremony	4	86	8	27.91	26.18	27.89
opening-ceremony	4	86	9	27.88	28.33	27.26
opening-ceremony	4	86	10	27.93	27.35	27.64
opening-ceremony	4	87	1	27.50	27.45	26.69
opening-ceremony	4	87	2	27.68	27.14	27.83
opening-ceremony	4	87	3	27.70	27.08	26.81
opening-ceremony	4	87	4	27.68	27.26	23.12
opening-ceremony	4	87	5	27.55	27.07	27.17
opening-ceremony	4	87	6	28.10	28.11	28.16
opening-ceremony	4	87	7	27.64	27.84	27.74
opening-ceremony	4	87	8	28.03	27.94	28.33
opening-ceremony	4	87	9	27.81	27.46	27.03
opening-ceremony	4	87	10	27.60	27.75	28.17
opening-ceremony	4	88	1	27.42	27.06	27.41
opening-ceremony	4	88	2	27.15	25.81	27.52
opening-ceremony	4	88	3	26.94	26.94	27.03
opening-ceremony	4	88	4	27.13	27.04	27.38
opening-ceremony	4	88	5	27.54	27.33	27.73
opening-ceremony	4	88	6	27.37	26.95	27.55
opening-ceremony	4	88	7	27.57	27.03	27.50
opening-ceremony	4	88	8	27.35	26.58	27.22
opening-ceremony	4	88	9	27.48	25.72	26.98
opening-ceremony	4	88	10	27.13	27.11	27.26
opening-ceremony	4	90	1	28.04	28.09	28.16
opening-ceremony	4	90	2	27.48	27.40	28.02
opening-ceremony	4	90	3	27.83	27.83	28.21

Continued on next page

Table V.3 – continued from previous page

Sequence	SNR (dB)	Frame	Run	JM 16.0	STBMA+PDE	SO-MLD
opening-ceremony	4	90	4	27.74	27.83	27.87
opening-ceremony	4	90	5	27.58	26.92	27.80
opening-ceremony	4	90	6	27.74	27.76	28.09
opening-ceremony	4	90	7	28.16	27.26	28.50
opening-ceremony	4	90	8	27.62	27.60	26.86
opening-ceremony	4	90	9	27.61	26.97	28.01
opening-ceremony	4	90	10	27.54	27.53	27.34
opening-ceremony	4	100	1	27.74	27.48	27.50
opening-ceremony	4	100	2	27.73	27.09	27.99
opening-ceremony	4	100	3	27.54	27.28	27.55
opening-ceremony	4	100	4	27.41	27.24	27.99
opening-ceremony	4	100	5	27.78	26.98	24.74
opening-ceremony	4	100	6	28.02	27.42	28.09
opening-ceremony	4	100	7	27.49	26.86	27.32
opening-ceremony	4	100	8	27.36	27.26	27.81
opening-ceremony	4	100	9	27.45	27.45	27.60
opening-ceremony	4	100	10	27.77	27.48	27.95
opening-ceremony	5	62	1	29.03	29.56	29.61
opening-ceremony	5	62	2	29.65	29.85	29.85
opening-ceremony	5	62	3	29.29	29.50	30.00
opening-ceremony	5	62	4	29.22	27.51	29.57
opening-ceremony	5	62	5	29.23	29.49	29.85
opening-ceremony	5	62	6	29.60	29.82	29.90
opening-ceremony	5	62	7	29.64	29.56	29.77
opening-ceremony	5	62	8	29.51	29.60	29.69
opening-ceremony	5	62	9	29.02	27.44	29.11
opening-ceremony	5	62	10	28.95	29.46	29.62
opening-ceremony	5	63	1	29.10	29.33	29.65
opening-ceremony	5	63	2	29.29	29.39	28.51
opening-ceremony	5	63	3	29.07	29.23	29.59
opening-ceremony	5	63	4	28.68	28.91	29.18
opening-ceremony	5	63	5	28.64	28.84	28.65
opening-ceremony	5	63	6	29.33	29.12	29.87
opening-ceremony	5	63	7	28.51	28.88	29.41
opening-ceremony	5	63	8	29.40	29.52	29.72
opening-ceremony	5	63	9	28.78	28.83	29.31
opening-ceremony	5	63	10	29.13	29.45	29.36
opening-ceremony	5	68	1	28.75	29.20	28.73
opening-ceremony	5	68	2	28.72	29.13	28.99
opening-ceremony	5	68	3	27.90	27.81	28.84
opening-ceremony	5	68	4	28.78	29.16	29.22

Continued on next page

Table V.3 – continued from previous page

Sequence	SNR (dB)	Frame	Run	JM 16.0	STBMA+PDE	SO-MLD
opening-ceremony	5	81	6	29.18	29.46	29.65
opening-ceremony	5	81	7	28.92	28.93	29.28
opening-ceremony	5	81	8	28.92	29.27	29.45
opening-ceremony	5	81	9	28.78	29.07	28.21
opening-ceremony	5	81	10	28.77	28.73	28.83
opening-ceremony	5	84	1	28.83	29.28	29.40
opening-ceremony	5	84	2	28.56	28.98	28.81
opening-ceremony	5	84	3	28.01	28.58	28.78
opening-ceremony	5	84	4	28.60	28.94	28.78
opening-ceremony	5	84	5	28.80	29.12	28.67
opening-ceremony	5	84	6	28.77	27.80	28.10
opening-ceremony	5	84	7	29.12	29.45	29.28
opening-ceremony	5	84	8	28.68	29.14	29.38
opening-ceremony	5	84	9	28.84	29.03	28.67
opening-ceremony	5	84	10	28.66	28.60	28.59
opening-ceremony	5	86	1	28.65	29.09	29.05
opening-ceremony	5	86	2	28.70	29.14	28.81
opening-ceremony	5	86	3	28.78	28.89	28.59
opening-ceremony	5	86	4	29.21	29.46	29.28
opening-ceremony	5	86	5	28.28	28.46	28.89
opening-ceremony	5	86	6	29.02	28.89	29.12
opening-ceremony	5	86	7	28.50	28.63	28.46
opening-ceremony	5	86	8	29.03	28.84	29.34
opening-ceremony	5	86	9	29.02	29.21	29.32
opening-ceremony	5	86	10	28.94	29.00	29.38
opening-ceremony	5	87	1	29.09	27.77	29.28
opening-ceremony	5	87	2	28.19	28.08	28.60
opening-ceremony	5	87	3	28.21	28.34	28.89
opening-ceremony	5	87	4	28.44	28.80	28.77
opening-ceremony	5	87	5	28.61	28.58	28.77
opening-ceremony	5	87	6	28.39	28.19	28.68
opening-ceremony	5	87	7	28.86	28.93	28.70
opening-ceremony	5	87	8	28.82	29.08	29.34
opening-ceremony	5	87	9	28.06	28.12	28.70
opening-ceremony	5	87	10	28.64	28.81	28.94
soccer	4	63	1	22.03	22.03	24.56
soccer	4	63	2	22.40	24.53	25.02
soccer	4	63	3	22.03	22.57	25.49
soccer	4	63	4	21.91	22.38	25.44
soccer	4	63	5	22.19	22.96	24.99
soccer	4	63	6	22.32	23.19	24.47

Continued on next page

Table V.3 – continued from previous page

Sequence	SNR (dB)	Frame	Run	JM 16.0	STBMA+PDE	SO-MLD
soccer	4	85	8	22.72	21.15	23.80
soccer	4	85	9	23.02	22.20	24.42
soccer	4	85	10	22.36	22.35	23.65
soccer	4	88	1	21.67	22.00	24.32
soccer	4	88	2	21.64	22.59	25.32
soccer	4	88	3	21.37	21.86	23.59
soccer	4	88	4	21.00	21.17	22.91
soccer	4	88	5	21.65	22.40	24.95
soccer	4	88	6	21.48	22.12	23.26
soccer	4	88	7	21.17	21.47	22.58
soccer	4	88	8	21.55	22.53	24.25
soccer	4	88	9	21.11	20.68	22.14
soccer	4	88	10	21.28	21.23	23.11
soccer	4	92	1	23.39	24.52	25.40
soccer	4	92	2	23.51	24.17	26.51
soccer	4	92	3	22.57	21.99	25.78
soccer	4	92	4	22.81	22.90	24.25
soccer	4	92	5	22.44	22.74	23.36
soccer	4	92	6	22.47	22.37	24.66
soccer	4	92	7	22.46	22.80	23.88
soccer	4	92	8	22.38	22.63	25.08
soccer	4	92	9	22.03	21.52	23.74
soccer	4	92	10	22.71	23.16	24.69
soccer	4	101	1	20.58	22.67	23.00
soccer	4	101	2	20.68	22.80	22.99
soccer	4	101	3	20.74	23.24	22.09
soccer	4	101	4	20.00	20.96	22.51
soccer	4	101	5	21.24	25.11	24.41
soccer	4	101	6	20.36	22.00	22.47
soccer	4	101	7	20.00	20.51	22.14
soccer	4	101	8	20.58	22.29	23.45
soccer	4	101	9	20.28	21.51	22.33
soccer	4	101	10	20.23	21.26	21.96
soccer	4	106	1	18.51	22.30	20.35
soccer	4	106	2	17.89	22.55	18.38
soccer	4	106	3	17.82	22.41	18.76
soccer	4	106	4	18.10	21.22	19.57
soccer	4	106	5	17.70	20.29	18.37
soccer	4	106	6	18.15	22.34	19.88
soccer	4	106	7	18.03	21.21	19.04
soccer	4	106	8	17.41	17.41	18.24

Continued on next page

Table V.3 – continued from previous page

Sequence	SNR (dB)	Frame	Run	JM 16.0	STBMA+PDE	SO-MLD
soccer	5	85	10	24.53	25.66	27.49
soccer	5	86	1	25.05	27.80	27.73
soccer	5	86	2	24.51	26.58	28.05
soccer	5	86	3	25.24	27.12	28.40
soccer	5	86	4	24.36	23.92	28.82
soccer	5	86	5	24.79	27.12	28.27
soccer	5	86	6	25.97	28.67	29.38
soccer	5	86	7	26.46	29.30	30.07
soccer	5	86	8	24.39	26.11	28.75
soccer	5	86	9	25.01	28.47	27.63
soccer	5	86	10	25.36	27.20	27.97
soccer	5	87	1	24.67	27.78	26.79
soccer	5	87	2	25.27	26.63	27.35
soccer	5	87	3	26.39	29.00	28.60
soccer	5	87	4	23.84	25.47	25.96
soccer	5	87	5	25.74	27.23	28.01
soccer	5	87	6	22.88	24.30	26.39
soccer	5	87	7	23.91	26.30	26.27
soccer	5	87	8	24.71	27.59	26.77
soccer	5	87	9	25.77	28.21	29.61
soccer	5	87	10	24.10	25.23	27.82
soccer	5	88	1	24.55	26.06	27.27
soccer	5	88	2	25.07	26.48	28.30
soccer	5	88	3	23.73	25.56	26.01
soccer	5	88	4	23.26	24.34	26.69
soccer	5	88	5	24.16	25.17	27.91
soccer	5	88	6	25.20	28.18	27.13
soccer	5	88	7	23.78	25.65	26.53
soccer	5	88	8	24.22	27.10	26.02
soccer	5	88	9	25.53	27.72	27.87
soccer	5	88	10	23.95	25.67	26.72
soccer	5	89	1	24.53	25.73	26.86
soccer	5	89	2	24.10	25.91	27.07
soccer	5	89	3	25.01	24.90	26.93
soccer	5	89	4	25.52	28.68	29.79
soccer	5	89	5	23.06	23.18	26.08
soccer	5	89	6	25.21	27.28	27.38
soccer	5	89	7	24.62	26.53	27.79
soccer	5	89	8	27.47	28.67	30.02
soccer	5	89	9	24.24	24.60	27.05
soccer	5	89	10	25.10	27.82	27.24

Continued on next page

Table V.3 – continued from previous page

Sequence	SNR (dB)	Frame	Run	JM 16.0	STBMA+PDE	SO-MLD
walk	4	71	2	15.49	16.66	19.13
walk	4	71	3	16.78	20.60	19.97
walk	4	71	4	15.70	17.61	18.48
walk	4	71	5	17.01	21.11	19.68
walk	4	71	6	16.53	22.52	19.06
walk	4	71	7	16.30	19.40	20.33
walk	4	71	8	16.88	22.65	19.12
walk	4	71	9	16.17	17.98	19.74
walk	4	71	10	15.93	17.12	20.63
walk	4	73	1	16.22	17.37	18.52
walk	4	73	2	15.94	16.27	19.23
walk	4	73	3	16.07	18.90	20.22
walk	4	73	4	15.92	18.59	18.84
walk	4	73	5	15.96	18.62	18.87
walk	4	73	6	15.81	16.78	18.97
walk	4	73	7	15.54	16.44	19.22
walk	4	73	8	16.54	20.84	20.22
walk	4	73	9	16.43	19.36	18.78
walk	4	73	10	15.99	17.35	18.76
walk	4	77	1	13.50	14.28	16.70
walk	4	77	2	13.90	17.27	16.06
walk	4	77	3	14.14	20.09	16.49
walk	4	77	4	13.85	16.86	16.38
walk	4	77	5	14.32	16.26	18.42
walk	4	77	6	14.44	18.37	20.44
walk	4	77	7	14.83	17.42	18.91
walk	4	77	8	14.00	15.93	17.76
walk	4	77	9	13.76	15.04	17.84
walk	4	77	10	13.63	15.47	16.92
walk	4	83	1	17.42	20.56	20.86
walk	4	83	2	17.44	18.66	20.53
walk	4	83	3	17.77	20.69	20.74
walk	4	83	4	17.42	18.76	20.88
walk	4	83	5	17.25	19.17	20.99
walk	4	83	6	17.73	20.81	20.17
walk	4	83	7	17.64	18.95	21.97
walk	4	83	8	17.59	18.68	21.77
walk	4	83	9	17.45	19.64	20.68
walk	4	83	10	17.80	20.10	21.67
walk	4	84	1	19.44	21.26	22.75
walk	4	84	2	18.15	18.64	20.18

Continued on next page

Table V.3 – continued from previous page

Sequence	SNR (dB)	Frame	Run	JM 16.0	STBMA+PDE	SO-MLD
walk	4	110	4	18.11	18.45	22.96
walk	4	110	5	18.03	18.21	22.49
walk	4	110	6	18.33	20.51	21.75
walk	4	110	7	17.81	18.22	17.97
walk	4	110	8	17.67	17.67	20.51
walk	4	110	9	19.28	22.22	22.15
walk	4	110	10	18.34	19.85	21.84
walk	5	65	1	20.87	23.87	24.50
walk	5	65	2	20.81	25.13	26.22
walk	5	65	3	22.07	26.24	25.75
walk	5	65	4	22.77	25.70	25.61
walk	5	65	5	21.55	26.86	26.89
walk	5	65	6	19.55	20.87	21.74
walk	5	65	7	21.61	25.75	28.97
walk	5	65	8	20.07	24.96	26.23
walk	5	65	9	19.21	21.19	23.57
walk	5	65	10	22.51	26.14	25.49
walk	5	67	1	23.87	25.96	27.03
walk	5	67	2	21.97	24.68	23.48
walk	5	67	3	21.07	24.32	24.74
walk	5	67	4	19.93	21.91	24.31
walk	5	67	5	21.45	24.43	25.92
walk	5	67	6	22.13	26.04	25.03
walk	5	67	7	20.85	22.68	24.63
walk	5	67	8	21.17	23.92	25.16
walk	5	67	9	20.81	22.98	25.15
walk	5	67	10	21.98	25.01	24.00
walk	5	68	1	22.29	25.63	26.85
walk	5	68	2	20.18	22.44	24.27
walk	5	68	3	21.67	24.04	26.13
walk	5	68	4	23.02	26.22	26.64
walk	5	68	5	21.96	25.38	24.48
walk	5	68	6	24.37	28.18	28.47
walk	5	68	7	22.96	25.45	28.61
walk	5	68	8	22.43	23.96	27.48
walk	5	68	9	23.93	26.44	25.52
walk	5	68	10	22.85	22.94	26.82
walk	5	74	1	19.05	25.88	26.32
walk	5	74	2	19.60	25.42	24.09
walk	5	74	3	18.25	23.84	22.65
walk	5	74	4	18.91	24.29	23.94

Continued on next page

Table V.3 – continued from previous page

Sequence	SNR (dB)	Frame	Run	JM 16.0	STBMA+PDE	SO-MLD
walk	5	101	7	21.87	24.31	24.22
walk	5	101	8	23.57	26.86	27.39
walk	5	101	9	22.06	25.71	25.33
walk	5	101	10	21.68	25.23	26.52
walk	5	106	1	24.28	26.16	27.82
walk	5	106	2	23.79	25.96	26.21
walk	5	106	3	24.71	26.57	27.56
walk	5	106	4	24.49	26.18	26.50
walk	5	106	5	24.69	26.86	26.83
walk	5	106	6	25.66	27.37	27.78
walk	5	106	7	26.12	27.76	28.72
walk	5	106	8	26.68	28.33	28.08
walk	5	106	9	26.79	28.48	27.48
walk	5	106	10	25.09	26.73	27.09
walk	5	108	1	20.63	22.24	23.26
walk	5	108	2	21.73	24.60	23.77
walk	5	108	3	21.53	26.79	25.12
walk	5	108	4	20.42	21.52	25.31
walk	5	108	5	23.78	26.58	26.60
walk	5	108	6	22.56	24.61	27.35
walk	5	108	7	25.63	26.21	27.07
walk	5	108	8	21.91	27.26	27.39
walk	5	108	9	20.67	22.35	22.57
walk	5	108	10	22.49	25.59	25.94
whale-show	4	61	1	21.91	21.90	20.29
whale-show	4	61	2	21.96	21.97	20.06
whale-show	4	61	3	22.15	22.13	21.71
whale-show	4	61	4	21.97	21.97	20.77
whale-show	4	61	5	21.89	21.88	20.19
whale-show	4	61	6	21.95	21.95	20.80
whale-show	4	61	7	21.99	21.98	20.36
whale-show	4	61	8	21.78	21.78	20.23
whale-show	4	61	9	22.01	22.00	20.51
whale-show	4	61	10	21.78	21.77	20.58
whale-show	4	63	1	22.56	22.60	23.22
whale-show	4	63	2	22.02	21.95	22.87
whale-show	4	63	3	21.97	21.91	22.65
whale-show	4	63	4	22.15	22.04	22.98
whale-show	4	63	5	21.99	22.00	22.97
whale-show	4	63	6	22.03	22.10	23.04
whale-show	4	63	7	21.99	21.98	21.14

Continued on next page

Table V.3 – continued from previous page

Sequence	SNR (dB)	Frame	Run	JM 16.0	STBMA+PDE	SO-MLD
whale-show	4	74	9	22.81	22.66	23.11
whale-show	4	74	10	22.89	22.84	23.51
whale-show	4	77	1	22.81	22.63	22.66
whale-show	4	77	2	23.04	22.93	22.90
whale-show	4	77	3	22.62	22.47	23.10
whale-show	4	77	4	22.90	22.89	23.09
whale-show	4	77	5	22.61	22.61	22.70
whale-show	4	77	6	23.07	23.13	22.03
whale-show	4	77	7	22.53	22.53	22.93
whale-show	4	77	8	22.84	22.72	22.97
whale-show	4	77	9	22.53	22.53	23.02
whale-show	4	77	10	23.04	22.93	23.47
whale-show	4	83	1	22.35	22.91	22.58
whale-show	4	83	2	22.51	22.89	22.88
whale-show	4	83	3	21.88	21.96	21.70
whale-show	4	83	4	21.84	21.90	22.25
whale-show	4	83	5	21.90	21.95	22.94
whale-show	4	83	6	22.28	22.82	23.09
whale-show	4	83	7	22.37	22.97	23.01
whale-show	4	83	8	21.94	21.73	22.73
whale-show	4	83	9	22.05	22.47	22.61
whale-show	4	83	10	22.31	22.51	23.18
whale-show	4	90	1	22.42	22.33	22.88
whale-show	4	90	2	22.43	22.45	22.15
whale-show	4	90	3	22.15	22.15	21.98
whale-show	4	90	4	22.22	22.12	22.26
whale-show	4	90	5	22.39	22.26	22.87
whale-show	4	90	6	22.45	22.20	22.34
whale-show	4	90	7	22.77	22.67	22.81
whale-show	4	90	8	22.50	22.42	21.95
whale-show	4	90	9	22.43	22.50	22.61
whale-show	4	90	10	22.46	22.62	22.68
whale-show	4	91	1	22.77	22.78	21.37
whale-show	4	91	2	22.70	22.70	20.42
whale-show	4	91	3	22.79	22.79	20.61
whale-show	4	91	4	22.76	22.76	20.60
whale-show	4	91	5	22.73	22.73	21.27
whale-show	4	91	6	22.73	22.73	20.87
whale-show	4	91	7	22.60	22.60	20.63
whale-show	4	91	8	22.73	22.73	21.05
whale-show	4	91	9	22.88	22.87	20.66

Continued on next page

Table V.3 – continued from previous page

Sequence	SNR (dB)	Frame	Run	JM 16.0	STBMA+PDE	SO-MLD
whale-show	4	91	10	22.67	22.67	20.32
whale-show	5	62	1	24.64	24.78	24.72
whale-show	5	62	2	23.26	23.34	25.00
whale-show	5	62	3	24.73	24.91	24.92
whale-show	5	62	4	23.98	24.16	24.57
whale-show	5	62	5	24.38	24.51	24.75
whale-show	5	62	6	24.20	24.44	24.67
whale-show	5	62	7	24.20	24.36	24.59
whale-show	5	62	8	24.24	24.35	24.65
whale-show	5	62	9	22.72	22.77	24.11
whale-show	5	62	10	23.00	23.15	24.13
whale-show	5	67	1	24.10	24.06	24.26
whale-show	5	67	2	23.63	23.50	23.88
whale-show	5	67	3	23.71	23.49	24.05
whale-show	5	67	4	23.52	23.34	23.80
whale-show	5	67	5	24.34	24.04	24.44
whale-show	5	67	6	23.51	23.50	24.37
whale-show	5	67	7	23.47	23.17	23.83
whale-show	5	67	8	23.82	23.61	24.12
whale-show	5	67	9	23.63	23.53	23.91
whale-show	5	67	10	23.47	23.08	23.80
whale-show	5	72	1	24.22	24.32	24.42
whale-show	5	72	2	23.89	23.95	24.35
whale-show	5	72	3	24.29	24.30	24.77
whale-show	5	72	4	24.27	24.10	24.30
whale-show	5	72	5	23.97	23.91	24.26
whale-show	5	72	6	23.95	23.95	24.48
whale-show	5	72	7	24.31	24.32	24.63
whale-show	5	72	8	24.25	24.30	24.75
whale-show	5	72	9	23.43	23.33	23.79
whale-show	5	72	10	23.63	23.65	24.04
whale-show	5	77	1	23.47	23.57	23.97
whale-show	5	77	2	23.74	23.82	23.82
whale-show	5	77	3	24.15	24.07	24.29
whale-show	5	77	4	23.94	23.68	24.25
whale-show	5	77	5	23.73	23.76	23.97
whale-show	5	77	6	23.43	23.42	23.65
whale-show	5	77	7	23.61	23.66	23.88
whale-show	5	77	8	24.10	24.13	24.45
whale-show	5	77	9	24.00	23.90	24.47
whale-show	5	77	10	24.08	24.07	24.22

Continued on next page

Table V.3 – continued from previous page

Sequence	SNR (dB)	Frame	Run	JM 16.0	STBMA+PDE	SO-MLD
whale-show	5	83	1	24.66	24.79	24.96
whale-show	5	83	2	24.02	24.03	24.18
whale-show	5	83	3	23.15	23.66	24.24
whale-show	5	83	4	23.20	23.45	23.68
whale-show	5	83	5	23.75	23.88	24.13
whale-show	5	83	6	23.32	23.33	24.24
whale-show	5	83	7	23.39	23.47	24.37
whale-show	5	83	8	23.77	24.10	24.41
whale-show	5	83	9	23.61	23.79	24.37
whale-show	5	83	10	23.83	23.97	24.34
whale-show	5	85	1	23.87	23.90	24.29
whale-show	5	85	2	23.59	23.73	24.31
whale-show	5	85	3	23.73	23.84	24.38
whale-show	5	85	4	23.75	23.87	24.28
whale-show	5	85	5	24.01	23.90	23.88
whale-show	5	85	6	23.32	23.49	23.96
whale-show	5	85	7	23.46	23.38	23.51
whale-show	5	85	8	23.39	23.40	23.79
whale-show	5	85	9	23.62	23.76	23.94
whale-show	5	85	10	23.40	23.36	23.81
whale-show	5	87	1	23.70	23.68	24.14
whale-show	5	87	2	23.55	23.71	23.78
whale-show	5	87	3	23.07	23.04	23.42
whale-show	5	87	4	23.98	24.08	24.06
whale-show	5	87	5	23.59	23.69	23.88
whale-show	5	87	6	23.51	23.71	23.99
whale-show	5	87	7	23.99	24.05	23.94
whale-show	5	87	8	23.13	23.16	23.53
whale-show	5	87	9	23.83	23.79	23.87
whale-show	5	87	10	23.90	23.90	24.31
whale-show	5	91	1	24.06	24.06	23.78
whale-show	5	91	2	24.60	24.59	23.78
whale-show	5	91	3	24.76	24.76	23.48
whale-show	5	91	4	24.25	24.25	23.12
whale-show	5	91	5	24.44	24.44	22.74
whale-show	5	91	6	24.43	24.43	23.14
whale-show	5	91	7	24.25	24.25	23.08
whale-show	5	91	8	24.31	24.30	21.78
whale-show	5	91	9	24.28	24.28	23.67
whale-show	5	91	10	24.62	24.62	23.75
whale-show	5	98	1	23.93	23.95	23.94

Continued on next page

Table V.3 – continued from previous page

Sequence	SNR (dB)	Frame	Run	JM 16.0	STBMA+PDE	SO-MLD
whale-show	5	98	2	23.90	23.96	24.34
whale-show	5	98	3	23.77	23.78	24.03
whale-show	5	98	4	24.11	24.05	24.48
whale-show	5	98	5	23.88	23.96	24.52
whale-show	5	98	6	23.97	24.00	24.57
whale-show	5	98	7	23.23	23.14	23.46
whale-show	5	98	8	23.68	23.69	24.19
whale-show	5	98	9	23.13	23.18	23.70
whale-show	5	98	10	23.47	23.48	23.75
whale-show	5	102	1	23.79	23.75	24.08
whale-show	5	102	2	23.83	23.72	24.04
whale-show	5	102	3	23.50	23.44	23.80
whale-show	5	102	4	23.99	23.98	24.38
whale-show	5	102	5	23.79	23.69	24.07
whale-show	5	102	6	23.55	23.51	23.78
whale-show	5	102	7	24.09	24.11	24.25
whale-show	5	102	8	23.53	23.03	23.93
whale-show	5	102	9	23.67	23.58	23.64
whale-show	5	102	10	23.96	23.95	23.91

BIBLIOGRAPHY

- Aign, S. October 1995. "Error Concealment Enhancement by Using the Reliability Outputs of a SOVA in MPEG-2 Video Decoder". In *International Symposium on Signals, Systems and Electronics*. p. 59-62. URSI.
- Bergeron, C. and C. Lamy-Bergot. October 2004. "Soft-input decoding of variable-length codes applied to the H.264 standard". In *6th Workshop on Multimedia Signal Processing*. p. 87-90. IEEE.
- Caron, F. and S. Coulombe. 2012a. "Method and System for Video Error Correction Based on Maximum Likelihood". US patent No. 61/646,852 (provisional), submitted May 14th 2012.
- Caron, F. and S. Coulombe. September 2012b. "A Maximum Likelihood Approach to Video Error Correction Applied to H.264 Decoding". In *6th International Conference on Next Generation Mobile Applications, Services and Technologies*. p. 1-6. IEEE.
- Caron, F. and S. Coulombe. 2013a. "Method and System for Video Error Correction Based on Maximum Likelihood Using Hard or Soft Information From the Channel Decoder". US patent No. 61/754,724 (provisional), submitted January 21th 2013.
- Caron, F. and S. Coulombe. September 2013b. "A Maximum Likelihood Approach to Correct Transmission Errors for Joint Source-Channel Decoding of H.264 Coded Video". In *20th International Conference on Image Processing*. IEEE.
- Caron, F. and S. Coulombe. May 2013c. Video Error Correction Using Soft-Output Maximum Likelihood Decoding Applied to H.264 Baseline Profile. Submitted to IEEE Transactions on Circuits and Systems for Video Technology.
- Caron, F. and S. Coulombe. 2013d. "Method and System for Video Error Correction". Patent number CA/2013/050370, submitted May 14th 2013.
- Chen, M.-J., Liang-Gee Chen, and Ro-Min Weng. June 1997. "Error Concealment of Lost Motion Vectors with Overlapped Motion Compensation". *IEEE Transactions on Circuits and Systems for Video Technology*, vol. 7, n. 3, p. 560-563.
- Chen, Y., Y. Hu, O. Au, H. Li, and C.W. Chen. January 2008. "Video Error Concealment Using Spatio-Temporal Boundary Matching and Partial Differential Equation". *IEEE Transactions on Multimedia*, vol. 10, n. 1, p. 2-15.
- Connie, A. T., P. Nasiopoulos, V. C. M. Leung, and Y. P. Fallah. January 2008. "Video Packetization Techniques for Enhancing H.264 Video Transmission over 3G Networks". In *5th Consumer Communications and Networking Conference*. p. 800-804. IEEE.
- Ding, X. and K. Roy. 2004. "A Novel Bitstream Level Joint Channel Error Concealment Scheme for Realtime Video Over Wireless Networks". In *23rd Annual Joint Conference of the IEEE Computer and Communications Societies INFOCOM*. p. 2163-2173.

- Farrugia, R. and C.J. Debono. 2009. "A Robust Error Detection Mechanism for H.264/AVC Coded Video Sequences Based on Support Vector Machines". *IEEE Transactions on Circuits and Systems for Video Technology*, vol. 18, n. 12, p. 1766-1770.
- Farrugia, R. and C.J. Debono. 2010. "A Hybrid Error Control and Artifact Detection Mechanism for Robust Decoding of H.264/AVC Video Sequences". *IEEE Transactions on Circuits and Systems for Video Technology*, vol. 20, n. 5, p. 756-762.
- Farrugia, R. and C.J. Debono. 2011. "Robust decoder-based error control strategy for recovery of H.264/AVC video content". *IET Communications*, vol. 5, n. 11, p. 1928-1938.
- Huang, S. C. and S. Kuo. September 2008. "Optimization of Hybridized Error Concealment for H.264". *IEEE Transactions on Broadcasting*, vol. 54, n. 3, p. 499-516.
- International Telecommunications Union. November 2007. ITU-T Recommendation H.264 : Advanced video coding for generic audiovisual services. <http://www.itu.int/rec/T-REC-H.264/en>.
- Joint Video Team. November 2011a. "H.264/AVC JM reference software". <http://iphome.hhi.de/suehring/tml/>.
- Joint Video Team. August 2011b. "0000277: using RTP mode, when dropping some packets with rtp_loss.exe decoder can not decode". <https://ipbt.hhi.fraunhofer.de/mantis/view.php?id=277>.
- Kumar, S., M. Mandal L. Xu, and S. Panchanathan. April 2006. "Error Resiliency Schemes in H.264/AVC Standard". *Journal of Visual Communication and Image Representation*, vol. 17, n. 2, p. 425-450.
- Kwok, W. and H. Sun. August 1993. "Multi-Directional Interpolation for Spatial Error Concealment". *IEEE Transactions on Consumer Electronics*, vol. 39, n. 3, p. 455-460.
- Lam, W.-M. M., Amy R. Reibman, and Liu Bede. April 1993. "Recovery of Lost or Erroneously Received Motion Vector". In *International Conference on Acoustics, Speech, and Signal Processing*. p. 417-420. IEEE.
- Lambert, P., W. De Neve, Y. Dhondt, and R. Van de Walle. April 2006. "Flexible macroblock ordering in H.264/AVC". *Journal of Visual Communication and Image Representation*, vol. 17, n. 2, p. 358-375.
- Larzon, L., M. Degermark, and M. Pink, S. Degermark. 1999. *UDP Lite for Real Time Multimedia Applications*. Technical report. In Proceedings of the QoS mini-conference of IEEE International Conference of Communications.
- Lee, J.-B. and Hari Kalva, 2008. *The VC-1 and H.264 Video Compression Standards for Broadband Video Services*. Springer.

- Lee, W.-T., H.-J. Chen, Y.-S. Hwang, and J.-J. Chen. July 2007. "Joint Source-Channel Decoder for H.264 Coded Video Employing Fuzzy Adaptive Method". In *International Conference on Multimedia and Expo*. p. 755-758. IEEE.
- Levine, D., W. E. Lynch, and T. Le-Ngoc. May 2007. "Iterative Joint Source-Channel Decoding of H.264 Compressed Video". In *International Symposium on Circuits and Systems*. p. 1517-1520. IEEE.
- Ma, X. and W. E. Lynch. May 2004. "Iterative Joint Source-Channel Decoding Using Turbo Codes for MPEG-4 Video Transmission". In *International Conference on Acoustics, Speech, and Signal Processing*. p. 657-660. IEEE.
- Montgomery, D. C. and George C. Runger, 2011. *Applied Statistics and Probability for Engineers*. Fifth ed. John Wiley and Sons, Inc.
- Nguyen, H. and P. Duhamel. October 2004. "Iterative joint source-channel decoding of variable length encoded sequences exploiting source semantics". In *International Conference on Image Processing*. p. 3221-3224. IEEE.
- Nguyen, N., W. E. Lynch, and T. Le-Ngoc. May 2010. "Iterative Joint Source-Channel Decoding for H.264 Video Transmission Using Virtual Checking Method at Source Decoder". In *23rd Canadian Conference on Electrical and Computer Engineering*. p. 1-4. IEEE.
- Persson, D. and T. Eriksson. May 2009. "Mixture Model- and Least Squares-Based Packet Video Error Concealment". *IEEE Transactions on Image Processing*, vol. 18, n. 5, p. 1048-1054.
- Postel, J. August 1980. "User Datagram Protocol". <http://www.ietf.org/rfc/rfc768.txt>.
- Postel, J. September 1981. "Transmission Control Protocol - DARPA Internet Program Protocol Specification". <http://www.ietf.org/rfc/rfc793.txt>.
- Qian, X., G. Liu, and H. Wang. June 2009. "Recovering Connected Error Region Based on Adaptive Error Concealment Order Determination". *IEEE Transactions on Multimedia*, vol. 11, n. 4, p. 683-695.
- Richardson, I. E. G., 2003. *H.264 and MPEG-4 Video Compression - Video Coding for Next-generation Multimedia*. John Wiley and Sons, Inc.
- Rosen, K. H., 2007. *Discrete Mathematics and Its Applications*. Sixth ed. McGraw Hill Higher Education.
- Sabeva, G., S. Ben Jamaa, M. Kieffer, and P. Duhamel. October 2006. "Robust Decoding of H.264 Encoded Video Transmitted over Wireless Channels". In *8th Workshop on Multimedia Signal Processing*. p. 9-13. IEEE.
- Sklar, B., 2001. *Digital Communications Fundamentals and Applications*. Second ed. Prentice Hall.

- Stockhammer, T., M. M. Hannuksela, and T. Wiegand. July 2003. "H.264/AVC in Wireless Environments". *IEEE Transactions on Circuits and Systems for Video Technology*, vol. 13, n. 7, p. 657-673.
- Sun, H. and W. Kwok. April 1995. "Concealment of Damaged Block Transform Coded Images Using Projections onto Convex Sets". *IEEE Transactions on Image Processing*, vol. 4, n. 4, p. 478-477.
- Trudeau, L., S. Coulombe, and S. Pigeon. September 2011. "Pixel Domain Referenceless Visual Degradation Detection and Error Concealment for Mobile Video". In *18th International Conference on Image Processing*. p. 2229-2232. IEEE.
- van der Schaar, M. and Philip A. Chou, 2007. *Multimedia Over IP and Wireless Networks Compression, Networking, and Systems*. Academic Press.
- Wang, Y. and S. Yu. November 2005. "Joint Source-Channel Decoding for H.264 Coded Video Stream". *IEEE Transactions on Consumer Electronics*, vol. 51, n. 4, p. 1273-1276.
- Wang, Y., Q. F. Zhu, and L. Shaw. October 1993. "Maximally Smooth Image Recovery in Transform Coding". *IEEE Transactions on Communications*, vol. 41, n. 10, p. 1544-1551.
- Wang, Y., Jorn Ostermann, and Ya-Qin Zhang, 2002. *Video Processing and Communications*. Prentice Hall.
- Wang, Y. and Qin-Fan Zhu. May 1998. "Error control and concealment for video communication: a review". *Proceedings of the IEEE*, vol. 86, n. 5, p. 974-997.
- Weidmann, C., P. Kadlec, O. Nemethova, and A. A. Moghrabi. October 2004. "Combined Sequential Decoding and Error Concealment of H.264 Video". In *6th Workshop on Multimedia Signal Processing*. p. 299-302. IEEE.
- Wenger, S. July 2003. "H.264/AVC Over IP". *IEEE Transactions on Circuits and Systems for Video Technology*, vol. 13, n. 7, p. 645-656.
- Wenger, S., M.M. Hannuksela, T. Stockhammer, M. Westerlund, and D. Singer. February 2005. "RTP Payload Format for H.264 Video". <http://www.ietf.org/rfc/rfc3984.txt>.
- Wiegand, T., G. J. Sullivan, G. Bjontegaard, and A. Luthra. July 2003. "Overview of the H.264/AVC Video Coding Standard". *IEEE Transactions on Circuits and Systems for Video Technology*, vol. 13, n. 7, p. 560-576.
- Wu, J., X. Liu, and K. Y. Yoo. November 2008. "A Temporal Error Concealment Method for H.264/AVC Using Motion Vector Recovery". *IEEE Transactions on Consumer Electronics*, vol. 54, n. 4, p. 1880-1885.
- Xu, Y. and Y. Zhou. November 2004. "H.264 Video Communication Based Refined Error Concealment Schemes". *IEEE Transactions on Consumer Electronics*, vol. 50, n. 4, p. 1135-1141.

- Y. K. Wang, M. M. H, V. V. and A. Hourunranta. September 2002. "The error concealment feature in the H.26L test model". In *International Conference on Image Processing*. p. 729-732. IEEE.
- Y. Wang, S. W, J. W. and A. K. Katsaggelos. July 2000. "Error resilient video coding techniques". *IEEE Signal Processing Magazine*, vol. 17, n. 4, p. 61-82.
- Yan, B. and H. Gharavi. January 2010. "A Hybrid Frame Concealment Algorithm for H.264/AVC". *IEEE Transactions on Image Processing*, vol. 19, n. 1, p. 98-107.